

Helsinki University of Technology Water Resources Publications

Teknillisen korkeakoulun vesitalouden ja vesirakennuksen julkaisuja

Espoo 2004

TKK-VTR-12

RELATIONSHIPS OF PARTICLE SIZE DISTRIBUTION CURVE, SOIL WATER RETENTION CURVE AND UNSATURATED HYDRAULIC CONDUCTIVITY AND THEIR IMPLICATIONS ON WATER BALANCE OF FORESTED AND AGRICULTURAL HILLSLOPES

Mikko Jauhiainen

Dissertation for the degree of Doctor of Philosophy to be presented with due to permission of the Department of Civil and Environmental Engineering for public examination and debate in Auditorium R1 at Helsinki University of Technology (Espoo, Finland) on the 3rd of September, 2004, at 12 noon.

Helsinki University of Technology
Department of Civil and Environmental Engineering
Laboratory of Water Resources

Teknillinen korkeakoulu
Rakennus- ja ympäristötekniikan osasto
Vesitalouden ja vesirakennuksen laboratorio

Jauhiainen, M., Relationships of particle size distribution curve, soil water retention curve and unsaturated hydraulic conductivity and their implications on water balance of forested and agricultural hillslopes, Helsinki University of Technology, Water Resources Publications, TKK-VTR-12, Espoo, 2004, 165 pp.

Distribution:

Helsinki University of Technology

Laboratory of Water Resources

P.O.Box 5300

FIN-02015 HUT

Tel. +358-9-451 3821

Fax. +358-9-451 3856

E-mail: contact@water.hut.fi

© Mikko Jauhiainen 2004

ISBN 951-22-7194-X

ISSN 1456-2596

Otamedia OY

Espoo 2004

HELSINKI UNIVERSITY OF TECHNOLOGY P.O. Box 1000, FIN-02015 HUT, http://www.hut.fi		ABSTRACT OF DOCTORAL DISSERTATION	
Author		Mikko Jauhiainen	
Relationships of particle size distribution curve, soil water retention curve and unsaturated hydraulic conductivity and their implications on water balance of forested and agricultural hillslopes			
Date of the manuscript June 17, 2002		Date of the dissertation September 3, 2004	
Monograph			
Department	Civil and Environmental Engineering		
Laboratory	Water Resources		
Field of research	Hydrology		
Opponent	Professor Hannu Ilvesniemi (Finnish Forest Research Institute)		
Supervisor	Professor Tuomo Karvonen (HUT)		
Pre-examiners	Professor Hannu Mannerkoski (University of Joensuu) Professor Juhani Virta (University of Helsinki)		
<p>The primary objectives of this study were to determine selected soil water retention curves for Finnish forest sites and to develop a methodology that predicts the water retention curve and unsaturated hydraulic conductivity from the particle size distribution curve. The method was obtained by modifying Andersson's method. Selected soil water retention curves were determined for four Finnish forest site types. Parameters of 360 soil samples were estimated. The samples were collected from 90 forest soil profiles. In each profile four podzol horizons were selected for sampling. The parameters are usable for water balance calculations of various scales. The study includes results of numerous water retention characteristics and hydraulic conductivity predictions from the particle size distribution curve. These predictions were accomplished for both forested and agricultural soils. Predicting water retention characteristics from particle size distribution curve could be accomplished at a reasonable level of accuracy when the semi-physical and van Genuchten's methods were used. Predicting the water retention characteristics using Jonasson's method was successful when clay content of soil was less than 25 percent. Implications of soil hydraulic properties on water balance of forested and agricultural hillslopes showed reasonable agreement with the measured values. The best overall fit between measured and calculated values was obtained in the case that water retention curve was estimated from particle size distribution curve and unsaturated hydraulic conductivity using Andersson's method.</p>			
Keywords: hydrology, soil water flow, water retention, hydraulic conductivity			
UDC 556.16:556.12:51.001.57:004.94		Number of pages 165	
ISBN (printed) 951-22-7194-X		ISBN (pdf) 951-22-7195-8	
ISBN (others)		ISSN 1456-2596	
Publisher HUT, Laboratory of Water Resources			
Print distribution contact@water.hut.fi		Fax +358 9 451 3856, E-mail	
<input checked="" type="checkbox"/> The dissertation can be read at http://lib.hut.fi/Diss/2003/isbn9512271958			

TEKNILLINEN KORKEAKOULU PL 1000, 02015 TKK, http://www.hut.fi	VÄITÖSKIRJAN TIIVISTELMÄ
Tekijä	Mikko Jauhainen
Partikkelikokojakauman, maan vedenpidätyskäyrän ja kyllästymättö- män maan hydraulisen johtavuuden väliset suhteet sekä niiden vaikutus metsäisten ja maatalousvaltaisten rinteiden vesitaseeseen.	
Käsikirjoituksen jättämispäivämäärä 17.6. 2002 Väitöstilaisuuden ajankohta 3.9. 2004	
Monografia	
Osasto	Rakennus- ja ympäristötekniikka
Laboratorio	Vesitalous ja vesirakennus
Tutkimusala	Hydrologia
Vastaväittäjä	Professori Hannu Ilvesniemi (Metsäntutkimuslaitos)
Työn valvoja	Professori Tuomo Karvonen (TKK)
Esitarkastajat	Professori Hannu Mannerkoski (Joensuun yliopisto) Professori Juhani Virta (Helsingin yliopisto)
<p>Tutkimuksen tärkeimpinä tavoitteina oli määrittää suomalaisille metsämaille valitut vedenpidätyskäyrät ja kehittää menetelmä, jolla ennustetaan maan par- tikelikokojakauman avulla vedenpidätyskäyrä ja kyllästymättöman maan hyd- raulinen johtavuus. Menetelmä kehitettiin laajentamalla Anderssonin menetel- mää. Neljälle suomalaiselle metsämaalle määritettiin valitut maan vedenpidätys- käyrät. Kaikkiaan 360 maanäytteen vedenpidätyskäyrän parametrit estimoitiiin. Näytteet oli kerätty 90 metsämaaprofiilista. Kustakin profiilista valittiin 4 podso- lihorisonttia näytteen ottoa varten. Parametrit ovat käyttökelpoisia eri mittakaa- vojen vesitaselaskelmiin. Tutkimuksessa on esitetty lukuisia partikkelikokoja- kaumasta ennustettuja vedenpidätyskäyriä ja hydraulisia johtavuuksia. Näitä ennusteita oli sekä maatalous- että metsämaista. Partikkelikokojakaumasta voidaan ennustaa vedenpidätyskäyrä tarkasti käyttämällä kehitettyä menetel- mää. Hydraulisen johtavuuden ennustaminen van Genuchtenin ja semi-fysi- kaalisella menetelmällä onnistui hyvin kaikilla tutkimuksessa käytetyillä maan savipitoisuuden arvoilla. Jonassonin menetelmä soveltui hyvin vain savipito- isuuden ollessa pohjamaassa alle 30 % ja viljelykerroksessa alle 25 %. Rinteen vesitalouslaskelmat sopivat hyvin yhteen mitattujen ja laskettujen arvojen välillä saatiin silloin, kun vedenpidätyskäyrä oli ennustettu partikkelikokojakaumasta ja hyd- raulinen johtavuus oli saatu Anderssonin menetelmällä.</p>	
Avainsanat: hydrologia, maaveden liike, vedenpidätys, hydraulinen johtavuus	
UDK 556.16:556.12:51.001.57:004.94	Sivumäärä 165
ISBN (painettu) 951-22-7194-X	ISBN (pdf) 951-22-7195-8
ISBN (muut)	ISSN 1456-2596
Julkaisija	TKK, Vesitalouden ja vesirakennuksen laboratorio
Painetun väitöskirjan jakelu Telefaksi 09 451 3856, sähköposti contact@water.hut.fi	
<input checked="" type="checkbox"/> Luettavissa verkossa osoitteessa http://lib.hut.fi/Diss/2003/isbn9512271958	

ACKNOWLEDGEMENTS

This study was financed by the Academy of Finland (through 'The Research Program on Climate Change', SILMU and the Graduate School of Geohydrology). Sven Hallin research foundation, Salaojituksen tukisäätiö foundation, and the Land and water technology foundation provided scholarships.

The work has been carried out while the writer worked in the University of Helsinki in Department of Forest Ecology, at the Helsinki University of Technology, Laboratory of Water Resources in Espoo and in Häme Polytechnic in Lepaa.

Professor Tuomo Karvonen has been my supervisor. He has been always ready to serve me with my questions and needs for help. During the work there has occurred some times when the help was needed. I am also grateful to the Head of Laboratory of Water Resources, Professor Pertti Vakkilainen for his support during the progress of this thesis.

Professor Juhani Virta and Professor Hannu Mannerkoski reviewed the thesis. I am grateful for their encouragement, constructive criticism and valuable suggestions.

Päivi, Otso and Ida have been my supporting home team with good ability to remind me of more important things existing than writing the thesis.

Espoo, 12.8.2004

Mikko Jauhiainen

TABLE OF CONTENTS

Abstract of doctoral dissertation	3
Väitöskirjan tiivistelmä	4
Acknowledgements	5
Table of contents	6
List of symbols	9
List of tables and appendices	13
List of figures	16
1 Introduction.....	21
1.1 General overview.....	21
1.2 Soil physical properties	22
1.2.1 Indirect estimation methods of the WRC	23
1.2.1.1 Discrete matric potential regression methods.....	23
1.2.1.2 Functional regression methods	24
1.2.1.3 Semi-physical methods.....	26
1.2.2 Fractal models	27
1.2.3 Spatial variability	28
1.2.4 Soil organic matter	29
1.2.5 Use of neural networks to develop pedotransfer functions	
30	
1.3 Estimation of the hydraulic conductivity function	30
1.3.1 Direct measurement of unsaturated hydraulic	
conductivity	30
1.3.2 Inverse methods for estimating soil hydraulic properties	
31	
1.3.3 Empirical models for predicting unsaturated hydraulic	
conductivity	32
1.3.4 Estimation of $K(\theta)$ from the PSDC and/or the WRC	32
1.4 Aims of the study.....	33
2 Material	35
2.1 Finnish forest soils.....	35
2.2 Swedish agricultural soils	36
2.3 Soils of UNSODA database	36
2.4 Rudbäcken hillslope.....	37
2.5 Mämmilampi experimental site.....	38
2.6 Sjäkkulla agricultural field	38
3 Estimation of unsaturated hydraulic functions from soil physical	
properties.....	40
3.1 Introduction.....	40
3.2 Andersson's models for describing the PSDC, WRC and	
relative hydraulic conductivity.....	40
3.2.1 Andersson's model for the particle size distribution	
function	40
3.2.2 Andersson's model for the water retention function.....	41
3.2.3 Andersson's work related to pedotransfer functions.....	42
3.2.4 Relative hydraulic conductivity function of Andersson..	43
3.3 Modifications and extensions to Andersson's models.....	45
3.3.1 Particle size distribution function	45

3.3.2	Water retention function.....	46
3.3.3	Relative hydraulic conductivity	46
3.4	Development of a semi-physical approach to predict WRC from PSDC	47
3.5	Mualem- and van Genuchten-type models	50
3.5.1	Water retention curve	50
3.5.2	van Genuchten type hydraulic conductivity function	50
3.5.3	Development of a semi-physical approach to predict WRC from PSDC using the van Genuchten-type functions	51
3.6	Testing of the developed methods in water balance modeling 53	
3.6.1	Introduction	53
3.6.2	Modeling of water balance of forested hillslopes.....	56
3.6.2	Modeling of water balance of an agricultural hillslope...	57
4	Results	60
4.1	Average water retention curves of podzol soil horizons of four Finnish forest site types	60
4.2	Selected water retention curves of profiles of four Finnish forest site types	62
4.3	Estimation of Andersson's and van Genuchten's parameters for Finnish forest mineral soil profiles.....	67
4.4	Estimation of Andersson's parameters for selected Finnish forest humus layer data	72
4.5	Prediction of the WRC from the PSDC using the semi- physical methods	76
4.5.1	Finnish forest sites	77
4.5.2	Swedish agricultural soils.....	84
4.6	Prediction of hydraulic conductivity from the WRC using modification of Andersson's method and van Genuchten's method 88	
4.6	Sensitivity analysis of the water retention characteristics.	92
5	Implications of soil hydraulic properties on the water balance of forested and agricultural hillslopes	93
5.1	Forested hillslope in Rudbäcken.....	93
5.1.1	Estimation of the WRC from the PSDC	93
5.1.2	Comparison of unsaturated hydraulic conductivity	96
5.1.3	Comparison of measured and estimated pressure heads in Rudbäcken hillslope	99
5.2	Forested soil profile in Mämmilampi, Hyytiälä.....	103
5.2.1	Setting up the model	103
5.2.2	Estimation of soil hydraulic properties from the PSDC	103
5.2.2	Comparison of measured and calculated pressure heads 105	
5.3	Sjökulla experimental field	110
5.3.1	Estimation of the WRC from the PSDC.....	110
5.3.2	Comparison of unsaturated hydraulic conductivity	111
5.3.3	Calculation of the water balance components of an agricultural hillslope	113
5.3.3.1	Lower part of the hillslope, macropore model included	114
5.3.3.2	Lower part of the hillslope, macropore model not included 117	

5.3.3.3	Upper part of the hillslope, macropore model included	120
5.3.3.4	Upper part of the hillslope, macropore model not included	122
6	Discussion and conclusions	125
7	Summary	132
8	References	134

LIST OF SYMBOLS

Latin letters

A	cross-sectional area
b	parameter in PSDC
b_1	parameter that defines the slope of the WRC at the inflection point
b_2	parameter in pipe-size distribution curve
c	derivative of the curve at the inflection point (x_0, y_0)
c_{sat}	constant including the effects of fluid characteristics and the porous media
$c_{sat,opt}$	optimum value of c_{sat}
C_p	pedotransfer function
$C(b)$	derivative of the WRC, $d\theta/db$
d_{25}	grain diameter at 25 cumulative % by weight
d_{75}	grain diameter at 75 cumulative % by weight
d_{COEF}	empirical fitting parameter
d_W	density of water
D	pipe diameter
D_{max}	maximum pipe diameter
D_{min}	minimum pipe diameter
D_p	mean particle diameter
D_g	particle-size scale parameter
D_d	depth from drain level to impermeable bottom of the profile
D_e	effective depth
D_{6-2}	fraction(%) of particle size values from 600 μm to 2000 μm
e	void ratio, V_v/V_s
E_{ave}	average errors of different pressure heads
E_{min}	minimum values of errors at different pressure heads
E_{max}	maximum values of errors at different pressure heads
ET	evaporation
f_∞	parameter defining macropore decrease as a function of depth
$f(h)$	pore capillary pressure distribution function, Kosugi (1996)
$f(r)$	pore radius distribution function, Kosugi (1996)
F_{CLAY}	clay content of the sample (%).
$100-F_{CLAY}$	range of the particle-size distribution function
g	acceleration due to gravity
h	soil water pressure head
h_i	soil water pressure head, Haverkamp and Parlange (1986)
h_B	bubbling pressure
$h_{B,opt}$	optimum bubbling pressure
h_g	water retention scale parameter
$h_{t,0}$	pressure head of the inflection point

b_M	difference between water level midway between two drains and drain level
$b(\theta)$	water retention characteristic
I	gradient causing flow
k_M	parameter
k_m	parameter, van Genuchten (1980), Burdine (1953), Mualem (1976)
K_H	bulk hydraulic conductivity
$K_{i,m}$	measured hydraulic conductivity
$K_{i,c}$	calculated hydraulic conductivity
$K_{s,tG}$	estimated saturated hydraulic conductivity, (App. 8/II)
$K_{s,bb}$	estimated saturated hydraulic conductivity, (App. 8/II)
K	parameter from Mualem's (1976a) model for hydraulic conductivity function
K_R	relative hydraulic conductivity
K_M	hydraulic conductivity of the macropores
$K_{M,MAX}$	hydraulic conductivity of the macropores at the soil surface
$K(\theta)$	hydraulic conductivity
$K(b)$	hydraulic conductivity
L	distance of the profile from the nearest main ditch
m	van Genuchten (1980) water retention shape parameter
M	number of measured points of the PSDC
M	number of measurements in soil sample, App. 8/II
M_1	number of measured points of the water retention curve
M_s	cumulative particle-size shape parameter
n	number of spherical particles with radius, r
n	van Genuchten (1980) water retention shape parameter
n_p	porosity
N	total number of particles in a gram soil sample
N	cumulative particle-size shape parameter
O	objective function
p	parameter in PSDC
p_1	parameter in WRC
p_2	parameter in pipe-size distribution curve
$P_1...P_4$	parameters of the multi- regression equation
PSDC	particle size distribution curve
q	total flow of the pipes
q_D	flow towards subsurface drains or open ditches, Hooghoudt's equation
r	diameter at the top of any pore
r_e	effective drain radius
R_i	mean pore radius, Haverkamp and Parlange (1986)
R	radius of the main pore
S_{dev}	standard deviation of errors
$S(b)$	sink term

$S_q(b)$	term which accounts the influence of deep subsurface flow
SP_i	sensitivity of parameter i
$u(y)$	pedotransfer function
v	vertical coordinate
V_f	volume of pores
V_s	volume of solids
V_{MAX}	maximum volume of the macropores
V_{MAX}	maximum volume of the macropores
W_{ditch}	water level elevation in the main ditch
WRC	water retention curve
x	particle size diameter
x_0	particle diameter of the inflection point of the PSDC
x_0	particle diameter of the most frequent particle diameter
x_v	pore (void) size diameter
y	cumulative particle-size distribution function
y_0	cumulative percent
y_{50}	cumulative percent of particles of inflection point
y_D	cumulative pipe size distribution curve (%)
$y_{Meas,i}$	measured values of particles, eq. 3-1
y_{ni}	calculated value of particles, eq 3-1
$y_G(x)$	cumulative particle size distribution function, Haverkamp et al. (1999).

Greek letters

α	parameter (van Genuchten 1978)
α_{COEF}	empirical fitting parameter
$\Phi(D)$	pore size distribution index
η	exponent of Karvonen's (1988) reduction factor
λ	fitting parameter (van Genuchten 1980)
λ_{opt}	optimised value of λ
μ	dynamic viscosity of water
θ	volumetric water content
θ_r	residual water content
θ_s	saturated water content
θ_0	water content at the inflection point
θ_I	estimated value of water content
$\theta_{Meas,i}$	measured value of water content
$\theta(b)$	water retention
$\theta_{2.0} - \theta_{4.2}$	plant available water
Θ	relative water content
ρ	pore interaction factor
ρ_d	bulk density
ψ_c	air entry value

LIST OF TABLES AND APPENDICES

- Table 1. Humus sample parameters of Andersson's ($h_{t,0}$, b_1 , θ_0 and p_1 , Eq. (3-2) and van Genuchten's (θ_s , θ_r , α and n , Eq. 3-28) functions of two *Vaccinium* and one *Oxalis-Myrtillus* forest sites.
- Table 2 Coefficient of determination, R^2 , average errors at different pressure heads, E_{ave} , standard deviation of errors, S_{dev} , minimum, E_{min} , and maximum, E_{max} , values of errors at different pressure heads for semi-physical, Jonasson's and van Genuchten's methods of WRC determination. Saturated water content θ_s and residual water content θ_r were estimated. S_E is the square sum of errors, θ_{ave} is the average value of all the measurements.
- Table 3 Coefficient of determination, R^2 , average errors at different pressure heads, E_{ave} , standard deviation of errors, S_{dev} , minimum, E_{min} , and maximum, E_{max} , values of errors at different pressure heads for semi-physical, Jonasson's and van Genuchten's methods of WRC determination. Saturated water content θ_s and residual water content θ_r were given as input values. S_E is the square sum of errors, θ_{ave} is the average value of all the measurements.
- Table 4. Particle size distributions and bulk densities ρ_b (kg dm^{-3}) of the Swedish arable soil samples.
- Table 5. Measured and calculated cumulative water balance components (mm) of the lower part of the Sjöckulla agricultural hillslope. Total precipitation during the period between 15.05 - 31.10.1998 was 608 mm and potential evapotranspiration was 420 mm. ΔW is the change (mm) in total water content of the profile. Macropore model included in calculations.
- Table 6. Measured and calculated cumulative water balance components (mm) of the lower part of the Sjöckulla agricultural hillslope. Total precipitation during 15.05 - 31.10.1998 was 608 mm and potential evapotranspiration was 420 mm. ΔW is the change (mm) in total water content of the profile. Macropore model was not included in calculations.
- Table 7. Calculated cumulative water balance components (mm) of the upper part of the Sjöckulla agricultural hillslope. Total precipitation during 15.05 - 31.10.1998 was 608 mm and potential evapotranspiration was 420 mm. ΔW is the change (mm) in total water content of the profile. Macropore model was included in calculations.
- Table 8. Calculated cumulative water balance components (mm) of the upper part of the Sjöckulla agricultural hillslope. Total precipitation during 15.05 - 31.10.1998 was 608 mm and potential evapotranspiration was 420 mm. ΔW is the change (mm) in total water content of the profile. Macropore model was NOT included in calculations.

- Appendix 1. Particle size distributions of the mineral soil samples and bulk densities ρ_b (kg dm^{-3}) and loss of ignition (%) (108 samples from four forest types and from four different layers).
- Appendix 2. Measured soil water retention curves as a function of pressure head h (cm) (108 samples from four forest types and from four different layers).
- Appendix 3 (I-II). Average WRCs of four forest types from four different layers as a function of pressure head h (cm). *Std* is standard deviation ($\text{m}^3 \text{m}^{-3}$), *max* and *min* are maximum and minimum volumetric water content, respectively (data based on 360 samples).
- Appendix 4. Parameters of Andersson's function ($h_{t,0}$, b_1 , θ_0 and p_1 , Equation 3-2) for 108 soils.
- Appendix 5. Horizon, texture bulk density (ρ_b , g cm^{-3}) and organic matter content (*OM*, %) of the selected UNSODA samples.
- Appendix 6 (I-VIII). Summary of the fitted parameters (α and n estimated, θ_s and θ_r given) of van Genuchten WRC equation to soil data (360 samples).
- Appendix 7/I. Swedish arable soil data. R^2 is the coefficient of determination, E_{ave} is the average error at different pressure heads, S_{dev} is the standard deviation of errors, E_{min} is the minimum value and E_{max} is the maximum value of errors at different pressure heads using semi-physical, Jonasson's and van Genuchten's methods of WRC determination. Saturated water content (θ_s) and residual water content (θ_r) were estimated. S_E is the square sum of errors and θ_{ave} is the average value of all the measurements.
- Appendix 7/II. Swedish arable soil data. R^2 is the coefficient of determination, E_{ave} is the average error at different pressure heads, S_{dev} is the standard deviation of errors, E_{min} is the minimum value and E_{max} is the maximum value of errors at different pressure heads using semi-physical, Jonasson's and van Genuchten's methods of WRC determination. Saturated water content (θ_s) and residual water content (θ_r) were estimated. S_E is the square sum of errors and θ_{ave} is the average value of all the measurements.
- Appendix 8/I. Results of the prediction of the saturated hydraulic conductivity for the UNSODA samples using modified form of Andersson's method and van Genuchten method. K_s is the measured saturated hydraulic conductivity (cm d^{-1}), h_B is the bubbling pressure (cm) determined using the Mualem's method (1976a), K_s , h_B is the estimated saturated hydraulic conductivity using Andersson's method (see Eq. (3-11)), $h_{B,opt}$ is the optimum bubbling pressure that gives accurate prediction of K_s in Andersson's method, $K_{s,vG}$ is the estimated saturated hydraulic conductivity using Eq. (3-36) and $c_{sat,opt}$ is the optimum value for parameter c_{sat} ($108 \text{ cm}^3 \text{ s}^{-1}$) that gives accurate prediction of K_s (see Eq. (3-36)).
- Appendix 8/II. Results of the prediction of the hydraulic conductivity function for the UNSODA samples using modified form of

Andersson's method and van Genuchten method. E_{ave} is the absolute value of the average logarithmic error: $|\log(K_{i,m}) - \log(K_{i,c})|$, where $K_{i,m}$ is the measured value, $K_{i,c}$ is the calculated value, and M is the number of measurements in soil sample. Average error is given for three different pressure head ranges representing wet ($-100 < h < 0$ cm), medium ($-500 < h < -100$ cm) and dry ($h < -500$ cm) conditions. $E_{ave}/h_{B,opt}$ is the average error when optimum value for bubbling pressure given in App. 8/I was used. E_{ave}/λ_{opt} is the average error in van Genuchten's method when the exponent λ in Eq. (3-29) was optimized (standard value for $\lambda = 0.5$ was used otherwise).

LIST OF FIGURES

- Figure 1. The location of the forested hillslope at Rudbäcken, Siuntio.
- Figure 2. The location of drainage pipes, groundwater observation tubes and weirs for measuring the runoff components of the agricultural hillslope at Sjökkulla, Kirkkonummi (Paasonen-Kivekäs 1999). Soil surface elevation shown in cm above an unknown reference level.
- Figure 3. Schematic curve of Andersson's particle size distribution function.
- Figure 4. Shape similarity of the particle size distribution curve (a, Eq. 3-1) and the water retention curve (b, Eq. 3-2). If the PSDC (a) is turned 90° counter-clockwise, it has the same shape as the WRC (b). x_{min} and x_{max} are the minimum and maximum particle diameters, respectively
- Figure 5. The basic principle of the calculation of the deep subsurface flux and the division of the hillslope to upper, middle and lower parts.
- Figure 6. Average WRCs of *Calluna*, *Vaccinium*, *Myrtillus* and *Oxalis-Myrtillus* forest site types; a = subsoil, b = bottom half of illuvial layer, c = top half of illuvial layer and d = eluvial layer.
- Figure 7. Selected soil water retention curves of mineral soil samples taken from the *Calluna* site type, (solid line = stand 1, dotted line = stand 30), a = C-horizon, b = bottom half of B-horizon, c = top half of B-horizon and d = A-horizon.
- Figure 8. Selected soil water retention curves of mineral soil samples taken from the *Vaccinium* site type, (solid line = stand 22, dotted line = stand 29), a = C-horizon, b = bottom half of B-horizon, c = top half of B-horizon and d = A-horizon.
- Figure 9. Selected soil water retention curves of mineral soil samples taken from the *Myrtillus* site type, (solid line = stand 13, dotted line = stand 15), a = C-horizon, b = bottom half of B-horizon, c = top half of B-horizon and d = A-horizon.
- Figure 10. Selected soil water retention curves of mineral soil samples taken from the *Oxalis-Myrtillus* site type, (solid line = stand 14, dotted line = stand 28), a = C-horizon, b = bottom half of B-horizon, c = top half of B-horizon and d = A-horizon.
- Figure 11. Example of water retention characteristics of the *Calluna* forest site a = the subsoil, b = bottom half of the illuvial horizon, c = top half of the illuvial horizon and d = the eluvial horizon fittings of Andersson's and van Genuchten's functions.
- Figure 12. Example of water retention characteristics of the *Vaccinium* forest site a = the subsoil, b = bottom half of the illuvial horizon, c = top half of the illuvial horizon and d = the eluvial horizon fittings of Andersson's and van Genuchten's functions.
- Figure 13. Example of water retention characteristics of the *Myrtillus* forest site a = the subsoil, b = bottom half of the illuvial horizon, c = top half of the illuvial horizon and d = the eluvial horizon fittings of Andersson's and van Genuchten's functions.

- Figure 14. Example of water retention characteristics of the *Oxalis-Myrtillus* forest site a = the subsoil, b = bottom half of the illuvial horizon, c = top half of the illuvial horizon and d = the eluvial horizon fittings of Andersson's and van Genuchten's functions.
- Figure 15. Selected soil water retention curves of humus samples taken from two *Vaccinium* (solid line) and the *Oxalis-Myrtillus* (dotted line) sites.
- Figure 16. Water retention characteristics of the *Vaccinium1* site, the humus layer, a = pit 1, b = pit 2 and c = pit 3, fittings of Andersson's and van Genuchten's functions.
- Figure 17. Water retention characteristics of the *Vaccinium2* site, the humus layer, a = pit 1, b = pit 2 and c = pit 3, fittings of Andersson's and van Genuchten's functions.
- Figure 18. Water retention characteristics of the *Oxalis-Myrtillus* site, the humus layer, a = pit 1, b = pit 2 and c = pit 3, fittings of Andersson's and van Genuchten's functions.
- Figure 19. Average WRC of 108 samples. Jonasson's, van Genuchten's and semi-physical (θ_s and θ_r estimated) methods.
- Figure 20. Average WRC of 108 samples. Jonasson's, van Genuchten's and semi-physical (θ_s and θ_r given as input data) methods.
- Figure 21. Predictions of the WRC from the PSDC, a = subsoil, b = bottom half of the illuvial horizon, c = top half of the illuvial horizon and d = eluvial horizon, the *Vaccinium* forest site type.
- Figure 22. Predictions of the WRC from the PSDC, a = subsoil, b = bottom half of the illuvial horizon, c = top half of the illuvial horizon and d = eluvial horizon, the *Oxalis-Myrtillus* forest site type.
- Figure 23. Semi-physical, Jonasson's and van Genuchten's predictions of the WRC from the PSDC, Swedish agricultural topsoils, a1 = clay content < 2.0 % (θ_r and θ_s given), a2 = (θ_r and θ_s estimated) b1 = clay content 6-10 % (θ_r and θ_s given), b2 = (θ_r and θ_s estimated) and c1 = clay content 26-30 % (θ_r and θ_s given) and c2 = (θ_r and θ_s estimated).
- Figure 24. Semi-physical, Jonasson's and van Genuchten's predictions of the WRC from the PSDC, Swedish agricultural subsoils, a1 = clay content < 2.0 % (θ_r and θ_s given), a2 = (θ_r and θ_s estimated), b1 = clay content 6-10 % (θ_r and θ_s given), b2 = (θ_r and θ_s estimated) c1 = clay content 31-35 % (θ_r and θ_s given), c2 = (θ_r and θ_s estimated) and d1 = clay content 51- 55 % (θ_r and θ_s given) and d2 = (θ_r and θ_s estimated).
- Figure 25. Predictions of hydraulic conductivity function of van Genuchten's and Andersson's equations, a = Hoffmeister Schlag (3360) silt loam soil, b = Lille (4001) sand soil, c = Helecine I (4030) silt loam soil and d = Helecine II (4031) silt loam soil.
- Figure 26. Predictions of hydraulic conductivity function of van Genuchten's and Andersson's equations, a = Retie (4040) sand soil b = Lubbeek II (4043) silt loam soil, c = Beerse (4061) podzol sand soil and d = Endingen I (4080) silt loam soil.
- Figure 27. Variation of the relative sensitivity as a function of the percentage of change in parameter value for the four parameters

(b_1 , $h_{t,0}$, θ_0 and p_1) of Andersson's model (Equation 3-2) for one horizon.

- Figure 28. Measured water retention characteristics and curve estimated from the PSDC, curves for the humus layer using Andersson's and van Genuchten's functions and estimated relative hydraulic conductivity, $K_r(\theta)$, of forested hillslope in Mämmilampi.
- Figure 29. Measured water retention characteristics and curve estimated from the PSDC for the lower part of the forested hillslope in Siuntio. Fitted curves using the Andersson's and van Genuchten's functions are also shown.
- Figure 30. Measured water retention characteristics and curve estimated from the PSDC. Fitted curves using the Andersson's and van Genuchten's functions are also shown (middle part of the forested hillslope in Siuntio).
- Figure 31. Measured water retention characteristics and curve estimated from the PSDC. Fitted curves using the Andersson's and van Genuchten's functions are also shown (upper part of the forested hillslope in Siuntio).
- Figure 32. Estimated unsaturated hydraulic conductivity curves for the lower part of the forested hillslope in Siuntio using $K(h)$ estimated from the PSDC, Andersson's and van Genuchten's functions.
- Figure 33. Estimated unsaturated hydraulic conductivity curves for the middle part of the forested hillslope in Siuntio using $K(h)$ estimated from the PSDC, Andersson's and van Genuchten's functions.
- Figure 34. Estimated unsaturated hydraulic conductivity curves for the upper part of the forested hillslope in Siuntio using $K(h)$ estimated from the PSDC, Andersson's and van Genuchten's functions.
- Figure 35. Measured and calculated pressure heads at three different depths in the lower part of the forested hillslope in Siuntio. Hydraulic properties estimated from a) the PSDC (WRC estimated from the PSDC) b) using Andersson's functions (WRC fitted to data) c) using van Genuchten's functions (WRC fitted to data).
- Figure 36. Measured and calculated pressure heads at three different depths in the middle part of the forested hillslope in Siuntio. Hydraulic properties estimated a) from the PSDC b) using Andersson's functions (WRC fitted to data) c) using van Genuchten's functions (WRC fitted to data).
- Figure 37. Measured and calculated pressure heads at three different depths in the upper part of the forested hillslope in Siuntio. Hydraulic properties estimated a) from the PSDC. b) using Andersson's functions (WRC fitted to data) c) using van Genuchten's functions (WRC fitted to data).
- Figure 38. Measured water retention characteristics and curve estimated from the PSDC. Fitted curves using the Andersson's and van Genuchten's functions are also shown (forested profile in Hyytiälä).
- Figure 39. Estimated unsaturated hydraulic conductivity curves for the soil profile in Hyytiälä using $K(h)$ estimated from the the PSDC, Andersson's and van Genuchten's functions.

- Figure 40. Four separately measured tensiometers and calculated pressure heads (negative soil matric potential) in Hyytiälä at three different depths using hydraulic properties estimated from the PSDC (option 1). Upper curve immediately below the humus layer, middle curve 0.2 m and lower curve 0.4 m below the humus layer.
- Figure 41. Four separately measured tensiometers and calculated pressure heads in Hyytiälä at three different depths: hydraulic properties estimated using Andersson's method (option 2), a) eluvial layer, b) 0.2 m below the humus layer and c) 0.4 m below the humus layer.
- Figure 42. Four separately measured tensiometers and calculated pressure heads (negative soil matric potential) in Hyytiälä at three different depths: hydraulic properties estimated using van Genuchten's method (option 3), a) eluvial layer, b) 0.2 m below the humus layer and c) 0.4 m below the humus layer.
- Figure 43. Four separately measured tensiometers and calculated pressure heads in Hyytiälä: hydraulic properties estimated using van Genuchten's method (option 3 with very large saturated K_s -value), a) eluvial layer, b) 0.2 m below the humus layer, and c) 0.4 m below the humus layer.
- Figure 44. Measured particle size distribution curves at four different depths in the Sjäokulla experimental field.
- Figure 45. Measured water retention characteristics and estimated WRC's fitted to experimental data, a) depth 5-10 cm, b) 35-40 cm and c) 65-70 cm.
- Figure 46. Estimated relative unsaturated hydraulic conductivity curves: 1) estimate from particle size distribution curve, 2) using the modified Andersson's method 3) van Genuchten-type function at Sjäokulla, a) depth 5-10 cm, b) 35-40 cm and c) 65-70cm.
- Figure 47. Measured and computed depth to water table using three different options of modelling unsaturated hydraulic conductivity (Sjäokulla, lower part of the agricultural hillslope, macropores included in the model).
- Figure 48. Measured and computed cumulative drainage flux using three different options of modelling unsaturated hydraulic conductivity (Sjäokulla, lower part of the agricultural hillslope, macropores included in the model).
- Figure 49. Measured and computed cumulative surface runoff using three different options of modelling unsaturated hydraulic conductivity (Sjäokulla, lower part of the agricultural hillslope, macropores included in the model).
- Figure 50. Measured and computed depth to water table using three different options of modelling unsaturated hydraulic conductivity (Sjäokulla, lower part of the agricultural hillslope, macropores not included in the model).
- Figure 51. Measured and computed cumulative surface runoff using three different options of modelling unsaturated hydraulic conductivity (Sjäokulla, lower part of the agricultural hillslope, macropores not included in the model).

- Figure 52. Measured and computed cumulative drainage flux using three different options of modelling unsaturated hydraulic conductivity (Sjökulla, lower part of the agricultural hillslope, macropores not included in the model).
- Figure 53. Measured and computed depth to water table using three different options of modelling unsaturated hydraulic conductivity (Sjökulla, upper part of the agricultural hillslope, macropores included in the model).
- Figure 54. Measured and computed depth to water table using three different options of modelling unsaturated hydraulic conductivity (Sjökulla, lower part of the agricultural hillslope, macropores not included in the model).

1 INTRODUCTION

1.1 General overview

Plants need water for their growth and they take their water from the soil, which typically is a porous medium. The storage of water in the soil is therefore of crucial importance to plants. In Finland precipitation is relatively evenly distributed during the year. However in late autumn and winter there is little evapotranspiration loss and the water storage of the soil becomes full. In summer, evapotranspiration is greater than rainfall and the soil water storage decreases. Especially during this time of the year the soil water flow processes are dominated by the unsaturated hydraulic conductivity properties of the soil. The most important factors in this respect are the soil water retention characteristics (WRC) and the hydraulic conductivity function.

Knowledge concerning the water balance of forest soils is important not only to forest growth per se, but also because it is linked to the nutrient supply of the soil. The soil water balance of forested areas determines the runoff from whole watershed areas. Hydraulic properties of the soil are used in water balance calculations and in various model simulations of forest growth and climate change impact studies and questions related to unsaturated flow in soils require determination of the hydraulic properties, or their derivatives.

After the glacial age the uncovered soil was seeded with grasses, deciduous and coniferous trees. When the plants grew it started the formation of organic matter on soil because of debris from plants and fauna. Humus layer of the soil developed. Rain water passing through the eluvial layer transported iron and aluminium compounds into the illuvial layer. This soil forming process of acid soils is called podzolisation, which can last thousands of years. Parent material under the eluvial and illuvial layer is called subsoil.

Subsoil of podzol represents the parent material in the process of profile development. The horizons above subsoil have been evolved after the glacial age. Subsoil is a priori the most representative horizon to show the difference of WRC between various forest site types. This soil layer has less organic matter than the podzolic horizons above it. The chemical changes are more rapid and abundant in the horizons above the subsoil. Subsoil has its basic effects on plant growth, because there are roots situated also in subsoil. Hillel (1971) divides the rooting system to an upper layer and a lower layer. The importance of these subsoil

roots is fundamental during the dry growing periods. At such times trees take the water from the subsoil. If the subsoil has a good ability to retain water there is plant water available during dry periods. This kind of soil also represents the good forest site type.

When this research was started there were few studies on the hydraulic properties of Finnish forest soils (e.g. Päivänen 1973, Heiskanen 1988 and Mannerkoski and Möttönen 1990). The soil profiles in forests of cold regions have their own features, e.g. they have humus layer and profiles that are seasonally frozen and covered with snow, and therefore the results from studies made in other countries may not be directly usable in Finland. In the late 1980s an investigation by the department of Forest Ecology of the Helsinki University was started. Thirty sites belonging to four forest site types were established. The forest site type was an important classifying factor of this study. As part of this study soil samples were taken for determination of WRCs. However, for such curves to be utilized in mathematical water balance models they have to be parameterized.

Quantification of the hydraulic properties of porous media is a concern shared by soil scientists, hydrologists, agricultural engineers, and petroleum engineers. As our ability to numerically simulate complicated flow and transport systems increases, the accuracy of future simulations may well depend on the accuracy with which we can estimate model parameters. Hydraulic conductivity is difficult to measure and indirect estimation methods based on several more easily measured physical soil properties, e.g. soil bulk density, organic matter content, particle size distribution function and water retention characteristics have to be developed.

1.2 Soil physical properties

The soil hydraulic properties that are needed in soil water balance calculations (e.g. Richards 1931) are the water retention characteristics, $\theta(h)$, which describes the relationship between the volumetric water content of the soil θ and the water pressure head h and the hydraulic conductivity functions, $K(\theta)$ or $K(h)$, which define the relationships between volumetric water content and hydraulic conductivity or pressure head and hydraulic conductivity respectively. Many recent studies have shown that essential problems exist in the description of the water retention and hydraulic conductivity functions near saturation (e.g., Jarvis and Messing 1995, De Vos 1997, Zavarotto et al. 1999 and van Dam and Feddes 2000). Several direct methods have been developed for measuring K

as a function of h or θ . They are often based on solving the inverse problem, i.e. an analytical or numerical solution of the hydraulic model describing the flow process is optimized with respect to measurements of water content and pressure head (Russo et al. 1991). These methods are expensive and difficult to implement. Therefore attention has been paid to the development of indirect methods, which predict the hydraulic properties from more easily measured data, including water retention data and pore- or particle size distributions (e.g. van Genuchten et al. 1999). Indirect methods generally are more convenient, far less costly to implement and generally give hydraulic estimates accurate enough for most applications.

The flow of water in soil can be either microscopic or macroscopic (Mualem 1992). The microscopic flow in each continuous pore can be theoretically analysed using Navier-Stokes equations (Bear 1972). The macroscopic or phenomenological flow relates to the entire cross-section of the soil and operates at areal scales of cm^2 to m^2 . In order to emphasize the fact that water does not flow through the solid phase, the term flux density is used to describe the flow.

1.2.1 Indirect estimation methods of the WRC

The water retention characteristic curve can be determined directly in the laboratory, but it is tedious to accomplish, especially for fine-textured soils. The main emphasis in this work is to discuss the indirect estimation methods. Many attempts have been made at estimating the WRC from readily available data such as particle size distribution, organic matter content, dry bulk density and clay content. These relationships are referred to pedotransfer functions. Haverkamp et al. (1999) proposed three different approaches to predict soil water characteristics from particle size distribution data: i) discrete matric potential regression methods, ii) functional regression methods, and iii) semi-physical approaches.

1.2.1.1 Discrete matric potential regression methods

In discrete matric potential regression methods multiple linear regression functions are used to relate specific soil water pressure head values h (e.g. soil water pressure head at the inflection point of the WRC) to particle size distribution, porosity, organic matter content and bulk density. There are no presuppositions about the shape of the WRC's. Regression analysis that relates water contents at

specific soil water pressure heads to soil texture, bulk density and organic matter content have also been developed for estimating the water retention characteristics (e.g. Gupta and Larson 1979, Rawls and Brakensiek 1982 and Jonasson 1991). Vereecken et al. (1989) concluded that water retention characteristics can be estimated to a reasonable level of accuracy from such simple soil properties as particle size distribution, dry bulk density and carbon content. Williams et al. (1992) found that models which included even one known value of soil water content-matric potential relationship were much more valid than those based on soil texture and bulk density alone.

1.2.1.2 Functional regression methods

In the functional regression method the shape of the WRC is assumed and the relative water content, θ , as a function of soil water pressure head, h , is expressed (Haverkamp et al. 1999). The parameters of the models are derived through fitting (Clapp and Hornberger 1978, Bloemen 1980, Wösten and van Genuchten 1988 and Vereecken et al. 1989). This gives a continuous functional description of the water retention curve and thus this one tensiometer installed at each of the following depths: 5, 25, 50 and 75 cm. method is more effective in the water flow calculations than the discrete method.

The most often used functions are the Brooks and Corey function (1964), Campbell's function (1974), Mualem's function (1976a) and van Genuchten's function (1980). In the Brooks and Corey model the parameter ψ_c is the air entry value and is assumed to be related to the maximum size of pores forming a continuous network of flow paths within the soil. One weakness of the Brooks and Corey equation is the discontinuity in the derivative at air entry value. This drawback has been removed in the van Genuchten's function, which is nowadays the most often used function in soil water balance models. Cosby et al. (1984) found that textural soil properties can explain most of the variation in the parameters of the Brooks and Corey function. In some approaches knowledge about part of the soil moisture characteristic curve is required (e.g. Rogowski 1971 and Rawls et al. 1982). However, approaches using the Brooks and Corey model fail to provide a realistic shape of the moisture characteristic curve in the wet range. Tani (1982) and Russo (1988) have proposed equations resembling the Brooks and Corey model but which are continuous and therefore more easily applied e.g. in solving the Richard's equation.

Tyler and Wheatcraft (1989) have considered van Genuchten's (1980) m parameter as a fourth fitting parameter. This model has an inflection point, which allows better performance than the Brooks and Corey model for many soils, especially for when near saturation. Nimmo (1991) and Ross et al. (1991) found that van Genuchten model is successful at high and medium water contents but often gives poor results at low water contents.

Fuentes et al. (1992) concluded that van Genuchten's water retention function, $h(\theta)$, based on the Burdine (1953) theory ($m = 1 - 2/n$) together with the Brooks and Corey conductivity equation is valid for different types of soils without becoming inconsistent with the general water transfer theory. This is due to the rather limiting constraint that exists for parameter m when using the Mualem theory, i.e. $0.15 \leq m \leq 1$. Even though the residual water content, θ_r , has a well-defined physical meaning, this parameter behaves as a pure fitting parameter without any physical meaning. In order to better describe the WRC of multi-modal soils, Zhang and van Genuchten (1994) proposed two models of the WRC. The four fitting parameter model corresponds to a sigmoidal type WRC, while the five fitting parameters model leads to a bimodal type WRC.

Kosugi (1996) proposed a WRC model of three-parameter lognormal distribution laws applied to the pore radius distribution function and to the pore capillary head distribution function. In Kosugi's (1994) study, the water capacity function was regarded as the pore capillary pressure distribution function $f(h)$, which is related to the pore radius distribution function $f(r)$ by the capillary pressure function. Using Kosugi's water retention model, acceptable matches with observed water retention curves and adequate predictions of hydraulic conductivities in five out of six cases were obtained (Kosugi 1996). The estimated parameters of the model indicated that the water retention characteristics of Japanese undisturbed forest soils are related to the soil structure more closely than to the soil texture.

Assouline et al. (1998) introduced a conceptual model based on the assumption that soil structure evolves from a uniform fragmentation process to define the water retention function. The fragmentation process determines the particle size distribution of the soil. The model exhibits increased flexibility and improves the fit at both high and at low water contents range. According to Wu et al. (1990) aggregation had significant effect on pore-size distribution and water retention. Rajkai et al. (1996) showed in their study of Swedish soil water retention, particle size fraction, dry bulk density and organic matter content data that a significant correlation was found between the WRC and the particle size

distribution curve (PSDC) model parameters using linear regression.

1.2.1.3 Semi-physical methods

The shape similarity of the PSDC and the WRC is the presupposition for the two semi-physical models found in the literature (e.g. Arya and Paris 1981 and Haverkamp and Parlange 1986). Using the Arya and Paris model, the cumulative PSDC is divided into a number of fractions, giving a pore volume and a volumetric water content to each fraction and then counting a representative mean pore radius (R_p) and a corresponding water pressure head (h) value (Haverkamp et al. 1999). Arya and Paris derived a formulation showing the relationship between pore and particle radii for an assemblage of uniformly-sized spherical particles in a cubic packing. This relationship was extended to natural soil materials by means of an empirical parameter.

A similar model was later proposed by Haverkamp and Parlange (1986). They proposed a method that allows the direct estimation of the parameters of the Arya and Paris model (1981) for sandy soils without organic matter. The predicted $h(\theta)$ curve was then associated to the boundary wetting curve (BWC). Coupled with the hysteresis model proposed by Parlange (1976), a group of wetting curves can be predicted. This method has the advantage of interpreting the cumulative particle size distribution function in its continuous form. It uses the simple linear relationship between R_p and D_p (Haverkamp and Parlange 1986), which is valid for pure sand soils but certainly too crude for most field soils. Other extensions, modifications, and applications of relationships between the PSDC and the WRC are given by Wu and Vomocil (1992) and Gupta and Ewing (1992).

Haverkamp et al. (1999) proposed an improved physically based approach for estimating the water retention curve parameters from textural soil properties. The method relies upon the concept of shape similarity and uses the method of geometrical scaling. The approach involves three steps: the first concerns the link between the main wetting branch of the water retention curve and the cumulative pore-size distribution; the second step defines the relation between cumulative pore size and particle size distribution functions; and the third entails the problem imposed by hysteresis. The authors distinguish between hydraulic pore radius and matric pore radius and take into account the effect of tortuosity.

Jauhiainen (2000) introduced a new method to predict the water retention curve from particle size distribution curve,

organic matter content and bulk density. Development of the method started from Andersson's (1990a, b) original theory of particle size distribution and water retention characteristics. The shape similarity of the curves was utilized by developing equations that predict the parameters of the WRC from the parameters of the PSDC. The method was tested against data collected from three different measurement sites and two forest site types, *Vaccinium* site type and *Oxalis-Myrtillus* site type. The results showed good agreement between the measured and predicted values.

1.2.2 Fractal models

It has long been recognized that the behaviour of water in soils depends on pore space geometry. Quantification of this geometry by means of fractal concepts offers an opportunity to relate water properties to soil structural properties (Perrier et al. 1996) and fractal geometry has recently been used to describe both soil structure and soil hydraulic properties (Giménez et al. 1997). Structural properties seem to follow power law functions. The exponent of these functions can be interpreted in terms of fractal dimension, which may be related to soil structural characteristics (Perrier et al. 1996).

Pachepsky et al. (1995a) have shown deviation from the power law and explains this being due to the multifractal structure of soil porosity, which results in dependence of the fractal dimension on the radii. The WRC model of Pachepsky et al. (1995b) assumes fractal self-similarity of pore volumes by adding a correcting factor accounting for the dependence on the radii. The chosen factor, $f(r)$, is a log-normal probability distribution function of the pore radii.

The fractal model of Rieu and Sposito (1991a) contains seven predictive equations and they tested it experimentally with data on aggregate characteristics and soil water properties for structured soils. For the single set of aggregate/soil water properties data available, good agreement was found with the fractal model for water potential and scaling relationship and the moisture characteristic and hydraulic conductivity-water content relationships (Rieu and Sposito 1991b). Rieu and Sposito (1991a, b) have shown that power functions for the aggregate size distribution and the WRC directly stems from a fractal model of aggregate and pore space properties for structural soils.

The empirical constant (α) used in the Arya and Paris (1981) model was shown to be equivalent to the fractal dimension of a tortuous fractal pore (Tyler and Wheatcraft 1989). Ten soils for which water retention and particle size data were available were analysed to obtain both the fractal

dimension and subsequently the water retention data using the Arya and Paris model. The soil textures ranged from sand to silty clay loam. The results indicated that water retention characteristics data could be estimated with reasonable accuracy for soils in which the particle size data shows power law scaling with a fractal dimension of > 3.0 . Such soils are those with a wide range of particle sizes.

Perrier et al. (1996) concluded that although fractal objects provide idealized and simplified models of real porous media, they do give valuable insight into the geometrical coherence that must underlie any attempt to relate fractal dimensions corresponding to different physical definitions with those describing water retention curves. Perfect et al. (1996) derived a three parameter fractal model for $h(\theta)$. The equation was fitted to 36 $h(\theta)$'s for a silt loam soil with wide range of structural conditions. The equation was able to fit $h(\theta)$ for a variety of porous media, including sandstone, glass beads, sands, sieved soil and undisturbed soils ranging from very fine sandy loam to heavy clay.

1.2.3 Spatial variability

Several methods have been proposed to quantify the spatial variability of soil water retention (Kutilek and Nielsen 1983). Two major approaches have been used for describing spatial variability in watersheds (Mulla 1988). In the first approach detailed field measurements of soil properties are linked to the spatial models, which are based on the concepts of scaling, kriging or cokriging. The second approach is a stochastic and is based on probability densities and autocorrelation structure.

Greminger et al. (1985), Yeh (1986) and Burden and Selim (1989) measured field moisture retention and compared the spatial variance structure of water retention to that of other soil properties such as bulk density and particle size distribution. Burden and Selim (1989) found a significant cross correlation between water content at 0,03 MPa and bulk density for a silt loam soil.

Shouse et al. (1995) used the Burden and Selim (1989) data to investigate the ability of the van Genuchten (1980) model to describe a large number of measured soil water retention curves taken from a spatially variable field soil. The soil water retention model was found to be extremely flexible in fitting the measured data. Water content scale factors seemed to be normally distributed, which differ from similar media scale factors that have been found to be lognormal. One scale factor showed a structured variance, indicating a spatial correlation distance of greater than 30 m.

Forest soils contain abundant macropores, especially in surface layers as a result of faunal activity and high root density (Bonell 1993). Buttle and House (1997) concluded that bulk hydraulic conductivity, K_h , is the most important character to be measured for input to distributed hydrological models for determining the spatial scale of soil profiles. The influence of macropores on K_h for hillslope soils did not exhibit a systematic spatial pattern.

Nordén (1989) concluded that the vertical distribution of soil water retention capacity was similar in the different profiles at two Swedish forest sites. The coefficient of variation of soil water retention capacity was often larger within a profile than between profiles at a given soil depth and soil water tensions. The significantly higher soil water retention capacity in the spodic B-horizon, i.e. the illuvial horizon, Nordén (1989) attributed to the accumulated organic-sesquioxide material in this horizon.

1.2.4 Soil organic matter

Podzolic forest soils typically have humus layer above the mineral soil and considerable amount of organic matter incorporated into the mineral soil. The amount of organic matter is influenced by precipitation and temperature through (i) decomposition rates, (ii) biomass growth and litter production and (iii) transport from the humus layer to the mineral soil (Gärdenäs 1998). Highly decomposed organic matter in the mineral soil efficiently retains water. The WRC of peat (e.g. Weiss et al. 1998) resembles the curve of clay soil sample; in the wet range of the curve, the water content becomes only slowly smaller with decreasing matric potential. Westman (1983) proposed that the WRC of humus layer has a distinct correlation between density characteristics and the amount of organic matter. The WRC of soils rich in organic matter are difficult to determine accurately because of swelling and cracking of the material.

Torres et al. (1998) found that low density sandy loam is so highly permeable that saturated hydraulic conductivity could not be determined with the Guelph permeameter (Reynolds and Elrick 1985), because they could not maintain a constant head of water. The peat media shrank an average of 0-16 % during desorption (Heiskanen 1993). Coarse mineral soils usually retain less water than slightly decomposed Sphagnum peat, the water retention capacity of clay being of similar magnitude to that of moderately decomposed peat (Päivänen 1973). Weiss et al. (1998) noticed that their semiempirical model with only one shape parameter can be suitable for statistical investigations of peat samples. Forest humus layers retained less water at < -

10 cm than the conventionally graded peat growth media did (Heiskanen 1988). Hydraulic conductivity in the mor layer of Scots pine stand was measured using the constant-head permeater and instantaneous profile method (Laurén and Heiskanen 1997). The unsaturated hydraulic conductivity decreased from $3.1 \cdot 10^{-3}$ to $1.1 \cdot 10^{-8}$ m d⁻¹. Laurén and Mannerkoski (2001) found that the hydraulic conductivity and the water retention of the mor layers varied considerably within Finnish pine and spruce stands.

1.2.5 Use of neural networks to develop pedotransfer functions

Multilinear regression has been the main technique for deriving pedotransfer functions. Recent studies have shown that artificial neural networks can also be used to determine the relationship between routinely measured soil properties and soil water characteristics. Neural networks can be viewed as multivariate nonlinear regression tools (Tamari and Wösten 1999). Krenn (1999) found artificial neural networks provided better estimates of the water content of soils than two multiple regression models. Schaap et al. (1999) introduced a bootstrap neural network approach that also determines the reliability of pedotransfer function. An advantage of neural network approach is that they do not require any a priori model concept (e.g. linear, exponential). The optimal relationships between the input data and the output data are established in iterative calibration procedure. These capabilities make neural networks well-suited to implement pedotransfer functions and make them more accurate than existing techniques.

1.3. Estimation of the hydraulic conductivity function

1.3.1 Direct measurement of unsaturated hydraulic conductivity

Klute and Dirksen (1986) and Green et al. (1986) introduced direct laboratory methods and field methods for measuring the hydraulic conductivity of the unsaturated zone in soils. Steady-state methods are based on approximations of Darcy's equation. The transient methods of Bruce and Klute (1956) and the sorptivity method of Dirksen (1975) belong to the group of laboratory methods. Among the field-based methods are unit-gradient approaches (Nielsen et al. 1973) and sorptivity methods with ponding (Clothier and White 1981). One of the most popular methods is the instantaneous profile method of Rose et al. (1965) and

Watson (1966). Al-Soufi (1983) determined the unsaturated hydraulic conductivities of Finnish agricultural soils of various texture. Mecke and Ilvesniemi (1999) used the instantaneous profile method to determine the hydraulic conductivity of Finnish podzolic forest soils. Penttinen (2000) concluded that sites supporting Scots pine and Norway spruce differ as regards field saturated hydraulic conductivity reflecting differences in texture in the tills of Central Lapland in Finland.

1.3.2 Inverse methods for estimating soil hydraulic properties

A large number of laboratory and field methods have been developed for measuring K as a function of h or θ (van Genuchten and Leij 1992). They are based on solving the inverse problem, i.e. an analytical or numerical solution of the hydraulic model describing the flow process is optimized with respect to water content and pressure head measurements (Russo et al. 1991). The dependent variable can be expressed in terms of observable parameters.

A useful means of solving the inverse problem is by using parameter estimation methods. Simultaneous estimation of the retention and hydraulic conductivity functions from transient flow data can be done using these methods (Dane and Hruska 1983 and Russo et al. 1991). The solution of the inverse problem is called the indirect method by Neuman (1973). Kool et al. (1987) and Russo et al. (1991) consider the advantages of parameter estimation methods as: (i) there is no need to mathematically invert the governing equation, (ii) the method yields hydraulic properties over the full range of water contents, (iii) the method yields information about parameter uncertainty and model accuracy, and (iv) parameter estimation methods permit experimental conditions to be selected on the basis of convenience and expeditiousness, rather than by an overriding need to simplify the mathematics. The method is also useful in modelling infiltration (Russo et al. 1991), hysteretic water flow and for use with layered soils (Kool and Parker 1987).

While parameter estimation methods have several advantages, a number of problems related to computational efficiency, converge, and parameter uniqueness remain to be solved (Kool et al. 1987, Russo et al. 1991, van Dam et al. 1992), especially when many hydraulic parameters must be estimated simultaneously. Furthermore, substantial experimental effort may still be required to obtain sufficient data to warrant this type of estimation method.

1.3.3 Empirical models for predicting unsaturated hydraulic conductivity

Mathematical formulations can be used to represent hydraulic properties. The main advantages of empirical approaches are: (i) they allow a closed-form mathematical solution for some unsaturated flow problem, and thereby simplify its analysis. (ii) They simplify the computational requirements of a numerical solution, save computer time, and improve accuracy, (iii) they provide a systematic way for extrapolating the measured curve, (iv) they minimize the number of measurements required for statistical representations of hydraulic conductivity distribution of heterogeneous field soils, and (v) they permit the use of inverse methods for determining the hydraulic properties (Mualem 1992).

The most frequently used empirical functions for predicting hydraulic conductivity are given by Averjanov (1950), Gardner (1958) and Brooks and Corey (1964). The parameters of the empirical equations are usually obtained by fitting equations to the observed data.

1.3.4 Estimation of $K(\theta)$ from the PSDC and/or the WRC

One alternative to direct measurements of $K(\theta)$ is to use theoretical methods that predict unsaturated hydraulic conductivity from more easily measured particle size distribution data or laboratory water retention data. Theoretical methods are usually based on statistical pore-size distribution models, which assume water flow through cylindrical soil pores, and use the equations of Darcy and Hagen-Poiseuille. These models visualize the porous medium as a set of interconnected, randomly distributed pores. Pore-size distribution models give, a simplified picture of actual soils, especially of undisturbed, structured or macroporous field soils. A good review of these methods is given by Mualem (1992). His review indicates an abundance of methods for predicting the unsaturated hydraulic conductivity from measured water retention data. Of these, Raats (1992) identified three broad groups of models, i.e., those related to the theories by Childs and Collis-George (1950), Burdine (1953) and Mualem (1976a). Microscopic approaches include the models of Purcell (1949), Fatt and Dykstra (1951), Burdine (1953) and Mualem (1976a, b).

Measured input retention data for predictive models can be given either as point values or in terms of closed-form equations using parameters that are fitted to observed data. Inventories of analytical water retention functions are given by van Genuchten and Nielsen (1985) and Vereecken (1992).

Unfortunately, most available retention functions cannot be easily incorporated into pore-size distribution models to yield simple closed-form analytical expressions for hydraulic conductivity. Exceptions are the equations of Brooks and Corey (1964), Visser (1968), Campbell (1974) and van Genuchten (1980).

In microscopic models, an important parameter the pore-interaction factor, ρ , is used proposed for predicting $K(\theta)$ from soil water retention, $h(\theta)$. While Burdine (1953) interpreted ρ strictly as a function of soil tortuosity, Marshall (1958) and Millington and Quirk (1961) interpreted ρ as a property defined by the probability of occurrence of continuous pores. Mishra and Parker (1989) provided a methodology for quantifying the uncertainty in parameter estimates of soil hydraulic properties estimated from PSDC data. Schuh and Cline (1990) examined the variability of the pore-interaction factor, and ρ exhibited no trend relationship to any of the soil properties tested. The assumption of capillary flow may not be valid for water strongly influenced by soil electrical properties in the very dry range or for macropores where turbulent flow may occur (Schuh and Cline 1990). It has been generally concluded that $K(\theta)$ models fit best on coarse- and medium-textured soils without well-defined structure, i.e. in most Finnish forest soils.

Porous media models having uniform straight capillaries are too simple to describe the real structure of the soil in a proper way (Dullien 1979). Fatt and Dykstra (1951) and Burdine (1953) introduced tortuosity of the flow path to improve this. Childs and Collis-George (1950) simulated variations in the pore size by sectioning a porous column normal to the flow direction and randomly rejoining the opposite faces together.

1.4 Aims of the study

The broad objective of this study has been to develop indirect methods for quantification of the hydraulic properties of porous media. A new semi-physical method utilising the shape similarity of the particle size distribution curve and water retention characteristic curve has been developed in linking together these two curves. PSDC is easy and rapid to measure. Thus the indirect methods are very usable especially in the applications of models in large watershed areas due to the fact that WRC:s are laborious and expensive to determine in the laboratory. While there are many empirical relationships, the actual water retention curve is, in general, too complicated to allow a description with relatively simple mathematical function using a limited number of parameters. Often in water balance calculations it

can be useful to have average curves, which define soil physical properties.

Andersson (1990a, 1990b and 1990c) has determined both theoretical and empirical hydraulic characters of the Swedish agricultural soils. In this study Andersson's theories are further developed and the applicability of modified forms of Andersson's methods in Finnish forest soils have been tested in four forest site types.

The aims of this study are:

(i) To determine average water retention curves of four Finnish forest site types and from four different layers.

(ii) To determine selected soil water retention curves for various mineral soil layers of *Calluna* (CT), *Vaccinium* (VT), *Myrtillus* (MT) and *Oxalis-Myrtillus* (OMT) forest site types. The parameters of the models will also be presented.

(iii) To determine selected soil water retention curves for humus soil layers of *Vaccinium* and *Oxalis-Myrtillus* forest site types. The parameters of Andersson's model and van Genuchten's model (not humus) will also be presented.

(iv) To develop a new semi-physical method to predict WRC from PSDC. The method is an extension of the theories developed by Andersson. The method will be tested with the observations of 108 CT, VT, MT and OMT forest site types and 32 Swedish agricultural soils. The results obtained with the new method will also be compared to the estimated curves produced by a semi-physical method based on Mualem-van Genuchten-type equations. One aim is to develop regression equations to estimate saturated water content and residual water content from bulk density, particle size range and loss of ignition. These methods can be used in the semi-physical method in the case that saturated and residual water content values have not been measured.

(v) To develop a method which predicts hydraulic conductivity from water retention characteristics. This method will be tested with the observations of 20 (mostly Dutch) soils taken from UNSODA data base

(vi) To accomplish the sensitivity analysis of the WRC model parameters.

(vii) To evaluate the applicability of the semi-physical method developed in (iv) in performing water balance calculations of forested and agricultural hillslopes. The results obtained by the new method will be compared to computed values using two other methods to estimate soil water retention curve and unsaturated hydraulic conductivity function: 1) modified Andersson's functions and 2) van Genuchten-type equations.

2 MATERIAL

2.1 Finnish forest soils

The main objective of the study was to determine the water retention characteristics and particle size distribution curves of podzol soil layers for four Finnish forest site types. A total of 30 sites were studied. The sites were scattered over about 400 km² area surrounding the Hyytiälä Forestry Field Station of the University of Helsinki in central Finland (61°48' N, 24°19' E). The climate is relatively uniform throughout the area. The annual mean temperature is +2.9 °C and the annual precipitation averages 709 mm (Climatological statistics... 1991).

The soil samples were taken during the summer 1987 and 1988. The forest site types were *Calluna* type (CT), *Vaccinium* type (VT), *Myrtillus* type (MT) and *Oxalis-Myrtillus* type (OMT) according to the Finnish forest site type classification (Cajander 1926). A total of seven CT sites, seven VT sites, eleven MT sites and five OMT sites were selected for soil sampling. In each stand a 10 m * 30 m rectangular area was chosen and three soil pits dug at each. The podzol profile consisted of three mineral soil layers; the uppermost eluvial horizon (A), in the middle illuvial horizon (B) and lower, parent material (C) horizon. A single sample (150 cm³ cylinder, 5.8 cm diameter and 5.7 cm height) was taken from the eluvial and C-horizon and two samples from the illuvial layer. The two samples of the illuvial horizon were taken from the upper and middle of the horizon.

Altogether 360 mineral soil samples were collected. 360 WRCs were measured and PSDC was available from 108 samples. The depth of the subsoil sample was the thickness of eluvial and illuvial layers multiplied by 1.5. From each sample soil WRC was determined from desorption of the sample, the PSDC was determined and loss of ignition was measured. Measured particle size distribution curve, bulk density and loss of ignition are shown for 108 soil samples in App. 1 (seven CT sites, six VT sites, 11 MT sites and three OMT sites). Volumetric water content was computed on the basis of the total volume of the soil. For preparing the water retention characteristic curves water contents had been measured at pressure heads of 0.01, 0.10, 0.32, 0.63, 1.0, 10.0 and 152.0 m. The WRCs for 108 samples are listed in App. 2. In each of the 30 sample areas three 6.5 cm by 6.5 cm rectangular samples of the surface humus layer were taken for determination of WRC. The porosity calculated from the bulk density of the mineral soil samples of this

study was in good correspondence with the measured saturated water content (Sahlberg 1992). The WRCs of two sites for each four forest site types were selected randomly (Chapter 4.2).

PSDC was determined using the pipette method of Elonen (1971). The classification of the particle size fractions was according to the Finnish system: clay < 2 μm , fine silt 2-6 μm , coarse silt 6 – 20 μm , fine fine sand 20 – 60 μm , coarse fine sand 60 – 200 μm , medium sand 200 – 600 μm and coarse sand 600 – 2000 μm .

2.2 Swedish agricultural soils

Water retention characteristics of 32 Swedish agricultural soils (Andersson and Wiklert 1972) had been selected for comparing the modified Andersson's method (Jauhiainen 2000) and van Genuchten's method (1980). Thirteen of these WRCs were taken from the topsoil (0 – 20 cm depth) and nineteen subsoils (as a rule from 20 – 100 cm depth). The subdivision of these two main groups had been made according to the content of clay. The classifying limits for the topsoils were ≤ 2 , 3-5, 6-10, 11-15, 16-20, 21-25, 26-30, 31-35, 36-40, 41-45, 46-50, 51-55 and 56-60 percent clay. The classifying limits of the subsoils were ≤ 2 , 3-5, 6-10, 11-15, 16-20, 21-25, 26-30, 31-35, 36-40, 41-45, 46-50, 51-55, 56-60, 61-65, 66-70, 71-75, 75-80, 81-85 and 86-90 percent clay. The range of the clay content was from 1 % to 56 % in topsoil samples and from 0 % to 87 % in subsoil samples.

Bulk density and the organic matter content of the samples had been determined. The PSDC had been determined using the following particles size fractions: clay < 2 μm , fine silt 2-6 μm , coarse silt 6-20 μm , fine fine sand 20-60 μm , medium fine sand 60-200 μm , coarse fine sand 200-600 μm and coarse sand >600 μm . The measured water contents at pressure head values: 0.001, 0.05, 0.15, 0.2, 0.3, 0.5, 1.0, 2.0, 3.0, 5.0, 10.0, 50.0, 150.0 and 400.0 m had been used to determine the WRC.

2.3 Soils of UNSODA database

The UNSODA unsaturated soil hydraulic database contains approximately 800 data sets (Leij et al. 1999 and Nemes et al. 2001). The data sets allow model estimates of water retention and hydraulic conductivity derived from more easily measured data (e.g. particle size distribution, bulk density and organic matter content) to be compared to measured values and mathematical functions describing

hydraulic characteristics to be tested (Leij et al. 1999). In this study, 20 agricultural soil profiles from Central Europe were selected for testing the methods developed for predicting hydraulic conductivity function from soil water retention curve (results in the Chapter 4.6). Soil texture, bulk density, organic matter content and cumulative particle size distribution curves of the selected soil samples are shown in App. 5.

2.4 Rudbäcken hillslope

An experimental site in the catchment of the Rudbäcken river (60° 08'N, 24° 18'E) was established on an eastward facing slope (14°, length 90 m) passing from bedrock, glacial till to clay sediments downslope (Jauhiainen and Nissinen 1994) (Fig 1).

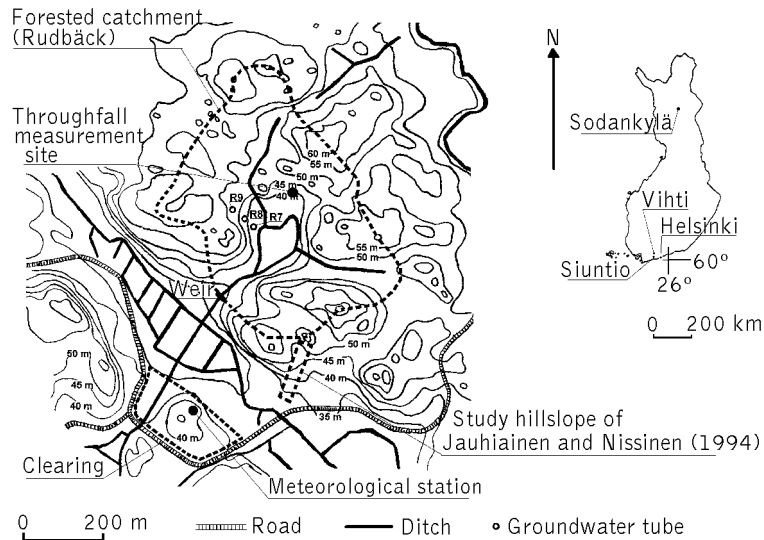


Figure 1. The location of the forested hillslope at Rudbäcken, Siuntio.

The tree stand on the slope is 90-years-old and has a standing volume of around 300 m³/ha. The main tree species is Norway spruce (*Picea abies*), but Scots pine (*Pinus sylvestris*), silver birch (*Betula pendula*), common alder (*Alnus glutinosa*) and European aspen (*Populus tremula*) are also present (Jauhiainen and Nissinen 1994).

Rectangular hillslope area (40 m * 80 m) had 35 tensiometer profiles in thirteen different rows. For the water balance calculations three rectangular areas (3 m * 40 m) upper, middle and lower part of the hillslope were established. In each smaller area five points were selected for

tensiometer installations. One tensiometer was installed at each of the following depths: 5, 25, 50 and 75 cm. These depths correspond to the eluvial horizon, the uppermost and middle illuvial horizon, and the C-horizon. In addition 18 rain gauges, 3 ground water wells and a snow collector were also installed (Jauhiainen and Nissinen 1994). Sampling for the soil texture and soil water retention measurements was made from three pits dug in each measurement area.

2.5 Mämmilampi experimental site

The Mämmilampi measurement site is situated near the Helsinki University Forestry Field Station in Hyytiälä in central Finland (61°51' N, 24°17' E, 150 m a.s.l.). The annual mean temperature of the area is +2.9 °C and the yearly precipitation averages 709 mm (Climatological statistics... 1991). The study site is located on a glaciofluvial sorted coarse sand deposit and the soil clearly podzolized.

The site was classified as *Vaccinium* type according to the Finnish classification of forest types (Cajander 1926). Scots pine (*Pinus sylvestris*) was the dominant tree species on the site. In order to investigate the small-scale variation of soil water balance a 2 m * 3 m area was defined. In each corner and middle of the sides a set of three tensiometers was installed. The 3 tensiometers in each set were installed at 0, 20 and 40 cm from the surface of mineral soil layer. Two thermo couples were installed in the corners of the area. The depths of thermo couples were 0 and 10 cm from the surface of mineral soil layer. Rain collectors were situated 150 m west from the experimental field.

In the Hyytiälä case study meteorological variables, precipitation, air temperature and radiation components, and soil matric potential values at three depths (0, 0.20 and 0.4 m below the humus layer) were measured every 10th minute, and data from the period between 17th of August and 27th of September in 1992 were available. Potential evapotranspiration was estimated using the Priestley-Taylor (1972) method. Interception losses were taken into account by assuming that the maximum interception storage is 0.002 m.

2.6 Sjököulla agricultural field

The experimental field was located in Kirkkonummi, in southern Finland (Paasonen-Kivekäs et al. 1999) (Fig 2). The topsoil was silty clay and subsoil silty to heavy clay. The soil cracked strongly during dry periods causing preferential flow

conditions. The field is typical for southern Finland, having clay contents of more than 30 percent.

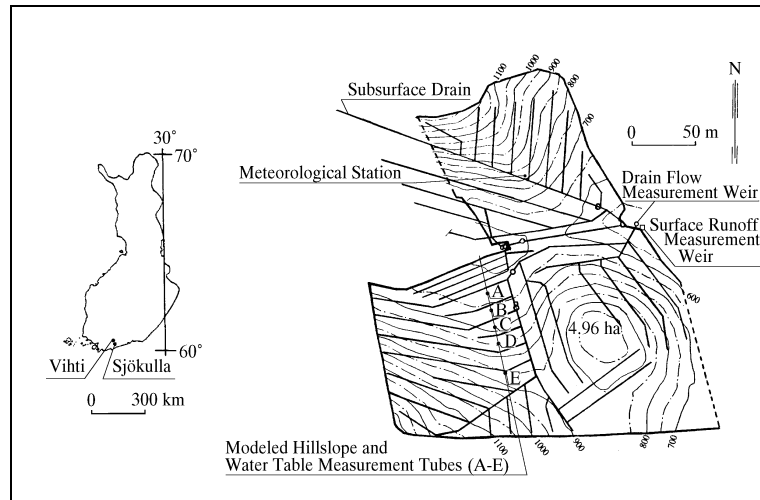


Figure 2. The location of drainage pipes, groundwater observation tubes and weirs for measuring the runoff components of the agricultural hillslope at Sjöckulla, Kirkkonummi (Paasonen-Kivekäs et al. 1999). Soil surface elevation shown in cm above an unknown reference level.

Typical of the arable land, the field is drained with subsurface tile drains. The drains, installed in 1938, are at depth of 1.3 m with spacing of 14 m. The field was cultivated with grain crops. The outflow and surface runoff from the field were measured with V-notch weirs (Fig 2). The water level at the weirs and was measured every 15 minutes using a pressure transducer or an ultrasonic sensor. The water level at the ground water tubes was measured automatically every 15 minutes, manual measurements were accomplished biweekly. Precipitation data from, the Vihti Meteorological station located 20 km to the north of the field were used.

3 ESTIMATION OF UNSATURATED HYDRAULIC FUNCTIONS FROM SOIL PHYSICAL PROPERTIES

3.1 Introduction

Andersson's (1990a, b) theory of the links between particle size distribution, water retention characteristics and unsaturated hydraulic conductivity are the basis of this study. The theory has been further developed in this work. Andersson's (1990a, b) publications were written only in Swedish and the theory is therefore briefly described here in English. A more detailed description of Andersson's theories has been given by Jauhiainen (2000). In this study one important goal is to develop a new semi-physical method to create a link between the measured particle size distribution curve (PSDC) and the soil water retention curve (WRC). New ideas to model the relationship between the WRC and the unsaturated hydraulic conductivity curve, $K(h)$, are also introduced. Mualem (1976a) and van Genuchten-type functions (1980) are used as the reference of the models developed here.

3.2 Andersson's models for describing the PSDC, WRC and relative hydraulic conductivity

3.2.1 Andersson's model for the particle size distribution function

Andersson (1990a) suggests that the log mass of the particles is arcus-tangent distributed (Cauchy distributed). Particle size distribution y can be represented using the curve:

$$y = y_0 + b \arctan \left[c \log \frac{x}{x_0} \right] \quad (3-1)$$

where x is particle diameter, and y_0 , b , c and x_0 are parameters. Parameter x_0 denotes the most frequent particle diameter corresponding to the cumulative percent y_0 . Consequently x_0 and y_0 correspond the coordinates of the inflection point and b and c determine the shape of the curve (see Fig. 3).

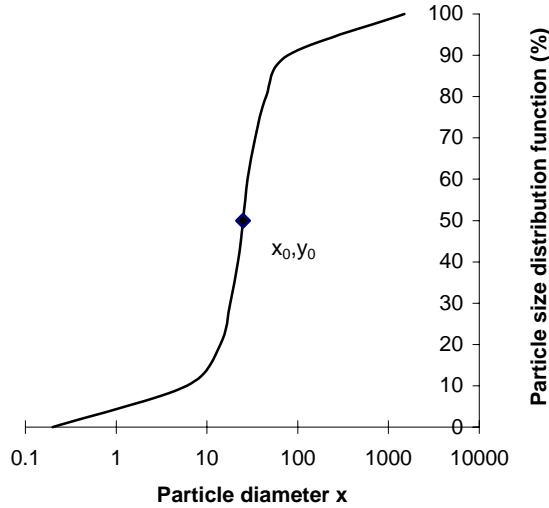


Figure 3. Schematic curve of Andersson's particle size distribution function.

The arctan-function provides values between $-\pi/2$ and $\pi/2$ and when the function approaches its maximum value $\pi/2$, y should be 100 %. This implies that $b = (100 - F_{\text{CLAY}}) / \pi$, where F_{CLAY} is the clay content of the sample (%). Parameter c defines how steep the particle size distribution curve is, i.e. c represents the derivative of the curve at the inflection point (x_0, y_0) .

3.2.2 Andersson's model for the water retention function

Andersson's (1990b) mathematical description of the water retention curve is:

$$\theta = \theta_0 - \frac{p_1}{\pi} \arctan \left[\frac{1}{b_1} \log \left(\frac{h}{h_{t,0}} \right) \right] \quad (3-2)$$

where θ is the volumetric water content, h is pressure head (cm), θ_0 is the volumetric water content of the inflection point and the corresponding soil matric potential is $h_{t,0}$ (cm). Parameter p_1 has the same kind of physical interpretation as parameter b of the particle size distribution curve: when arctan-function approaches its maximum value $\pi/2$, θ goes to saturated water content θ_s and $p_1 = 2(\theta_s - \theta_0)$ or $p_1 = \theta_s - \theta_t$ where θ_t is the residual water content. Parameter b_1 defines

the inverse of the slope of the WRC at the inflection point (θ_0 , $h_{t,0}$).

3.2.3 Andersson's work related to pedotransfer functions

As the measurement of WRC is a tedious and time-consuming process, it is useful to determine the WRC from the more easily measurable PSDC. Andersson (1990a, b) has given a mathematical description using arc-tangent functions for both the particle size distribution curve (Eq. 3-1) and the water retention curve (Eq. 3-2).

The basic idea of Andersson is to utilise the similarity of the particle size distribution curve and the water retention curve (see Fig. 4). Both are symmetric functions: the inflection point of the PSDC is (x_0 , y_{50}) and the corresponding inflection point in the WRC is (θ_0 , $h_{t,0}$). The key point is that using a pedotransfer function it is possible to derive the parameters of the WRC from the parameters of the PSDC. The pedotransfer function gives the relationship between pore (void) diameter x_v and particle diameter x . Andersson (1990b) uses the equation:

$$x_v = u(y)x \quad (3-3)$$

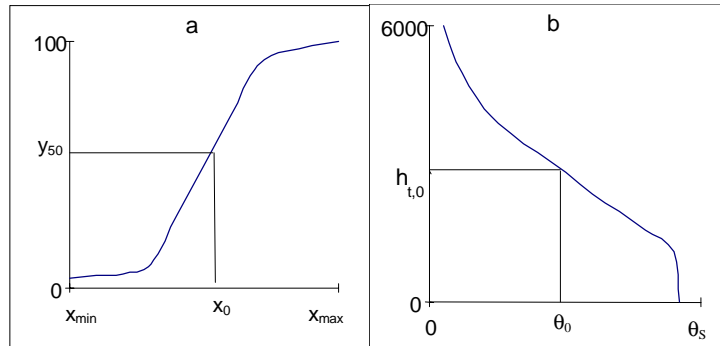


Figure 4. Shape similarity of the particle size distribution curve (a, Eq. 3-1) and the water retention curve (b, Eq. 3-2). If the PSDC (a) is turned 90° counter-clockwise, it has the same shape as the WRC (b). x_{min} and x_{max} are the minimum and maximum particle diameter, respectively.

where $u(y)$ is the pedotransfer function, which is assumed to be a function of the PSDC, i.e. y . Andersson (1990b) made calculations of the relation between x_v and x for two soil types, but he did not present any analytical function for the relationship. A new pedotransfer function has been developed in this study and details of the new method are given in Chapter 3.4.

Mualem (1992) introduced S-shaped WRC. In the present study there is introduced the V-shaped WRC which is typical for the humus samples. Both ends of the V-shaped curve approach closer the x and y coordinates asymptotically, x coordinate is reached in saturation point. In the present study, the V-type curve is also used if the curve is getting closer asymptotically the y coordinate although it does not behave same way at the other end of the curve.

3.2.4 Relative hydraulic conductivity function of Andersson

Andersson's (1969, 1990b) theoretical model for calculating the relative hydraulic conductivity is based on the assumption that the soil-water retention curve is known and the phenomena of hysteresis is not taken into account. The pore volume of soil is considered to be constituted of small pipes with differing diameter. The same type of idealization has been earlier suggested by Burdine (1953, ref. Bear 1972). The cumulative pipe-size distribution curve, y_D (%), is defined by Andersson (1990c) as:

$$y_D = y_{D_0} + \frac{100p_2}{n_p\pi} \arctan\left(\frac{1}{b_2} \log \frac{D}{D_0}\right) \quad (3-4)$$

where D is the pipe diameter, y_{D_0} , D_0 , p_2 and b_2 are parameters and n_p is porosity. Eq. (3-4) closely resembles Eq. (3-1) and parameters have the same type of physical interpretation. In Andersson's original formulation parameter p_2 is introduced, but since arctan-function provides values between $-\pi/2$ and $\pi/2$, it can be seen that p_2 equals n . Therefore p_2 could also be left out from the equation.

The Laplace surface-tension equation is used to define the relationship between the soil water tension h and the corresponding pipe diameter D (e.g. Burdine 1953 and Andersson 1969), i.e:

$$h = 0.3/D \quad (3-5)$$

If tension has a value then pipes with a diameter greater than D are empty and pipes with a diameter smaller than D are filled with water. The derivative of y_D with respect to D is the pore-size distribution index $\Phi(D)$:

$$\Phi(D) = \frac{100p_2 \log(e)}{n\pi b_2} \frac{1}{\left[1 + \left(\frac{1}{b_2} \log \frac{D}{D_0}\right)^2\right] D} \quad (3-6)$$

Consider a class of pipes, d_p , where the lower limit of the pipe diameter is $D - dD/2$ and the upper limit is $D + dD/2$. The percentage of pipes from the total pipe-size distribution in this class is $dy_D = \Phi(D)dD$. In a soil column with bottom area A and height L_h the total volume of pipes is $nAL_h/100$ and the total number of pipes in this class is:

$$dN = \frac{nAL_h}{100^2} \frac{\Phi(D)dD}{(\pi L_h D^2 / 4)} \quad (3-7)$$

where $\pi L_h D^2 / 4$ is the volume of a single pipe with diameter D and length L_h . According to the Hagen-Poiseuille law, the flow through a pipe with diameter D is $\frac{d_w \pi g I D^4}{128 \mu}$, where d_w is the density of water, g is the acceleration due to gravity, μ is the dynamic viscosity of water and I is the gradient causing the flow. All pipes belonging to pipe class $(D - dD/2, D + dD/2)$ can conduct an amount of water, dq , in a time unit:

$$dq = \frac{nA d_w g I}{32 * 100^2 \mu} D^2 \Phi(D) dD \quad (3-8)$$

The total flow through a completely saturated soil can be calculated as follows:

$$q = \int_{D_{min}}^{D_{max}} dq = \frac{nA d_w g I}{32 * 100^2 \mu} \int_{D_{min}}^{D_{max}} D^2 \Phi(D) dD \quad (3-9)$$

where D_{min} and D_{max} are the smallest and the largest pipe diameter taken into consideration, respectively. According to Darcy's law:

$$q = K_s A I \quad (3-10)$$

where K_s is the hydraulic conductivity at saturation. By equating Eqs. (3-9) and (3-10) a formula for calculating the saturated hydraulic conductivity is obtained:

$$K_s = C_c \int_{D_{min}}^{D_{max}} D^2 \Phi(D) dD \quad (3-11)$$

where

$$C_c = \frac{nd_w g}{32 * 100^2 \mu} \quad (3-12)$$

The relative hydraulic conductivity $K_r(h)$ and unsaturated hydraulic conductivity $K(h)$ can be estimated from equations:

$$K_R(h) = \frac{\int_{D_{min}}^D D^2 \Phi(D) dD}{\int_{D_{min}}^{D_{max}} D^2 \Phi(D) dD} \quad (3-13)$$

$$K(h) = K_R(h) K_s \quad (3-14)$$

Eq. (3-13) is a function of h since h and D can be related to each other using Eq. (3-5). It is not possible to solve analytically Eq. (3-13) and in this study a numerical solution to Eq. (3-13) is developed and it is described in Chapter 3.3.3.

3.3 Modifications and extensions to Andersson's models

3.3.1 Particle size distribution function

In Andersson's original formulation the parameters of the PSDC are estimated using either two or four selected points from the measured PSDC. Therefore, not all the measured points are used. In this study, the parameters x_0 , y_0 , b and c are estimated by minimizing the square sum of errors between the measured and estimated curve, i.e. the objective function to be minimized is:

$$F(x_0, y_0, b, c) = \sum_{i=1}^M (y_{n,i} - y_{Meas,i})^2 \quad (3-15)$$

where M is the number of measured points of the PSDC, $y_{Meas,i}$ is measured and $y_{n,i}$ is the corresponding estimated value calculated using Eq. (3-1). The minimization of Eq. (3-15) is accomplished using the SOLVER-option of EXCEL.

3.3.2 Water retention function

In Andersson's original formulation the parameters of the water retention function are estimated using either three or four selected points from the measured curve. Therefore, all the measured points are not utilised. The water retention curve shown in Eq. (3-2) can be written in the form, where parameter p_1 is replaced by $\theta_s - \theta_r$:

$$\theta = \theta_0 - \frac{\theta_s - \theta_r}{\pi} \arctan \left[\frac{1}{b_1} \log \left(\frac{h}{h_{t,0}} \right) \right] \quad (3-16)$$

A new formulation of Andersson's method allows the estimation of the parameters θ_0 , $h_{t,0}$, and b_1 simultaneously by minimizing the square sum of errors between the measured and estimated curve, i.e. the objective function to be minimized is:

$$F(h_{t,0}, \theta_0, b_1) = \sum_{i=1}^{M_1} (\theta_i - \theta_{Meas,i})^2 \quad (3-17)$$

where M_1 is the number of measured points of the water retention curve, $\theta_{Meas,i}$ is the measured and θ_i is the corresponding estimated value calculated using Eq. (3-16). The minimization of Eq. (3-17) is accomplished using the SOLVER-option of EXCEL. In this formulation saturated water content θ_s and residual water θ_r are not included in the optimisation procedure. If measured values of θ_s and θ_r are available, they should be used. However, this is not always the case and therefore new regression equations for estimating θ_s and θ_r from bulk density, particle size curve and loss of ignition have been developed the results are given in Section 4.5.1.

3.3.3 Relative hydraulic conductivity

Andersson's original hydraulic conductivity function (Eq. 3-13) does not take into account the effect of the tortuosity. The influence of tortuosity was inserted into the function by using the reduction factor Θ^η where $\Theta = (\theta - \theta_r)/(\theta_s - \theta_r)$ is relative saturation rate. The exponent η has been determined with the procedure suggested by Karvonen (1988) and value $\eta = 2$ was proposed. The equation for calculating the relative hydraulic conductivity function is given by:

$$K_R(h) = \Theta^\eta \frac{\int_{D_{\min}}^D D^2 \Phi(D) dD}{\int_{D_{\min}}^{D_{\max}} D^2 \Phi(D) dD} \quad (3-18)$$

The practical solution of Eq. (3-18) is carried out using numerical integration with the trapezoidal method starting from $h = 16\,000$ cm and ending at $h = h_B$ (cm), where h_B is the so called bubbling pressure which was determined using the method proposed by Mualem (1976a). The corresponding D , dD , D_{\min} and D_{\max} -values can be calculated from Eq. (3-5): $D = 0.3/h$, $dD = 0.3/dh$, and $D_{\min} = 0.3/16000$ (cm) and $D_{\max} = 0.3/h_B$. Interval $\log(16000) - \log(0.1)$ is divided to 50 steps in the numerical integration. The concept of bubbling pressure has to be included in the solution since numerical integration cannot be continued to h -value 0 cm; zero h would lead to infinite pipe diameter. The pore-size distribution index $\Phi(D)$ needed in solving Eq. (3-18) is calculated from Eq. (3-6).

3.4 Development of a semi-physical approach to predict WRC from PSDC

The shape similarity of the PSDC and the WRC is the presupposition for the semi-physical model developed here starting from Andersson's PSDC-function shown in Eq. (3-1). The same type of arctan-function can be used to relate θ with h . The aim is to predict the parameters θ_0 , p_1 , b_1 and $h_{i,0}$ of the WRC shown in Eq. (3-2)

$$\theta = \theta_0 - \frac{p_1}{\pi} \arctan \left[\frac{1}{b_1} \log \left(\frac{h}{h_{i,0}} \right) \right] \quad (3-2)$$

using the parameters y_0 , b , c and x_0 of the PSDC given in Eq. (3-1)

$$y = y_0 + b \arctan \left[c \log \frac{x}{x_0} \right] \quad (3-1)$$

It is possible to use the relationship between particle size x and pore size x_v using the transfer function given in Eq. (3-3), i.e. $x = x_v/u(y)$. Furthermore, by assuming that pipe diameter D in Eq. (3-5) can be replaced by pore size diameter x_v , it is possible to express particle diameter x as follows:

$$x = \frac{0.3}{u(y)h} \quad (3-19)$$

By substituting Eq. (3-19) to the PSDC given in Eq. (3-1) it can be written in the form

$$y = y_0 + b \arctan \left[c \log \frac{0.3}{x_0 u(y)h} \right] = y_0 - b \arctan \left[c \log \frac{h}{h_{t,0}} \right] \quad (3-20)$$

where parameter $h_{t,0}$ can be obtained from Eq. (3-21):

$$h_{t,0} = \frac{0.3}{u(y)x_0} \quad (3-21)$$

By comparing the arguments of the arctan-function in Eqs. (3-2) and (3-20) it can be seen that they are the same when

$$b_1 = \frac{1}{c} \quad (3-22)$$

The maximum and minimum values of arctan-function are $\pi/2$ and $-\pi/2$ respectively. Maximum value of y is 100 (%) and the minimum value of y is F_{CLAY} , the clay content of the sample (%). The corresponding maximum and minimum values of Eq. (3-2) are θ_s and θ_r , respectively. Parameter p_1 of the WRC function can then be obtained directly from parameter b of the PSDC function by appropriate scaling

$$p_1 = \frac{\pi b (\theta_s - \theta_r)}{100 - F_{CLAY}} \quad (3-23)$$

Parameter θ_o is the inflection point of the WRC and it can be determined from the simple relation

$$\theta_o = \theta_r + (\theta_s - \theta_r)/2 \quad (3-24)$$

Parameters of the water retention curve, $h_{t,0}$, b_1 , p_1 and θ_o can now be calculated from parameters of the PSDC, y_0 , b , c and x_0 using Eqs. (3-21) – (3-24) if the transfer function $u(y)$ is known. θ_s and θ_r can be taken from the measured values or from values estimated using the regression equations given in Chapter 4. 5.

In the original formulation of Andersson the pedotransfer function, $u(y)$, is assumed to be a function of the PSDC, i.e. y . Here this approach is simplified in such a way that $u(y)$ is

replaced by pedotransfer function C_p , which is based on multiple regression using the following variables: particle diameter at the inflection point x_0 (unit is mm), bulk density ρ_b , (kg dm^{-3}) and the difference between the saturated and residual water content $\theta_s - \theta_r$ (multiplied by 100 in Eq. 3-25):

$$\frac{1}{C_p} = P_1 + P_2 x_0 + 100 P_3 (\theta_s - \theta_r) + P_4 \rho_b \quad (3-25)$$

where $P_1 \dots P_4$ are the parameters of the multiple regression equation. In total 108 forest soils were used to estimate the parameters and the results are shown in Chapter 4.5.

Parameter $h_{t,0}$ can be computed by substituting C_p to Eq. (3-21):

$$h_{t,0} = \frac{0.3}{C_p x_0} \quad (3-26)$$

Jonasson (1991) suggested two non-linear regression equations that can be used to estimate $h_{t,0}$ directly from two characteristic values of the particle size distribution curve, d_{25} and d_{75} :

$$\alpha_p = \exp[\alpha_{COEF} \log(d_{75}/d_{25})] \quad (3-27a)$$

$$h_{t,0} = 100 d_{COEF} \frac{1}{e^{1/2}} \frac{1}{x_0^{(3\alpha_p - 1)/2}} \quad (3-27b)$$

where e is the void ratio and α_{COEF} and d_{COEF} are empirical fitting parameters. Jonasson (1991) suggested the following values for the parameters: $\alpha_{COEF} = 0.312$ and $d_{COEF} = 0.061$. In this study data was used to estimate the two parameters based on the same 108 soils that were used to determine the C_p -function. The following results were obtained: $\alpha_{COEF} = 0.311$ and $d_{COEF} = 0.069$, which are very close to the values suggested by Jonasson.

The results obtained with the semi-physical method are shown in Chapter 4.5. And two different methods to estimate $h_{t,0}$ are used: 1) the multiple regression equation (Eq. 3-25) and 2) the Jonasson's method, (Eqs. 3-27a,b) using the modified parameter values.

3.5 Mualem- and van Genuchten-type models

3.5.1 Water retention curve

Based on Burdine's (1953) and Mualem's (1976a) equations van Genuchten (1980) presented a flexible analytical equation that relates the pressure head h to volumetric water content θ .

$$\theta = \theta_r + \frac{\theta_s - \theta_r}{(1 + |\alpha h|^n)^m} \quad (3-28)$$

The parameters α and n are inversely related to the air-entry tension and width of the pore size distribution (van Genuchten 1978). For α , the lowest value reported is around 0.1 m^{-1} for a heavy clay soil while for n the upper limit is about 10 for materials with extremely narrow pore size distributions. High values of α and n generally correspond to sandy soils while fine-textured soils have lower values. Parameter m in Eq. (3-28) can be written as a function of parameters k_m and n : $m = 1 - k_m/n$ ($0 < m < 1$). In the Burdine theory parameter $k_m = 2$ and in the Mualem theory $k_m = 1$. In this study the Mualem theory is used. van Genuchten function is used in this study as a reference method to the functions described in Chapter 3.3.2. Moreover, the parameters of the Eq. (3-28) are determined for all the 360 measured water retention curves and the results are given in App. 6.

3.5.2 van Genuchten type hydraulic conductivity function

The particular form of Eq. (3-28) makes it possible to derive analytical expressions for the relative hydraulic conductivity, $K_r(h)$ when substituted in the predictive conductivity models of Burdine (1953) and Mualem (1976a).

The relative hydraulic conductivity is expressed in terms of water content (van Genuchten 1980):

$$K_r(\Theta) = \Theta^\lambda \left[1 - (1 - \Theta^{1/m})^m \right]^2 \quad (3-29)$$

where the relative saturation Θ can be calculated either as a function of volumetric water content θ or pressure head h . Parameter λ is usually 0.5, but it is also possible to take it as a parameter to be optimized.

$$\Theta = \frac{\theta - \theta_r}{\theta_s - \theta_r} = (1 + |\alpha h|^n)^{-m} \quad (3-30)$$

The parameters α and n are calculated using the SOLVER option of Excel in the same way than Eqs. (3-15) and (3-17). The relative hydraulic conductivity can also be expressed directly as a function of pressure head h as follows:

$$K_R(h) = \frac{(1 - (\alpha h)^{n-1} (1 + (\alpha h)^n)^{-m})^2}{(1 + (\alpha h)^n)^{m/2}} \quad (3-31)$$

$K_R(h)$ is obtained from Eq. (3-18). θ_r and θ_s can be obtained from laboratory measurements or estimated using the regression methods shown in Chapter 4.5.

3.5.3 Development of a semi-physical approach to predict WRC from PSDC using the van Genuchten-type functions

A new semi-physical method for estimation of WRC from PSDC was described in Chapter 3.4 starting from the theories of Andersson. The same type of approach can also be developed based on Burdine-Mualem-van Genuchten theories. The cumulative particle size distribution function, $y_G(x)$, is written in the form given by Haverkamp et al. (1999):

$$y_G(x) = \left[1 + \left(\frac{D_g}{x} \right)^N \right]^{-M_s} \quad \text{with } M = 1 - \frac{k_m}{k_M} \quad (3-32)$$

where x is the particle size, D_g is the particle size scale parameter and M_s and N are the shape parameters of the particle size distribution curve linked to each other in a similar way as the shape parameters used for the water retention function. The value of k_M is not obligatory equal to k_m (see Chapter 3.5.1) and the ratio k_m/k_M is a function of tortuosity and porosity. However, in this study it was assumed that $k_M = k_m$ and hence $M_s = 1 - 1/N$. Cumulative particle size data are easily accessible, and the values of D_g , M_s and N can be optimized using the SOLVER-option of Excel. The water retention curve parameter m is then calculated from M_s (Haverkamp et al. 1999):

$$m = \frac{M_s}{1 + p_\beta} \quad (3-33)$$

where p_β is a tortuosity factor and value 0.5 is used here. Parameter n can then be solved from

$$n = 1/(1 - m) \quad (3-34)$$

Parameter D_g of Eq. 3-32 has the same type of interpretation than parameter x_0 in Eq. (3-1). The second parameter of the van Genuchten-type curve, α , has unit m^{-1} and its inverse can be denoted as $h_g = 1/\alpha$ and h_g can be interpreted in the same way than parameter $h_{t,0}$ in Eq. (3-2). Therefore, it is possible to use the pedotransfer function C_p developed in Chapter 3.4 (Eq. 3-26) to calculate h_g and α from D_g :

$$h_g = \frac{0.3}{C_p D_g} \quad (3-35a)$$

$$\alpha = \frac{1}{h_g} \quad (3-35b)$$

The method suggested in this Chapter allows estimation of the parameters of the van Genuchten function, α , n and m from the parameters of the PSDC, (D_g , N and M_s) using Eqs. (3-33) - (3-35). The results obtained with this new method are compared against the results given by the semi-physical method described in Chapter 3.4. The comparison is shown in Chapter 4.5.

In the case that saturated hydraulic conductivity is not available as a measured value, it is possible to estimate it using Eq. (3-36) (Mishra and Parker 1990):

$$K_s = c_{sat} \frac{(\theta_s - \theta_r)^{2.5}}{h_g^2} \quad (3-36)$$

where c_{sat} is a constant including the effects of fluid characteristics and the porous media geometric factor; a value suggested in the literature is $108 \text{ cm}^3 \text{ s}^{-1}$ when K_s is expressed in cm s^{-1} ; $h_g = 1/\alpha$, where α is the parameter of the Van Genuchten-model (1980).

3.6 Testing of the developed methods in water balance modeling

3.6.1 Introduction

As our ability to numerically simulate complicated flow and transport systems increases, the accuracy of future simulations may well depend on the accuracy with which we can estimate model parameters, i.e. soil water retention curve and unsaturated hydraulic conductivity function. The applicability of the new semi-physical method to estimate soil water retention curve from particle size distribution curve needs to be tested using a soil water balance calculation model. The aim is to estimate WRC from the PSDC and determine hydraulic conductivity function $K(h)$ from WRC using the methods presented in this study. In the results shown in Chapter 5 hydraulic conductivity function is plotted as a function of soil water content θ , i.e. as $K(\theta)$ -curve.

This curve is obtained by calculating K as a function of h from Eq. (3-31) and then taking the corresponding water content values from function of Eq. (3-28). These curves are then used as input data for the CROPWATN-model, which is used to calculate the soil water balance. The applicability of the new method is evaluated by comparing the calculated water balance components with the measured values from three different field experiments. Moreover, the calculated values obtained with the curves estimated with the semi-physical method will be compared to results obtained by using Andersson's functions and van Genuchten-type functions for describing $\theta(h)$ - and $K(h)$ -relationships. The results of the comparison of the water balance components are given in Chapter 5.

In forested areas the usefulness of the estimation procedures is checked by comparing calculated pressure heads at four different depths with measured values. For agricultural hillslope additional measurements available for comparison are depth to water table, drainage flow and surface runoff. The water balance comparisons are carried out using three different methods to estimate the soil hydraulic properties: 1) use the new semi-physical method described in Sections 3.4 and 3.5 to estimate $\theta(h)$ and $K(h)$ from the PSDC, 2) fit Andersson function to measured $\theta(h)$ -curve and estimate $K(h)$ using Andersson's method given in Eq. (3-13), 3) use van Genuchten's function (3-29) to estimate $K(h)$ from $\theta(h)$ -curve. In option 1) measured soil water retention curve is not utilised at all and in methods 2) and 3) the PSDC is not used.

The PSDC and soil water retention curves measured in the three experimental sites (Rudbäcken, Mämmilampi and

Sjökulla) were not used in the development of the estimation procedures described earlier in Chapter 3 and therefore, the results of these applications are used as independent validation data sets for the procedures. Moreover, in water balance calculations the unsaturated hydraulic conductivity curve plays an important role and $K_r(\theta)$ -curves from the three methods described above in 1)..3) are also shown in order to get a better idea on the influence of the $\theta(h)$ - and $K(h)$ -curves on water balance components of forested and agricultural hillslopes.

The water balance of forested and agricultural hillslopes was calculated using the CROPWATN-model (Karvonen 1988, Karvonen and Kleemola 1995 and Karvonen 2002), which solves numerically the Richards equation:

$$C(h) \frac{\partial h}{\partial t} = \frac{\partial}{\partial z} \left[K(h) \left(\frac{\partial h}{\partial z} - 1 \right) \right] - S(h) - S_q(h) \quad (3-37)$$

where h is soil water pressure head (m), $C(h) = d\theta/dh$ is the derivative of the soil water retention curve (m^{-1}), z is the vertical coordinate (m), $K(h) = K_s K_r(h)$ is the hydraulic conductivity curve ($m d^{-1}$), K_s is the saturated hydraulic conductivity ($m d^{-1}$) and $K_r(h)$ is the relative value of the unsaturated hydraulic conductivity (0..1) calculated using either Andersson's or van Genuchten's functions. $S(h)$ is the sink term that is used to take into account the effect of evapotranspiration and $S_q(h)$ is the term that accounts the influence of deep subsurface flow and drainage flow in agricultural areas.

CROPWATN is a quasi-2D-model that solves numerically the Richards equation in a vertical column (Karvonen 2002). Deep horizontal subsurface fluxes and flow to subsurface drains and open ditches can be taken into account as additional sink-terms in Eq. (3-37). Surface runoff can be obtained in the model if groundwater level rises to the soil surface (profile is completely saturated) or rainfall is greater than the infiltration capacity at the soil surface. The model calculates soil water content and pressure head profiles and depth to groundwater level is taken as the point where pressure head is equal to zero (boundary between saturated and unsaturated zones).

Deep subsurface flow refers to saturated horizontal flux. This flux takes into account the horizontal flow of water into and out of the profile and it can be calculated by using Darcy's law. The unit of the calculated flux in $mm d^{-1}$ indicating that it is treated as the amount of water removed from the profile in the lateral direction. In the numerical solution this flux is taken away from all the nodes that lie below the groundwater level. Parameters needed to calculate deep subsurface flow are the saturated horizontal hydraulic

conductivity, the distance of the profile from the nearest main ditch (L) and water level elevation in the main ditch (W_{ditch}). Moreover, the thickness of the water conducting layer has an influence on the horizontal flux. In the model the thickness of the layer is obtained by subtracting the elevation of the groundwater level (the model calculates it) from the elevation of the impermeable bottom of the profile. The basic principle of the calculation of the deep subsurface flux and the division of the hillslope to upper, middle and lower parts is shown in Fig. 5.

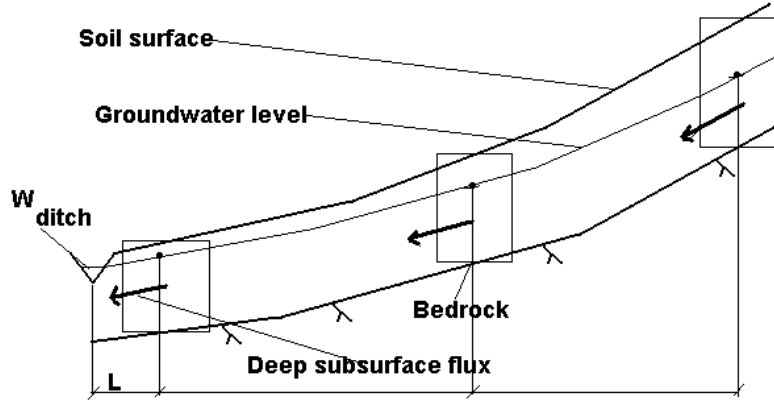


Figure 5. The basic principle of the calculation of the deep subsurface flux and the division of the hillslope to upper, middle and lower parts.

In agricultural applications the drainage flux is calculated using the Hooghoudt's equation. The Hooghoudt's equation for calculating flow towards subsurface drains or open ditches, q_D ($m\ d^{-1}$) is given in Eqs. (3-38) - (3-40) (Karvonen 1988):

$$q_D = \frac{8K_S D_e h_M + 4K_S h_M^2}{L^2} \quad (3-38)$$

$$D_e = \frac{D_d}{1 + \frac{D_d}{L} \left[\frac{8}{\pi} \ln \left(\frac{D_d}{r_e} \right) - a_e \right]} \quad (3-39)$$

$$a_e = 3.55 - \frac{1.6D_d}{L} + 2 \left(\frac{D_d}{L} \right)^2 \quad (3-40)$$

where K_S is the saturated hydraulic conductivity in horizontal direction ($m\ d^{-1}$), D_d is depth from drain level to

impermeable bottom of the profile (m), D_e is effective depth calculated from Eq. (3-39), h_M is the difference between water level midway between two drains and drain level (m). If h_M is negative, then water level is below the drain level and drainage flux is zero. L is the spacing between two drains (m) and r_e is the effective drain radius (m). In Finland subsurface drains are surrounded by a gravel envelope and r_e can be replaced by true drain radius. This is also the case in the Kirkkonummi experiment described in Section 3.6.3.

3.6.2 Modeling of water balance of forested hillslopes

The procedures developed in this study for estimating the water retention curve and the unsaturated hydraulic conductivity curve from the particle size distribution curve were tested using the measurements carried out at two forested experimental areas: Rudbäcken hillslope in Siuntio and Mämmilampi site in Hyytiälä. The three main goals were 1) to estimate the WRCs from the PSDCs and to compare them to the measured curves, 2) to calculate the pressure heads with CROPWATN-model at different depths using the estimated curves and compare calculated values to the measured values and 3) to calculate the pressure heads using water retention curves fitted to the measured WRCs.

In the Rudbäcken hillslope measurements of pressure head were available from the upper, middle and lower part of the hillslope and from the following depths: 0.05, 0.25, 0.50 and 0.75 m, respectively. CROPWATN-model was applied separately for the upper, middle and lower part of the hillslope. Horizontal fluxes along the hillslope had to be taken into account as additional sink terms in the model (deep subsurface flux). The parameters needed in this calculation are the horizontal hydraulic conductivity (calibrated value 0.2 m d^{-1} in all cases), distance from the centre point of the profile to the main ditch (10 m for the lower part, 30 m for the middle part and 50 m for the upper part of the hillslope) and distance of water level in the main ditch from the soil surface (1.9, 2.5 and 4.0 m for the lower, middle and upper part of the hillslope, respectively).

In the Rudbäcken hillslope the soil profile was taken to be 6.045 m thick. Initial depth to groundwater level was assumed to be 1.0 m in the lower part, 1.5 m in the middle part and 2.0 m in the upper part of the hillslope, respectively. The soil profile was divided into 20 layers. The thickness of the humus layer was assumed to be 0.05 m divided to two uniform layers, 0.02 and 0.03 m. Below the humus layer, the thickness of the nodes was 0.04, 0.04, 0.05, 0.055, 0.07, 0.08, 0.09, 0.09, 0.13, 0.15, 0.15, 0.25, 0.25, 0.4, 0.4, 0.6, and four nodes with thickness equal to

0.8 m. The measured PSDC and water retention curves were available from the mineral soil below the humus layer at the depths of 0-0.05 m, 0.1-0.2 m, 0.2-0.3 m; the fourth curve was assumed to represent the profile below 0.3 m. The curves were available for the lower, middle and upper part of the hillslope. The particle size distribution curves were available at depths of 0-0.1 m, 0.1-0.2 m, 0.2-0.3 m and 0.3 m below the humus layer. In the estimation procedure, the PSDCs were used to estimate the WRCs separately for the four depths. The soil water retention curve for the humus layer was taken from the Mämmilampi experimental site. The saturated vertical hydraulic conductivity was calibrated and the following values were used: 1.0 m d^{-1} in the humus layer, 0.6 m d^{-1} in the eluvial and illuvial layers and 0.2 m d^{-1} in the subsoil. The same K_s -values were used for the lower, middle and upper part of the hillslopes.

In the Hyytiälä site the soil profile was assumed to be 4.3 m thick with an initial depth to groundwater level known to be around 3-5 m and 4.0 m was selected. The soil profile was divided into 20 layers. The thickness of the humus layer was assumed to be 0.1 m divided to three uniform layers, 0.02, 0.04 and 0.04 m. Below the humus layer, 0.05 m thick nodes were used to a depth of 0.6 m, while below that the thickness of the layer increased gradually from 0.1 m to 0.6 m so that the total thickness of the profile was 4.3 m. The measured PSDC and water retention curves were available from the mineral soil below the humus layer at the depths of 0-0.1 m, 0.1-0.2 m, 0.2-0.3 m; the fourth curve was assumed to represent the profile below 0.3 m. The saturated vertical hydraulic conductivity was calibrated and the following values were used: 1.0 m d^{-1} in the humus layer, 0.24 m d^{-1} in the eluvial and illuvial layers and 0.10 m d^{-1} in the subsoil.

3.6.2 Modeling of water balance of an agricultural hillslope

The semi-physical method developed in this study for estimating the water retention curve and the unsaturated hydraulic conductivity curve from particle size distribution curve was also tested in agricultural hillslope using the measurements carried out at Sjökuilla experimental field in Kirkkonummi shown in Fig. 1. In this case the three main goals were 1) to estimate the WRCs from the PSDCs and to compare them to measured curves, 2) to calculate the water balance components using the estimated curves and compare the calculated drainage fluxes, surface runoff values and depth to the water table to measured values and 3) to calculate the water balance components using water retention curves fitted to the measured WRCs. In the

CROPWATN-model the influence of flow to subsurface drains was taken into account in the calculation of the water balance components. Additionally, the effect of the macropores was included in the testing of the estimated curves since the CROPWATN has an option to treat macropores separately from the micro-matrix.

In Kirkkonummi case the CROPWATN-model was calculated separately for the lower and upper part of the agricultural hillslope. Since the CROPWATN-model cannot treat the hillslope in truly 2-D domain, the difference between the upper and lower parts of the hillslope has to be taken into account via the deep subsurface flow component. Physically it represents a so called secondary drainage flow, i.e. flow from the profile towards the nearest main ditch. Deep subsurface flow has to be calculated as the net value, i.e. difference between incoming and outgoing fluxes. In the upper part of the hillslope the incoming flux is zero (the profile extends to the water divide there), but for the lower part of the hillslope the incoming flux is non-zero. The outgoing flux for the lower profile is calculated based on the difference between water level in the profile (calculated by the model) and the water level in the main ditch (given as input value to the model).

The depth to the water table was measured in several tubes and in this study calculated values were compared to the observations done both in the upper part (tubes 10 and 19) and in the lower part (tubes 7 and 23) of the hillslope. The measurements of drainage flux and surface runoff were also available as area-averaged values. Data from year 1998 was used in testing the methods.

In setting up the model for the upper and lower parts the soil water retention curves were the same and the two differences were as follows. For the first, in the upper part of the hillslope the macropores were assumed to extend to the depth of 2.0 m and in the lower part only to depth 1.1 m due to the fact that the lower part is usually much wetter and macropores were assumed to be in a shallower layer. For the second, in the calculation of the deep flux to the secondary drainage system the water level in the main ditch was different for the lower and upper part of the hillslope. In the lower part of the hillslope water level in the main ditch was 1.5 m below the soil surface and in the upper part of the hillslope the distance from soil surface to water level in the main ditch was 2.5 m.

The vertical profile was divided to 20 layers as follows: 0.01, 0.02, 0.04, 0.06, 0.08, 0.08 m, 4 * 0.1 m, 0.16 m, 7 * 0.2 m, and 2 * 0.3 m. The soil water retention curves were estimated for three different horizons: 0-0.3 m, 0.3-0.6 m and 0.6-2.85 m. The drain spacing used in the calculations was 16 m and depth of drains was 1.0 m. The maximum volume of the macropores, V_{MAX} was calibrated to be 2 % at

the soil surface and it decreased as a function of depth z (m) according to Eq. (3-41). Hydraulic conductivity of the macropores was calibrated and a value obtained for $K_{M,MAX}$ was 0.10 m h^{-1} (2.4 m d^{-1}) at the soil surface. The hydraulic conductivity of the macropores $K_M(z)$ decreases as a function of depth z according to Eq. (3-42) (see e.g. Karvonen et al. 2001).

$$V_M(z) = V_{MAX} e^{-f_z z} \quad (3-41)$$

$$K_M(z) = \left[\frac{V_M(z)}{V_{MAX}} \right]^2 K_{M,MAX} \quad (3-42)$$

where f_z is a parameter which defines how fast the macroporosity is decreased as a function of depth z (m). In this study a value 2.0 was used for f_z which implies that e.g. at depth 0.6 m $V_M(0.6) = 0.6 \%$ and $K_M(z) = 0.009 \text{ m h}^{-1}$ (0.216 m d^{-1}) Lateral hydraulic conductivity used to calculate the deep subsurface flux to the secondary drainage system was estimated to be 0.01 m h^{-1} (0.24 m d^{-1}). The soil water retention curves and unsaturated hydraulic conductivity curves were determined using the methods described earlier in this Chapter and the $\theta(h)$ and $K(h)$ -curves used in calculating the water balance will be discussed in Chapter 5.3.

4.1 Average water retention curves of podzol soil horizons of four Finnish forest site types

One aim of the study was to derive average soil water retention curves of podzolic soil horizons for four Finnish forest site types, *Calluna* (CT), *Vaccinium* (VT), *Myrtillus* (MT) and *Oxalis-Myrtillus* (OMT). The results shown in Fig. 6 are average curves for the four forest site types based on 360 samples. Average values, standard deviations, minimum and maximum values of soil water content θ at different pressure head values are shown in App. 3. Summary of the fitted parameters of van Genuchten WRC equation to the soil data is compiled in App. 6 (360 samples).

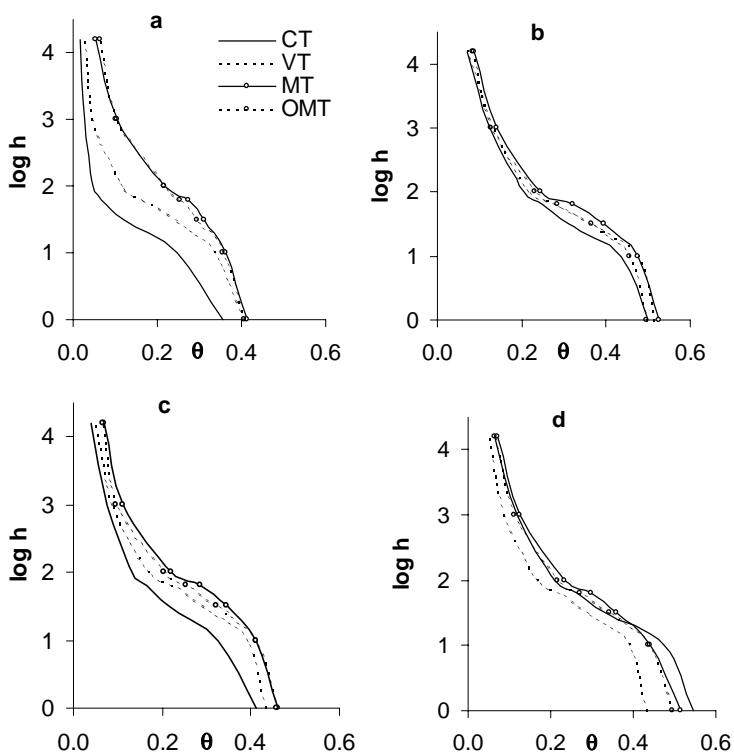


Figure 6. Average WRCs of *Calluna*, *Vaccinium*, *Myrtillus* and *Oxalis-Myrtillus* forest site types; a = subsoil, b = bottom half of illuvial layer, c = top half of illuvial layer and d = eluvial layer.

Subsoil of podzol represents the parent material in the process of profile development. The horizons above subsoil have been evolved after the glacial age. Subsoil of four

mineral soil horizons is a priori the most representative horizon to show the difference of WRC between various forest site types. This soil layer has less organic matter than the podzolic horizons above it. The chemical changes are more rapid and abundant in the horizons above the subsoil. Subsoil has its basic effects on plant growth, because there are roots situated also in subsoil. Hillel (1971) divides the rooting system to an upper layer and a lower layer. The importance of these subsoil roots is fundamental during the dry growing periods. At such times trees take the water from the subsoil. If the subsoil has good ability to retain water there is plant available water also in dry periods. This kind of soil also represents the good forest site type. The average WRCs of C-horizons soil from the four various site types can be utilized in the water balance calculations of regional scale.

The average WRC of C-horizon soil from the *Calluna* sites was V-type (Fig. 6a). The greatest variability in water content values was at the wet end of the curve (App. 3). The water contents at log pressure head values 1.0 and 1.5 varied more than water content at saturation. At the dry end of the curve, standard deviation was smallest in the CT type. This was one of three features clearly shown by the average WRC for the *Calluna* type C-horizons. The other two features were the V-shape and having the smallest water contents at saturation compared to the other forest site types. The amount of plant-available water was the smallest for the *Calluna* sites and would be insufficient for as large timber production as in more fertile site types during the dry growing periods. All four forest site types had their smallest deviation at the dry end of the WRC. At log pressure head value of 2.0, there is only a minor amount of water for plants in *Calluna* type.

The average WRC of C-horizon soil from the *Vaccinium* sites (Fig. 6a) was S-shaped (Mualem 1992). Variation in the moisture contents in the dry range of the curve was clearly larger than in the *Calluna* sites. The greatest variation in moisture contents occurred at a log pressure head values of 1.5 and 1.8. A typical feature of the WRC of the *Vaccinium* type was the large release of water between the two equilibrium log pressure head values of 1.0 and 2.0, which fall within the range important for plant growth.

The average WRC of C-horizon soil from the *Myrtillus* sites (Fig. 6a) was gentle S-shaped. Moisture contents of the C-horizon of the *Myrtillus* sites varied considerably at all log pressure head values (App. 3). The variation was the greatest in the range between log pressure head values 1.5 and 2.0. Two of the WRCs (App. 2) were V-shaped, indicating that the WRC of the C-horizon does not show the fertility of the forest site in these cases. The V-shape is clearly an indicator of soils with low water retention, namely those of *Calluna* site type and in some cases also *Vaccinium* site types.

The WRC for *Oxalis-Myrtillus* C-horizons resembled clearly the WRC of *Myrtillus* C-horizons (Fig. 6a). Three of the curves (App. 2) were V-shaped with a bimodal feature at a log pressure head value 1.8. The soils with V-shaped curves had greater water contents than *Calluna* site soils at the dry end of the curve. The slope of the curve in the dry range was not as steep as in *Calluna* site curves. It was shown in this study that there is a relationship between the WRC of subsoil and forest site type. This should especially be the case with respect to plant-available water.

The average WRCs of the upper layers of soil profiles (Fig. 6b-d) were S-shaped or gentle S-shaped. The smallest difference between the shapes of the curves was in bottom half WRCs (Fig. 6b). *Vaccinium* type WRCs of eluvial layer (Fig. 6d) had smallest water content values in the whole range of log pressure head. In other layers *Calluna* type had smallest values.

In the present study, there were the smallest variations of water content at the ends of the WRCs of all the layers (App. 3). The smallest variation at the dry end of the curve in the *Calluna* site type can be caused by the small amount of fine particles in this group. Rajkai et al. (1996) analysed the WRC data of the Swedish soils database. The average WRCs of 156 soils showed a large variation of water content in the whole range of the curve. In Rajkai et al. (1996), three textural (clay, silt and sand) groups were used in the WRC determinations. There was the greatest variation between the average WRCs (vol.) of the texture groups at the dry end of the average curves.

A V-type curve is characteristic for coarse graded soils. Residual water content is determined by the quantity of finer particles of graded soils (Karvonen 1988). In moraine soils the WRC is of a gentle S-type or S-type. On clayish soils, the shape of the curve is of the S-type (Andersson and Wiklert 1972). The shape is not dependent only on the particles of the sample. The amount of organic matter is an important factor of the shape of the WRC.

4.2 Selected water retention curves of profiles of four Finnish forest site types

Here are introduced altogether 96 curves of 24 profiles which were selected randomly after the WRC measurements were accomplished. There were six profiles in each forest site type. Measured PSDCs of the profiles (plot/profile: 1/1, 2/3, 3/3, 9/3, 13/1, 15/1 and 30/1), seen in this chapter) are shown in App. 1. The corresponding WRCs are given in App. 2. If someone wants to use these curves he can select a WRC which resembles his own PSDC.

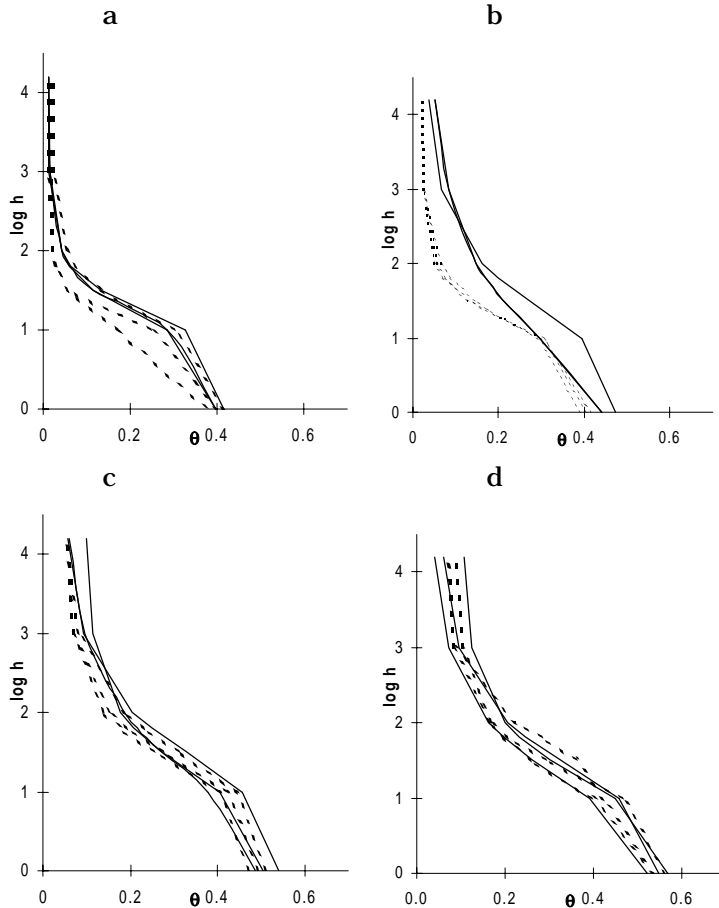


Figure 7. Selected soil water retention curves of mineral soil samples taken from the *Calluna* site type, (solid line = plot 1 (one profile with PSDCs), dotted line = plot 30 (one profile with PSDCs)) a = C-horizon, b = bottom half of B-horizon, c = top half of B-horizon and d = A-horizon.

The WRCs of *Calluna* site type for A-horizon, the top half of B-horizon, and the bottom half of B-horizon and C-horizon (the sampling depth for C-horizon was determined by multiplying the sum of A- and B-horizon thicknesses by 1.5) taken from two *Calluna*-type forest sites are shown in Fig. 7. The corresponding water retention curves for *Vaccinium* forest sites are given in Fig. 8. Curves for *Myrtillus* sites are shown in Fig. 9 and for *Oxalis-Myrtillus* sites in Fig. 10.

The saturated water content was the smallest in the subsoil horizon with no organic matter. The values of saturated water contents varied between 0.35 and 0.65. The upper illuvial horizon had a greater ability to retain water than the horizon below it.

The saturated water content, θ_s , was the greatest for A-horizons of *Calluna* site type and decreased in deeper horizons (Fig. 7). The shapes of the curves were similar to the gentle S. From curves for the *Calluna* site types, a distinct difference between the horizons can be seen.

Plant-available water contents ($\theta_{2.0} - \theta_{4.2}$) were the lowest in the C-horizon material (Fig. 7a). In two cases, the plant-available water content was almost zero and would be highly susceptible to drought. The lower B-horizon (Fig. 7b) had a better capacity to retain water at the dry end of the curve than the C-horizon. Three of the curves resembled those of the C-horizon. The other curves showed a better water retention capacity than the C-horizon curves.

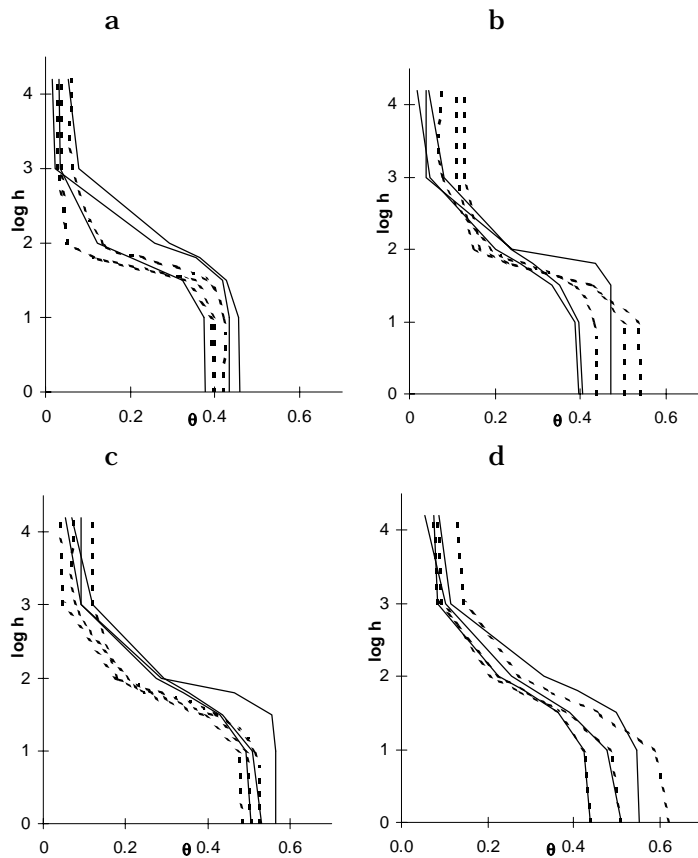


Figure 8. Selected soil water retention curves of mineral soil samples taken from the *Vaccinium* site type, (solid line = plot 2, dotted line = plot 9), a = C-horizon, b = bottom half of B-horizon, c = top half of B-horizon and d = A-horizon.

The saturated water content of the lower B-horizon was a little larger than that in the C-horizon under it. All the curves were typical for the poor forest site type (see Fig. 6a).

The samples of the top half of the illuvial horizon (Fig. 7c) and eluvial horizon (Fig. 7d) had a better ability to retain water than the layers under them. The saturated water content of the upper half of the B-horizon was larger than that in the C-horizon. The curves of the uppermost layer (Fig. 7d) resembled the curves of the layer below it. The eluvial horizons of the *Calluna* site had the largest saturated water contents of the profiles.

The subsoil (Fig. 8a) of the *Vaccinium* site type had the smallest water retention capacity at the dry end of the curve compared to the other horizons of this site type. Two of the six curves had larger water content values at a log pressure head value 2.0 than the four others. The four subsoil curves were of V-type. The saturated water content of the subsoil horizon was of same size as that of the *Calluna* site type.

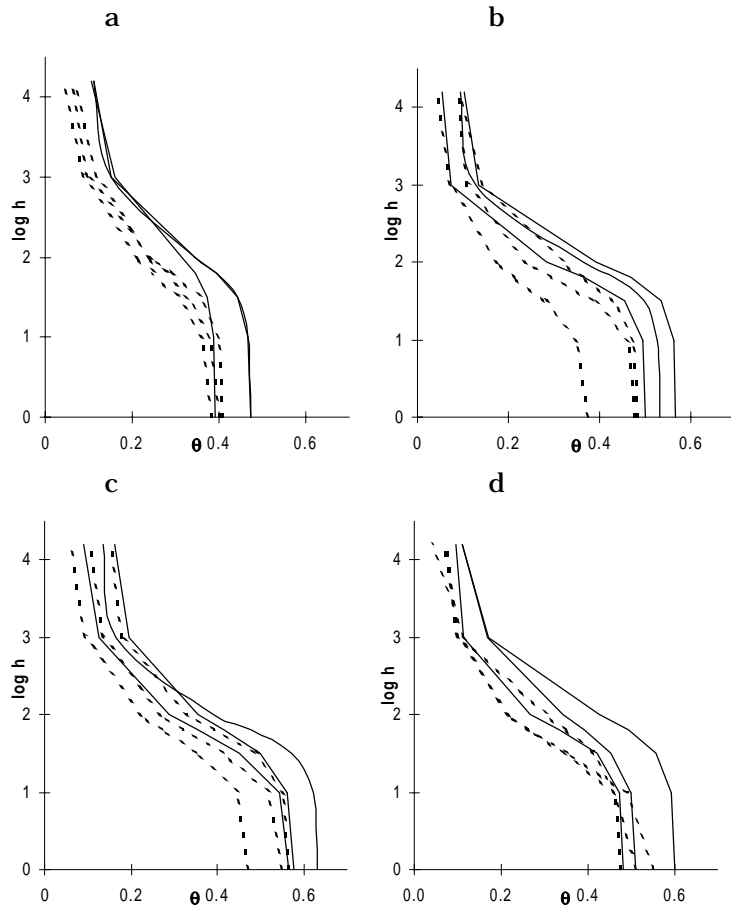


Figure 9. Selected soil water retention curves of mineral soil samples taken from the *Myrtillus* site type, (solid line = plot 13 (one profile with PSDCs), dotted line = plot 15 (one profile with PSDCs)), a = C-horizon, b = bottom half of B-horizon, c = top half of B-horizon and d = A-horizon.

The bottom half of the illuvial horizon (Fig. 8b) of the *Vaccinium* site type had clearly a larger water retention capacity than in the horizon under it. The variation of plant-available water was large in this horizon. In the top half of the B-horizon (Fig. 8c) there was clearly a greater amount of available water than in the subsoil of the *Vaccinium* site type. The saturated water content of this horizon was larger than in the horizons under it.

The variation between all the six curves of the eluvial layer (Fig. 8d) was smaller than in the two horizons under it. The measured amount of plant-available water was in this layer the greatest of the *Vaccinium* site type samples. The saturated water content of the eluvial horizon was as large as that of the top half of the illuvial layer.

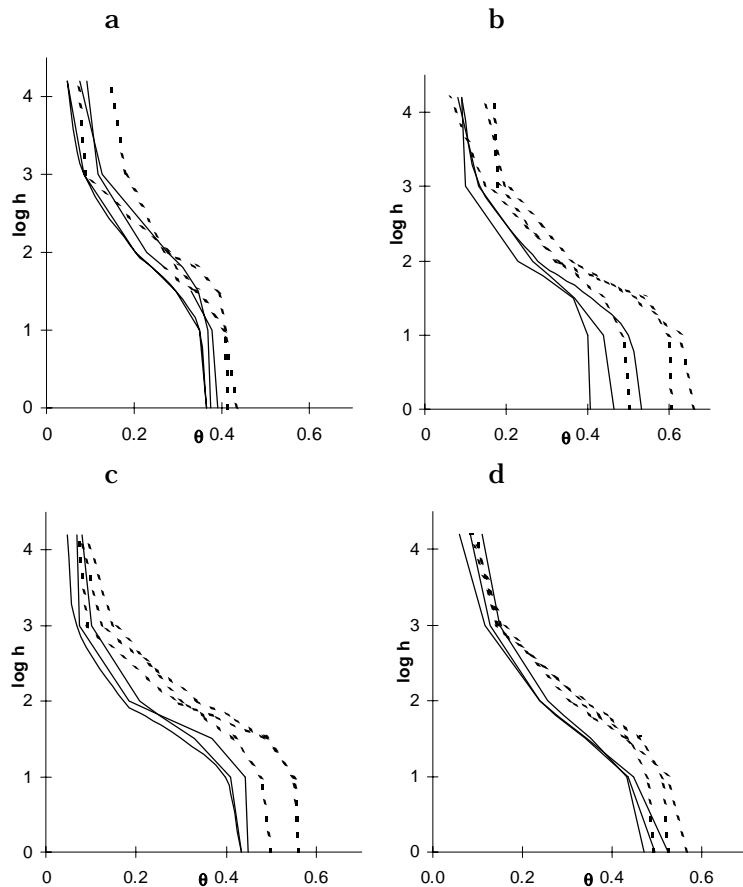


Figure 10. Selected water retention curves of mineral soil samples taken from the *Oxalis-Myrtillus* site type, (solid line = plot 3, dotted line = plot 28, not determined PSDCs), a = C-horizon, b = bottom half of B-horizon, c = top half of B-horizon and d = A-horizon.

The saturated water content of the subsoil of the *Myrtillus* site type (Fig. 9a) was of same size as in the *Calluna* and *Vaccinium* site types. The amount of plant-available water was distinctly greater in this site type than in the more barren site types. The WRCs of the subsoil (stand 13) resembled those of clay soils.

The WRC of the bottom half of the illuvial horizon of the *Myrtillus* site type (Fig. 9b) was of the S shape indicating a fertile forest site type. There was a lot of water for plants to use. The sample with the smallest porosity had a large amount of water for plants.

The saturated water content of the top half of the B-horizon (Fig. 9c) was clearly larger than that in subsoil. There was large variation in all parts of the WRCs. All the curves had a similar S shape.

The saturated water content of the uppermost horizon (Fig. 9d) was smaller than in the horizon under it. The variation of water contents of the horizon was also smaller than in the top half of the illuvial horizon.

The water retention curves of the C-horizon of *Oxalis-Myrtillus* site type (Fig. 10a) and *Myrtillus* site type (Fig. 9a), resembled the water retention curve of clay soil, with a gentle S-shape. The saturated water content and the variation of the WRCs were small in this horizon.

The variation of the water content values of the bottom half of illuvial horizon of *Oxalis-Myrtillus* site type (Fig. 10b) was largest at the wet end of the WRC. At the dry end of the curves there was the smallest variation of water content values. All the curves were of a gentle S shape.

Selected soil water retention curves of soil samples taken from the top half of the illuvial-horizon (Fig. 10c) of the *Oxalis-Myrtillus* site type had large variations. The saturated water content was distinctly larger than that of subsoil.

The shape of the curves of the uppermost horizon (Fig. 10d) of the *Oxalis-Myrtillus* site type was gentle S. The saturated water content of the horizon was clearly larger than the saturated water content of the subsoil. A distinct difference could be seen between the water retention capacities of the virgin subsoil and the horizons above it. This was the case in every four forest site types studied here. The exceptions were MT and OMT in the range of $\log h$ from 2.0 to 4.2.

4.3 Estimation of Andersson's and van Genuchten's parameters for Finnish forest mineral soil profiles

The aim of this part of the study was the estimation of Andersson's (1990c) and van Genuchten's (1980) parameters for selected Finnish forest soil profiles. Andersson's

parameters for these soils are shown in App. 4 and van Genuchten's parameters are given in App. 6. Van Genuchten's function was fitted for all 360 soils but Andersson's function only to those 108 profiles where PSDC was available.

Figures 11-14 show for four forest site types the fittings of Andersson's and van Genuchten's equations to the measured data. The curves selected to Figs. 11-14 are close to the average curves shown in Section 4.1. The *Calluna* forest site type belong to CT 1, plot1/hor1-4; *Vaccinium* site type to VT 2, plot3/hor1-4; *Myrtillus* site type to MT 15, plot 1/hor1-4; and the *Oxalis-Myrtillus* site type to OMT 3, plot3/hor1-4 (measured WRCs shown in App. 2).

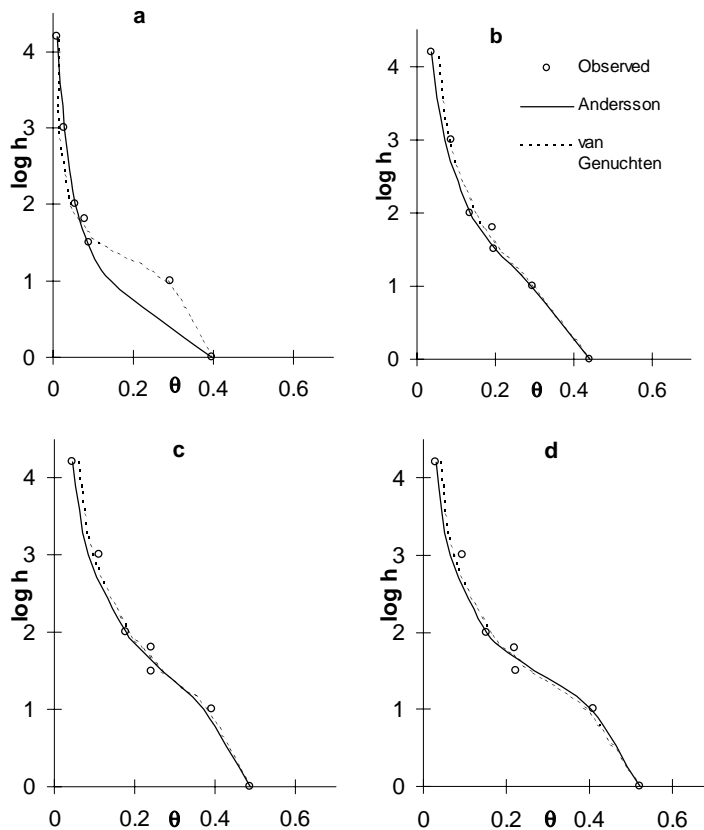


Figure 11. Example of water retention characteristics of the *Calluna* forest site a = the subsoil, b = bottom half of the illuvial horizon, c = top half of the illuvial horizon and d = the eluvial horizon fittings of Andersson's and van Genuchten's functions.

Both functions were accurate in fittings to soil water characteristics data in general. Andersson's function was

more sensitive to initial values in iteration of calculations than van Genuchten's function. Fitted curves were most accurate at the ends of curve. The poorest result of Andersson's function was obtained at log pressure head value 1.0 where the difference between the calculated and observed water contents was 0.12 (Fig. 11a). Another weak point was log pressure head value 3.0 at which differences were not so large, but there were many poor fits. However, all the fittings followed the observed values reasonably well. Log pressure head value of 1.8 was difficult to fit accurately, because of the bimodal structure of the samples.

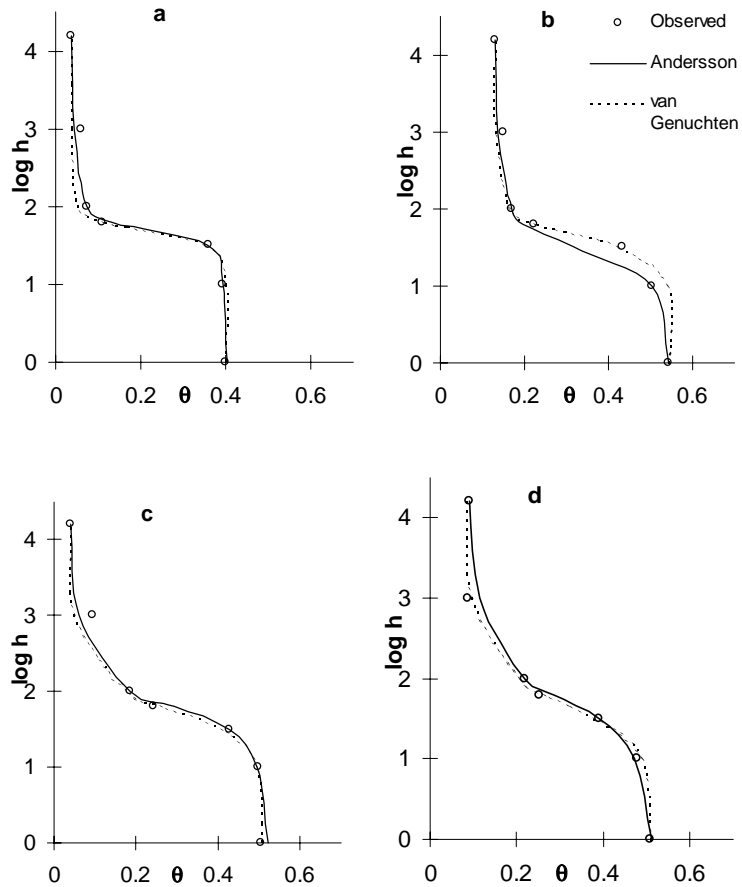


Figure 12. Example of water retention characteristics of the *Vaccinium* forest site a = the subsoil, b = bottom half of the illuvial horizon, c = top half of the illuvial horizon and d = the eluvial horizon fittings of Andersson's and van Genuchten's functions.

Fittings of van Genuchten's function did follow perfectly the observed values of the water retention characteristics of the eluvial horizon in the *Vaccinium* forest site type (Fig. 12d). Andersson's function was also successful in describing the

observed values. Both Andersson's and van Genuchten's functions followed the observed values of the water retention characteristics of the samples taken from the subsoil, the lower and upper illuvial horizon of the *Vaccinium* forest site type (Figs. 12a, b and c). The observed and modelled values varied slightly at the log pressure head of 3.0.

Comparison of the fittings of van Genuchten's and Andersson's functions in determining the soil water retention characteristics showed that van Genuchten's function had some difficulties in following the curve of subsoil of *Vaccinium* site type (Fig. 12a). Van Genuchten's function succeeded extremely well in the two uppermost horizons of the profile (Fig. 12c and d). The values given by Andersson's function for the saturated range of the curves of the upper illuvial horizon sample shown in Fig. 12c were too large. The curves of the deeper horizons of the horizon of *Vaccinium* site type (Figs. 12a and b) showed a narrow pore size distribution with an almost horizontal angle in the middle range of the curve. Van Genuchten's function was successful in describing the water retention characteristics of both deeper horizon samples.

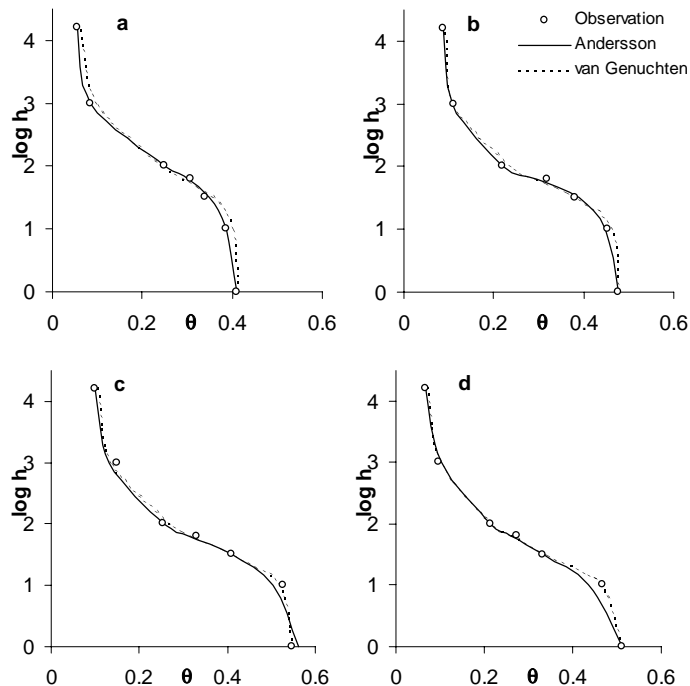


Figure 13. Example of water retention characteristics of the *Myrtillus* forest site a = the subsoil, b = bottom half of the illuvial horizon, c = top half of the illuvial horizon and d = the eluvial horizon fittings of Andersson's and van Genuchten's functions.

Van Genuchten's function followed the observed values of the WRC (*Myrtillus* type, Fig. 13) fairly well. At a log pressure head value of 3.0, the water content of the upper illuvial horizon (Fig. 13c) of the both functions was too small. Andersson's function did not follow the observed value of water content at log pressure head value of 1.0 (Fig. 13d) well. Both Andersson's and van Genuchten's functions were very successful in describing the WRC of two lower horizon samples (Fig. 13a and b).

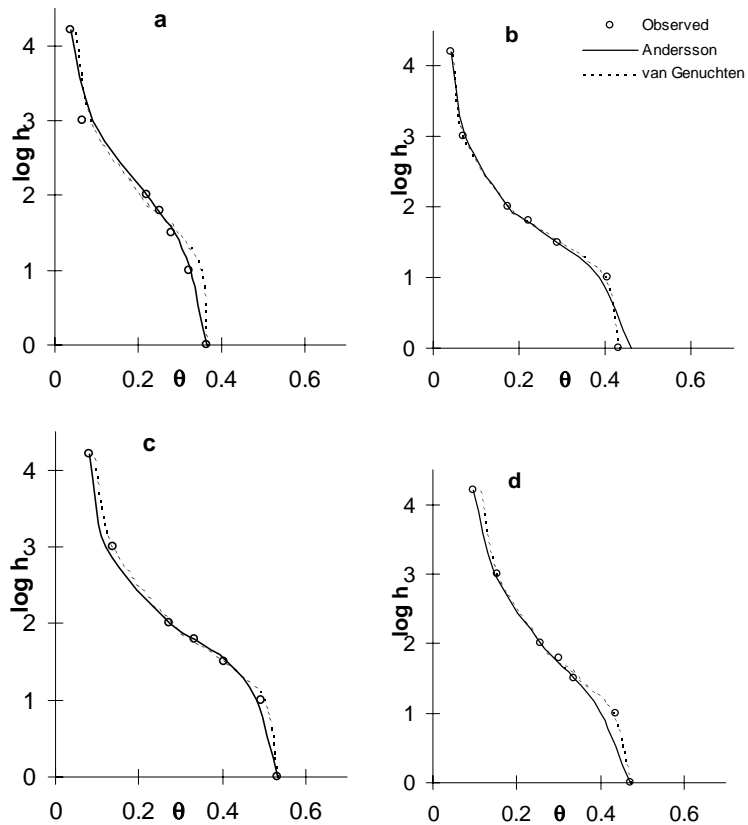


Figure 14. Example of water retention characteristics of the *Oxalis-Myrtillus* forest site a = the subsoil, b = bottom half of the illuvial horizon, c = top half of the illuvial horizon and d = the eluvial horizon fittings of Andersson's and van Genuchten's functions.

The WRCs of the *Oxalis-Myrtillus* forest site type (Fig. 14) showed a much wider pore size distribution than the curves of samples taken from the more barren *Vaccinium* site type. All four curves showed a rather similar S-shape. The values given by van Genuchten's function to water content values at both log pressure head values of 1.0 and 3.0 (Fig. 14a) were too large. Andersson's function also gave water content

values that were too large at log pressure head value of 3.0 (Fig. 14a) and too small at the pressure head value of 1.0 (Fig. 14d). Andersson's function was inflexible near the saturated range (Fig. 14b), giving values that were too large. In the other cases, the fittings of both functions were surprisingly good.

In nine of sixteen fittings, Andersson's equation gave smaller water content values than the observations for log pressure head value 3.0. Saturated water content was smaller than that observed in three cases when Andersson's function was fitted to data. Van Genuchten's function had its weakest point at the dry end of the curve where it gave values that were too large in eight of sixteen cases.

Neither of the functions was flexible enough to follow observation points, which were caused by bimodal structure of soil porosity (Durner 1994). Bimodality was characteristic for the *Calluna* forest site type (Fig. 11) and in a lesser degree for the *Myrtillus* forest site type (Fig. 13). Pachepsky et al. (1995a) have shown that one reason for the deviation from the power law is the multifractal structure of soil porosity, which results in dependence of the fractal dimension on the radii.

4.4 Estimation of Andersson's parameters for selected Finnish forest humus layer data

The aim of this part of the study was the estimation of Andersson's (1990c) parameters for selected Finnish forest humus layers. Andersson's and van Genuchten's functions for water retention characteristics were fitted for the humus samples (Table 1 and Figs. 15-18).

Table 1. Humus sample parameters of Andersson's ($h_{t,0}$, b_1 , θ_0 and p_1 , Eq. 3-2) and van Genuchten's (θ_s , θ_r , α and n , Eq. 3-28) functions of two *Vaccinium* and one *Oxalis-Myrtillus* forest sites.

		θ_0	p_1	b_1	$h_{t,0}$	θ_s	θ_r	α	n
VT 1	Pit 1	0.268	0.523	1.054	1	0.267	0.05	0.323	1.58
VT 1	Pit 2	0.17	0.233	0.633	10.5	0.246	0.069	0.187	1.65
VT 1	Pit 3	0.407	0.64	0.543	4.5	0.585	0.114	0.331	1.707
VT 2	Pit 1	0.568	0.901	0.822	7.7	0.756	0.059	0.531	1.399
VT 2	Pit 2	0.536	0.875	0.712	6.3	0.52	0.066	0.477	1.503
VT 2	Pit 3	0.551	0.893	0.67	7.3	0.631	0.083	0.49	1.474
OMT	Pit 1	0.752	1.61	1.124	1	0.805	0.195	0.239	1.57
OMT	Pit 2	0.518	1.037	0.908	1	0.771	0.157	0.273	1.606
OMT	Pit 3	0.629	1.261	0.969	1	0.81	0.168	0.241	1.653

All the WRCs of humus samples (Fig. 15) were of the V-type. Humus sample parameters of Andersson's WRC of two site types are presented in Table 1. The WRCs showed that this

type of humus soil behaved in such a way that the desorption was rapid from the beginning and in most samples half of the saturated water content had already been released at the log pressure head value of 1.0. Saturated water contents ranged from 0.23 to 0.81. Water content at the dry end of the WRC varied between 0.02 and 0.21.

Two VT samples (Fig. 15) differed from the rest of the samples. This indicated large variation of the material. VT samples had a very small capacity to retain water. One reason for this was that they were only 1 cm thick. In such humus samples, there was only a small amount of mature humus which could retain water. There could also have been a large measurement error in the sample. Saturated values of these two samples are strongly erroneous. Young humus mostly had matter that was in the early stage of decomposition.

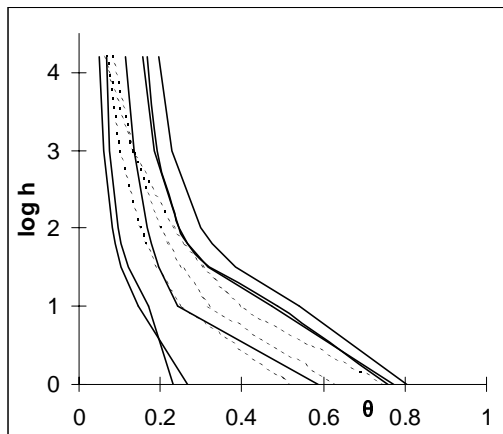


Figure 15. Selected soil water retention curves of humus samples taken from two *Vaccinium* (solid line) and the *Oxalis-Myrtillus* (dotted line) sites.

The fitting of Andersson's and van Genuchten's equations to the humus data succeeded well in each of the nine cases (Figs. 16-18). The fitting was successful both in the wet and dry range of the WRC.

In the *Vaccinium*1 stand (Fig. 16) the saturated water content of the sample was extremely small for two of the three pits, only around 0.25, which reflects the difficulties in measuring WRC for humus layers. This was very typical for some thin humus layers with many twigs and undispersed material. This curve showed a small amount of plant-available water. In the WRC of pits 1 and 2 of the *Vaccinium*1 site, the amount of plant-available water was very scarce. The saturated water content of the pit 3 was more than two times greater than that of the sample of pit 2, which was situated 10 m from the pit 3. The fitting of equations to the

observed data succeeded well. The log pressure head value of 1.0 was the only problematic point of the fitting. The calculated value was too small compared to the observed value.

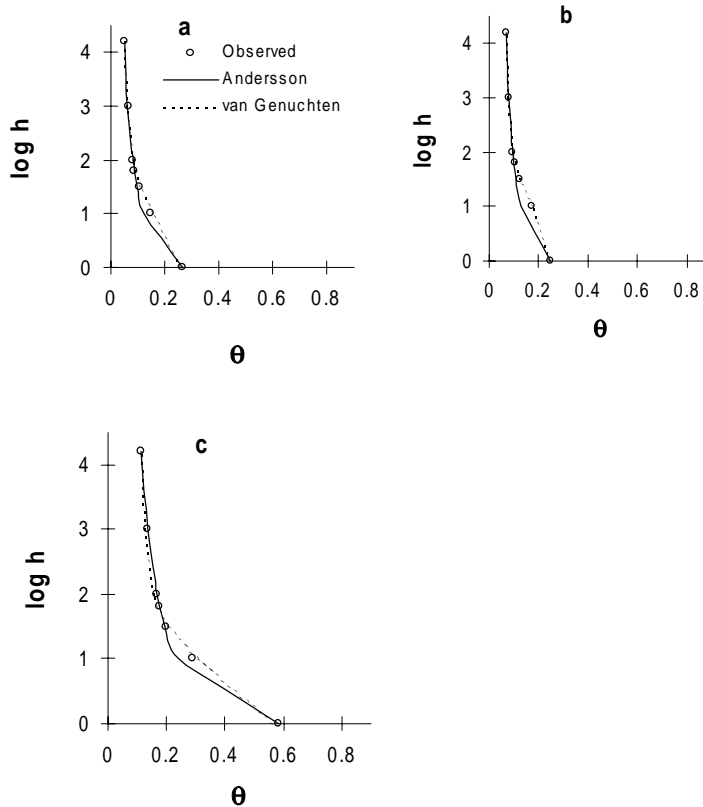


Figure 16. Water retention characteristics of the *Vaccinium1* site, the humus layer, a = pit 1, b = pit 2 and c = pit 3, fittings of Andersson's and van Genuchten's functions.

The amounts of plant-available water of the humus samples in the *Vaccinium2* site were larger than in the *Vaccinium1* site. Fittings of both equations to data were accurate (Fig. 17). Only at the log pressure head point 1.0 was the calculated value too high compared to the observed value (Fig. 17c).

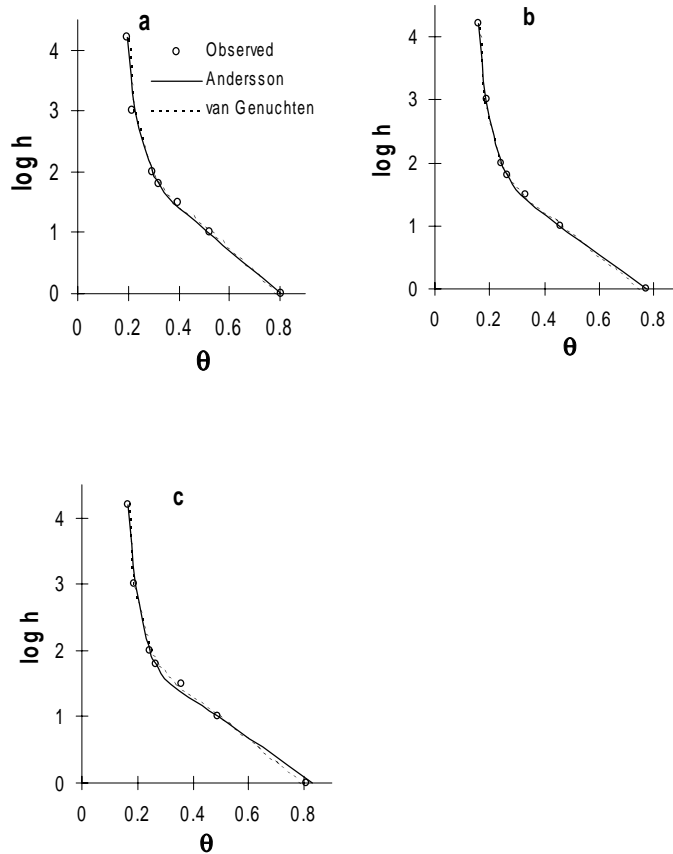


Figure 17. Water retention characteristics of the *Vaccinium2* site, the humus layer, a = pit 1, b = pit 2 and c = pit 3, fittings of Andersson's and van Genuchten's functions.

The water retention characteristics of the sample taken from pit number one in the *Oxalis-Myrtillus* forest site type (Fig. 18a) resembled the curves of the *Vaccinium* site type. The amount of available water was larger than the water amount of the *Vaccinium* site type.

The saturated water content of the sample (Fig. 18b) was the smallest of the *Oxalis-Myrtillus* site type humus samples, only about 0.5. Fitting was successful with no exceptions. The amount of plant-available water was smaller than in the other two samples of this site type. The amount of usable water was the same size as that of the sample taken from pit 1. Physical characteristics of humus differ distinctly from the characteristics of the mineral soil horizon. The humus layer swells and cracks when it gets wet and dries. As it can be more than 10 cm thick, the humus layer can be a very important for water storage.

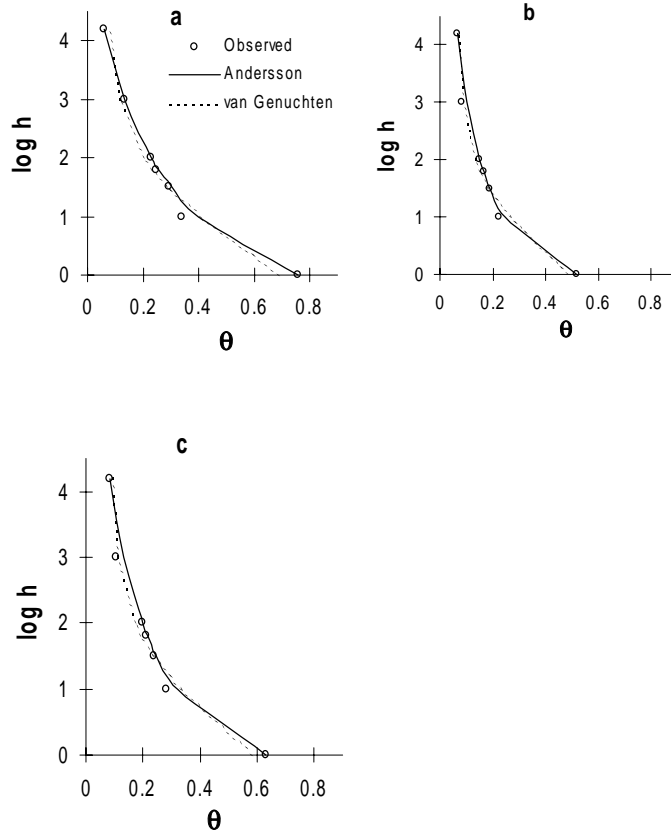


Figure 18. Water retention characteristics of the *Oxalis-Myrtillus* site, the humus layer, a = pit 1, b = pit 2 and c = pit 3, fittings of Andersson's and van Genuchten's functions.

The size of the water storage capacity is difficult to know exactly because of the unstable nature of the media. Forest floor water content dynamics is of crucial importance in water balance calculations. In numerous water flow and water balance calculations, the humus layer is neglected.

4.5 Prediction of the WRC from the PSDC using the semi-physical methods

108 Finnish forest soil samples and 7 Swedish agricultural field soil samples were used as test material for the methods for estimating the WRC from the PSDC. Three different methods were used: semi-physical method developed in this study (see Section 3.4), Jonasson's method (see Section 3.4) and van Genuchten-type method (see Section 3.5.3). The estimation of the WRCs was carried out both in the case that

saturated and residual water content values were assumed to be unknown (Fig. 19 and Table 2) and in the case that θ_s and θ_r were given as input values (Fig. 20 and Table 3).

In predicting the WRC from the PSDC it is necessary to utilize the transfer function C_p given in Eq. (3-25).

$$\frac{1}{C_p} = P_1 + P_2 x_0 + 100 P_3 (\theta_s - \theta_r) + P_4 \rho_d; \quad R^2 = 0.47 \quad (3-25)$$

where $P_1 \dots P_4$ are the parameters of the multiple regression equation. 108 forest profiles were used to determine the parameters of Eq. (3-25). The parameters of regression equation were $P_1 = -6.94$, $P_2 = 4.11$, $P_3 = 0.123$ and $P_4 = 4.875$. The same transfer function was used in the semi-physical method and in van Genuchten-type method. Jonasson's method predicts directly $h_{t,0}$ using Eqs. (3-27).

Eq. (3-25) includes saturated water content θ_s and residual water content θ_r . In real cases these values are not necessarily known and therefore simple regression equations were developed to predict θ_s and θ_r from bulk density ρ_d (kg dm⁻³) and PSDC.

$$\theta_s = 0.928 * (1 - \rho_d / 2.65) + 0.021; \quad R^2 = 0.61 \quad (4-1)$$

$$\theta_r = 0.185 - 0.0011 D_{6-2} - 0.07 * \rho_d \quad R^2 = 0.31 \quad (4-2)$$

where $D_{6.2}$ denotes the fraction (%) of particle size values from 600 μm to 2000 μm .

4.5.1 Finnish forest sites

Altogether thirteen observation points were used in predictions of the WRCs. Six of the points were interpolated between the measured points.

Semi-physical method was the most accurate of three methods in predicting WRC of average Finnish forest soil samples (Fig. 19) when θ_s and θ_r were estimated. Van Genuchten's method gave good shape for the curve but all the water content values were too large indicating that the transfer function developed originally for the semi-physical method was not suitable in van Genuchten's method. Jonasson's method gave the poorest result.

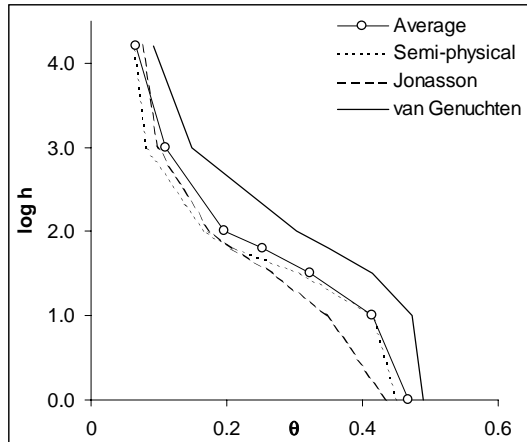


Figure 19. Average WRC of 108 samples. Jonasson's, van Genuchten's and semi-physical (θ_s and θ_r estimated) methods.

Coefficient of determination, R^2 , average errors at different pressure heads, E_{ave} , standard deviation of errors, S_{dev} , minimum, E_{min} , and maximum, E_{max} , values of errors at different pressure heads for semi-physical, Jonasson's and van Genuchten's methods of WRC determination are shown in Table 2 in the case that saturated water content θ_s and residual water content θ_r were estimated using Eqs. (4-1) and (4-2).

The smallest average difference between the measured and calculated water content value was achieved at pressure head 10 cm when semi-physical method was used (Table 2), the largest error was at pressure 1000 cm. Jonasson's predicting method had its most accurate values at both ends of the WRC. Van Genuchten's method gave its most inaccurate values in the middle range of the WRC.

Standard deviation of the WRC of the semi-physical method was smallest at the ends of the curve (Table 2). Deviation was of same size of magnitude in the whole range of the WRC. Jonasson's method had its largest deviation in two dry end points of the curve. Jonasson's method is not physically based and it can cause large errors in some soils. The predicted WRC values of van Genuchten's method were of same class of magnitude in the whole range of the curve.

Table 2. Coefficient of determination, R^2 , average errors at different pressure heads, E_{ave} , standard deviation of errors, S_{dev} , minimum, E_{min} , and maximum, E_{max} , values of errors at different pressure heads for semi-physical, Jonasson's and van Genuchten's methods of WRC determination. Saturated water content θ_s and residual water content θ_r were estimated. S_E is the square sum of errors, θ_{ave} is the average value of all the measurements.

h , cm	1	10	32	63	100	1000	16000
Semi-physical							
E_{ave}	-0.018	0.000	-0.012	-0.042	-0.030	-0.030	-0.005
S_{dev}	0.042	0.055	0.068	0.087	0.084	0.052	0.041
E_{max}	0.126	0.190	0.225	0.163	0.284	0.062	0.073
E_{min}	-0.099	-0.111	-0.216	-0.359	-0.264	-0.265	-0.216
			$S_E =$	$\theta_{ave} =$	$S_M =$		$R^2 =$
			3.477	0.261	19.64		0.823
Jonasson							
E_{ave}	-0.033	-0.066	-0.054	-0.046	-0.023	-0.013	0.008
S_{dev}	0.061	0.143	0.099	0.101	0.104	0.051	0.027
E_{max}	0.074	0.124	0.233	0.185	0.360	0.161	0.073
E_{min}	-0.467	-0.887	-0.367	-0.277	-0.241	-0.142	-0.102
			$S_E =$	$\theta_{ave} =$	$S_M =$		$R^2 =$
			7.449	0.261	19.64		0.621
van Genuchten							
E_{ave}	0.023	0.059	0.092	0.096	0.107	0.040	0.026
S_{dev}	0.055	0.077	0.074	0.058	0.065	0.070	0.065
E_{max}	0.195	0.329	0.279	0.240	0.311	0.274	0.257
E_{min}	-0.089	-0.078	-0.058	-0.062	-0.046	-0.087	-0.093
			$S_E =$	$\theta_{ave} =$	$S_M =$		$R^2 =$
			7.142	0.261	19.64		0.636

$$S_E = \sum_{j=1}^7 \sum_{i=1}^{108} (\theta_{i,j}^M - \theta_{i,j}^C)^2$$

$$S_M = \sum_{j=1}^7 \sum_{i=1}^{108} (\theta_{i,j}^M - \theta_{AVE}^M)^2$$

$$R^2 = \frac{S_M - S_E}{S_M}$$

Semi-physical method gave the most accurate results for the WRC when θ_s and θ_r were given (Fig. 20 and Table 3). However, coefficient of determination R^2 was smaller (0.809) than in the case when θ_s and θ_r were estimated (0.823). Van Genuchten's method behaved in opposite way giving larger values for R^2 when θ_s and θ_r were given (0.636 in Table 2 and

0.740 in Table 3). In the wet end of the curve all the methods were accurate (see Fig. 20 and Table 3).

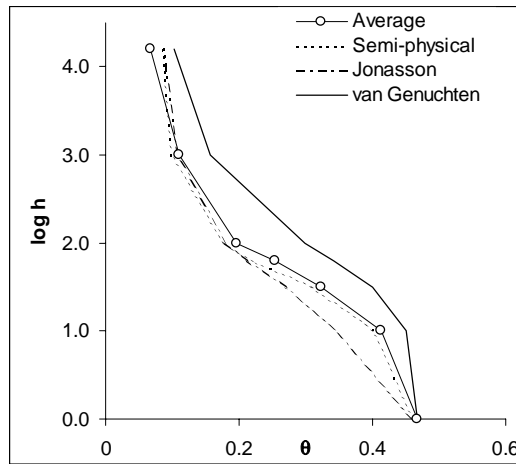


Figure 20. Average WRC of 108 samples. Jonasson's, van Genuchten's and semi-physical (θ_s and θ_r given as input data) methods.

The differences between the measured and calculated values of the WRC were of same size in the whole range of the curve when the semi-physical method was used (Table 3). The most accurate point of the curve was at pressure head 1000 cm when Jonasson's method was used.

Standard deviation of the WRC of semi-physical method was smallest in the driest point of the curve (Table 3). The WRC of Jonasson's method deviated most in the wet range of the curve. The smallest standard deviation point was the wettest part of the WRC when van Genuchten's method was used.

Examples of the estimation of the WRCs from PSDC for *Vaccinium* site are shown in Fig. 21. Predictions of the curves of the *Vaccinium* site were successful. Both the semi-physical and Jonasson's method followed the observed values of the WRCs accurately. The method was better predictor than Jonasson's method in three of the four cases.

In drawing the graphs shown in Figs 21 and 22 relative saturation θ was calculated using measured value for saturated water content and residual water content was estimated using van Genuchten's method.

Table 3. Coefficient of determination, R^2 , average errors at different pressure heads, E_{ave} , standard deviation of errors, S_{dev} , minimum, E_{min} , and maximum, E_{max} , values of errors at different pressure heads for semi-physical, Jonasson's and van Genuchten's methods of WRC determination. Saturated water content θ_s and residual water content θ_r were given as input values. S_E is the square sum of errors, θ_{ave} is the average value of all the measurements.

h , cm	1	10	32	63	100	1000	16000
Semi-physical							
E_{ave}	-0.037	-0.014	-0.013	-0.034	-0.021	-0.013	0.017
S_{dev}	0.047	0.061	0.080	0.086	0.088	0.052	0.032
E_{max}	0.000	0.163	0.287	0.193	0.311	0.114	0.143
E_{min}	-0.171	-0.162	-0.234	-0.249	-0.213	-0.108	0.000
			$S_E =$	$\theta_{ave} =$	$S_M =$		$R^2 =$
			3.741	0.261	19.64		0.809
Jonasson							
E_{ave}	-0.046	-0.072	-0.052	-0.041	-0.016	-0.003	0.019
S_{dev}	0.068	0.146	0.104	0.104	0.107	0.057	0.032
E_{max}	0.000	0.163	0.276	0.218	0.375	0.141	0.143
E_{min}	-0.477	-0.904	-0.339	-0.249	-0.213	-0.108	0.000
			$S_E =$	$\theta_{ave} =$	$S_M =$		$R^2 =$
			8.094	0.261	19.64		0.588
van Genuchten							
E_{ave}	0.000	0.038	0.077	0.087	0.102	0.047	0.036
S_{dev}	0.000	0.043	0.057	0.051	0.062	0.064	0.054
E_{max}	0.000	0.163	0.229	0.238	0.303	0.266	0.258
E_{min}	0.000	-0.013	-0.041	-0.057	-0.037	-0.043	0.001
			$S_E =$	$\theta_{ave} =$	$S_M =$		$R^2 =$
			5.105	0.261	19.64		0.740

$$S_E = \sum_{j=1}^7 \sum_{i=1}^{108} (\theta_{i,j}^M - \theta_{i,j}^C)^2$$

$$S_M = \sum_{j=1}^7 \sum_{i=1}^{108} (\theta_{i,j}^M - \theta_{AVE}^M)^2$$

$$R^2 = \frac{S_M - S_E}{S_M}$$

Jonasson's method predicted at dry end water content values smaller than θ_r , which gave negative values for relative saturation Θ (see Fig. 21a). In both methods saturated water content is not directly included in the equation for relating water content to pressure head (see Eq. (3-2)) and therefore it is possible that values greater than 1.0 for Θ can be obtained (see Fig. 21a). Moreover, relative saturation Θ can

be smaller than 1.0 for the same reason at pressure head value 1 cm (see Fig. 22).

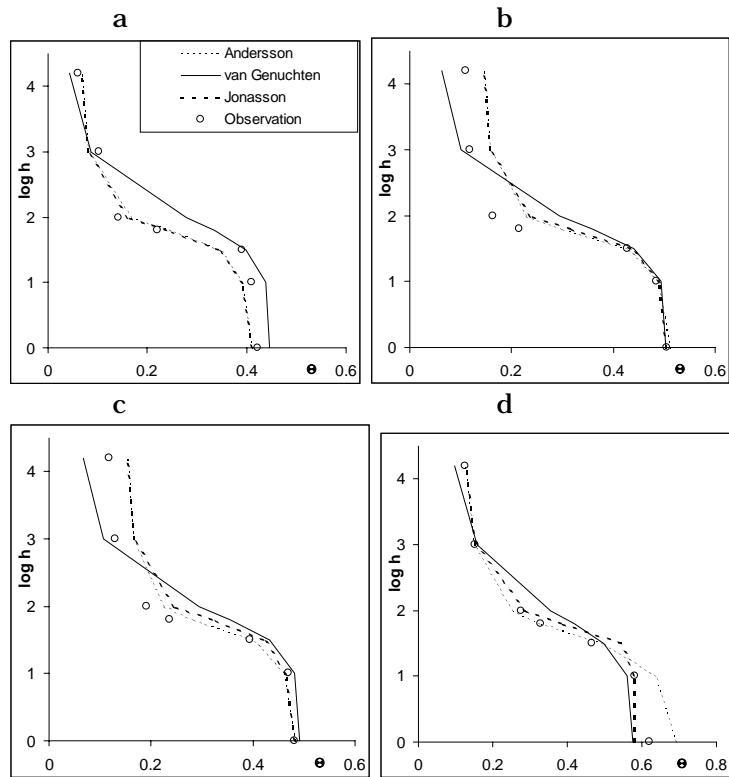


Figure 21. Predictions of the WRC from the PSDC, a = subsoil, b = bottom half of the illuvial horizon, c = top half of the illuvial horizon and d = eluvial horizon, the *Vaccinium* forest site type (plot 2, pit 2).

In the dry part of the WRC, the observed values of the A-horizon of the VT site were greater than the predicted ones (Fig. 21a). Relative water content values differed most on both sides of the pressure head value of 100 cm. Jonasson's method gave predictions which were larger than the observed values in almost the whole range of the curve. Predicted values of the semi-physical method closely followed the observations at the saturated and dry ends of the curve. In the middle of the curve, predicted values were a little smaller than those observed. Predictions of both methods were the same as the observations in the saturation point of the curve and also in the driest point of the water retention characteristics curve. The curves seemed realistic.

Both methods obtained the best predictions in two illuvial horizons of the VT site (Figs. 21b and c). Jonasson's method was the most accurate in predicting the WRC of the upper

illuvial horizon sample (Fig. 21c). In the saturation range, both curves had larger water content values than the observed values in the bottom half of illuvial horizon (Fig. 21b). At the dry end of the curve, both methods gave smaller values than the observed values in the bottom half of the illuvial horizon (Fig. 21b). In the middle range of the curve, the predictions closely matched the observations. At the dry end of the curve, Jonasson's method gave smaller water content values than zero giving unphysical values.

The semi-physical method predictions of subsoil (Fig. 21a) gave larger values of soil water potential than the observed values in the wet range of the curve. Jonasson's method already seemed to be unphysical from the pressure head values of 700 cm. The semi-physical method was also unphysical in the dry range of the WRC. Jonasson's method gave unrealistic values in the saturation range of the curve. The predicted values were greater than 1.0. The range approximating to water potential values of 100 cm was most difficult for both predicting methods to follow the observed values of the curve accurately. In this range, both methods gave predicted water content values that were too large.

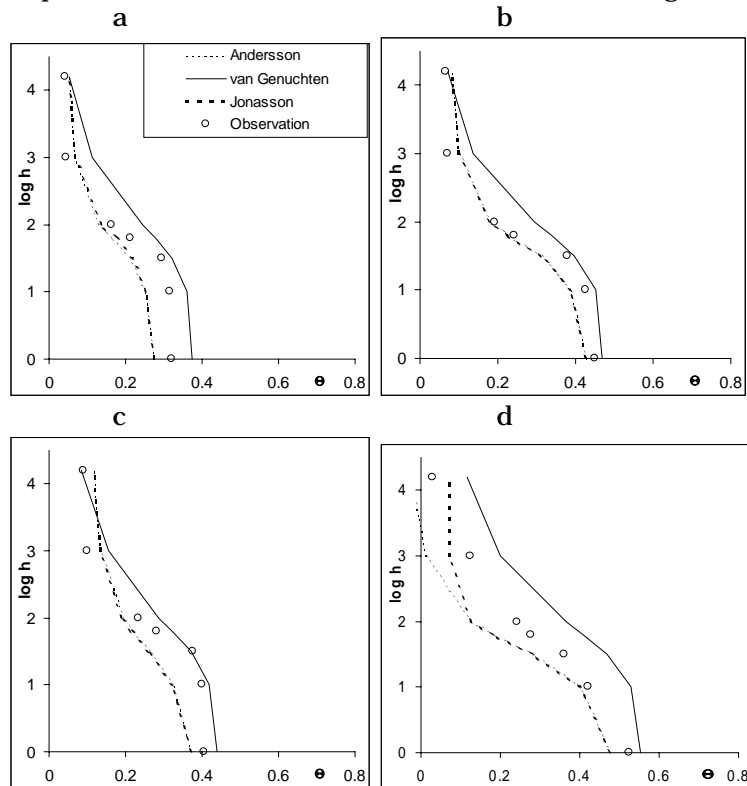


Figure 22. Predictions of the WRC from the PSDC, a = subsoil, b = bottom half of the illuvial horizon, c = top half of the illuvial horizon and d = eluvial horizon, the *Oxalis-Myrtillus* forest site type (plot 3, pit 2).

Examples of the estimation of the WRCs from PSDC for *Oxalis-Myrtillus* forest site are shown in Fig. 22. The semi-physical method closely followed the observed values of the A-horizon of the OMT site (Fig. 22d) in the wet part of the curve, but gave predictions that were too small in the dry ($\log h > 1.7$) range of the curve. Jonasson's method hit the observation when the pressure head was 100 cm. At the wet end of the curve, the values of Jonasson's predictions were too large, while in the dry part they were too small. Both methods gave water content values of zero at the wilting point.

Jonasson's method followed the observed values of the WRC of the top half of the illuvial horizon (Fig. 22c) extremely well; giving the best prediction of all the curves shown in this part of the study. The semi-physical method gave values that were too small when pressure head values were less than 1000 cm.

Predictions of both methods for the WRC of the lower part of the illuvial horizon (Fig. 22b) could not follow the observations in the dry and wet ends of the curve. At the wet end, the predicted values were too small and at the dry end too large. The predicted values of both methods followed the observed values well in the middle part of the WRC ($1.0 > \log h > 3.0$).

The semi-physical method could hit the observed value of the subsoil curve only in the wet part of the curve (Fig. 22a). At pressure head values greater than 5 cm the semi-physical method gave water content values that were too small. At a pressure head value of 10 000 cm, the water content value was zero, which was not physically based. Jonasson's method followed the observed values well when the pressure head was less than 1000 cm. The predictions at the dry end were too small, as in the case of the semi-physical method.

When the semi-physical method was used for predicting the WRCs for VT sites the error was smaller than that of more fertile *Oxalis-Myrtillus* site. OMT predictions were too small, especially at the dry end of the WRC. Only the dry part of the curve of the subsoil was too difficult for both methods to follow in a reasonable way.

4.5.2 Swedish agricultural soils

In order to test the applicability of the semi-physical method independent data from arable soils were used in predictions. The selected soils (3 topsoil and 4 subsoil samples) differed distinctly from the Finnish forest soils that were used in determining the parameters of the semi-physical method. The samples were selected by increasing clay content. The particle size distributions and bulk densities of the samples

are shown in Table 4. The estimation of the WRCs was carried out both in the case that saturated and residual water content values were assumed to be unknown and in the case that θ_s and θ_r were given as input values. The results for topsoil are shown in Fig. 23 and for subsoil in Fig. 24. App. 7/I shows the average coefficient of determination, R_2 , average errors at different pressure heads, E_{ave} , standard deviation of errors, S_{dev} , minimum, E_{min} , and maximum, E_{max} , values of errors at different pressure heads for semi-physical, Jonasson's and van Genuchten's methods of WRC determination in the case that saturated water content θ_s and residual water content θ_r were estimated. The corresponding results for the case that θ_s and θ_r were given as input data are shown in App. 7/II. The semi-physical method gave the best results when θ_s and θ_r were estimated. R^2 -values were 0.921, 0.729 and 0.872 for the semi-physical, Jonasson's, and van Genuchten's method, respectively. The coefficient of determination was not improved when θ_s and θ_r were given.

Table 4. Particle size distributions and bulk densities ρ_b (kg dm⁻³) of the Swedish arable soil samples.

μm	<2	2-6	6-20	20-60	60- 200	200- 600	600- 2000	>2000	ρ_b
Top soil/1	1	1	7	6	30	34	17	4	1.44
Top soil/2	8	4	8	20	25	23	7	5	1.25
Top soil/3	28	17	14	10	14	8	3	6	1.34
Subsoil/1	0	1	1	8	38	42	9	1	1.53
Subsoil/2	7	4	16	31	29	8	3	2	1.45
Subsoil/3	32	21	19	14	8	3	1	2	1.51
Subsoil/4	52	17	14	9	3	1	1	3	1.44

In most cases the correspondence between the predicted and the observed values was good when the methods were used. Jonasson's (1991) and semi-physical methods failed to follow the observed values accurately in the dry end of the curve when clay content of the topsoil sample was < 2 % (Fig. 23 a1 and a2). Jonasson's method failed to follow the observed WRC of topsoil when the clay content was 26-30 percent (Fig. 23 c1, c2) and the observed WRC of subsoil when the clay content greater than 30 % (24 c1, c2, d1, d2). The predictions of the semi-physical and Jonasson's method of topsoil with clay content < 2.0 % (Fig. 23 a1 and a2) were accurate in wet range of the curve. Dry end of the curve gave largest errors for both semi-physical and Jonasson's methods (App. 7/I and 7/II).

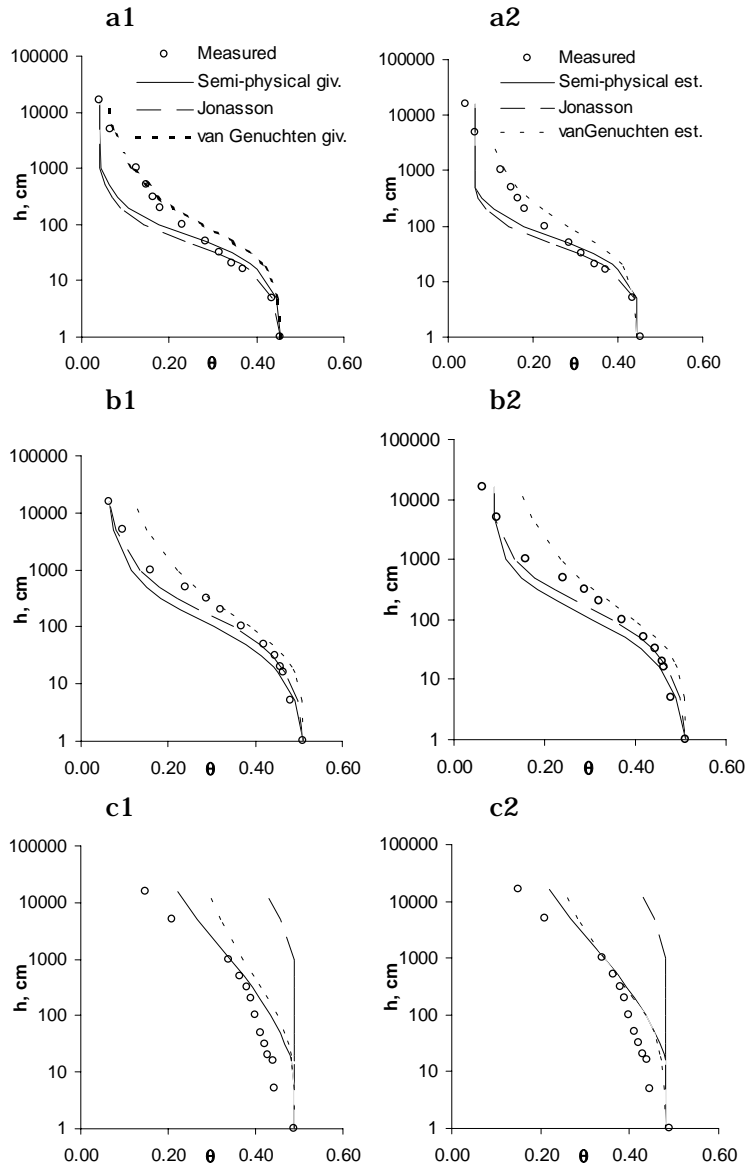


Figure 23. Semi-physical, Jonasson's and van Genuchten's predictions of the WRC from the PSDC, Swedish agricultural topsoils, a1 = clay content < 2.0 % (θ_r and θ_s given), a2 = (θ_r and θ_s estimated) b1 = clay content 6-10 % (θ_r and θ_s given), b2 = (θ_r and θ_s estimated) and c1 = clay content 26-30 % (θ_r and θ_s given) and c2 = (θ_r and θ_s estimated).

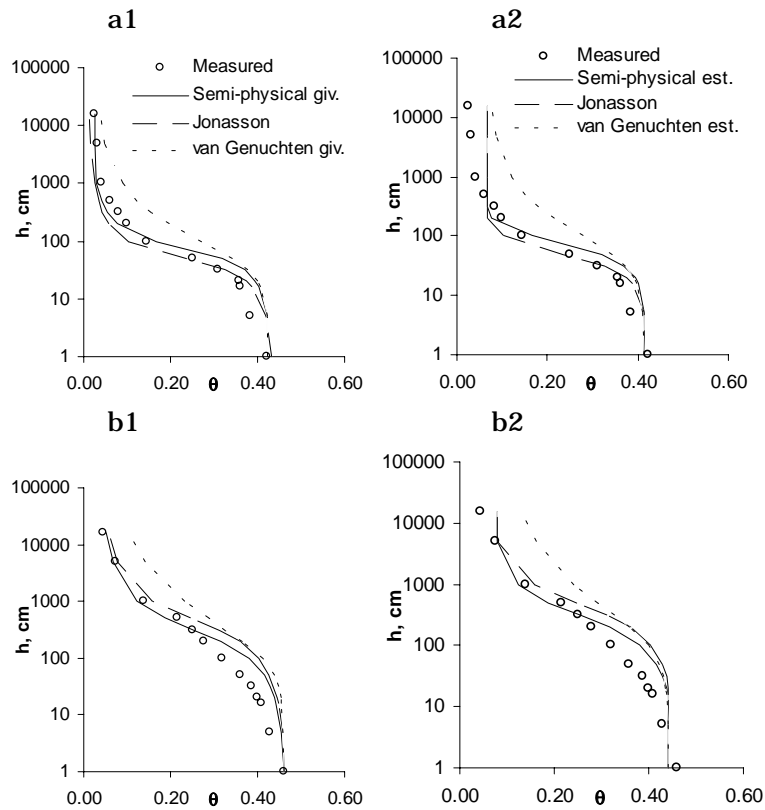


Figure 24/I. Semi-physical, Jonasson's and van Genuchten's predictions of the WRC from the PSDC, Swedish agricultural subsoils, a1 = clay content < 2.0 % (θ_r and θ_s given), a2 = (θ_r and θ_s estimated), b1 = clay content 6-10 % (θ_r and θ_s given), b2 = (θ_r and θ_s estimated).

Van Genuchten predictions of topsoils were best when the clay content was smallest (Fig. 23 a1 and a2). The dry end of the WRC was problematic for van Genuchten method (Fig. 23 b1-2 and c1-2), giving too large values. Greatest errors were seen in the driest point of the curve (App. 7). In van Genuchten's method the same difficulty was observed than for Finnish forest soils. The transfer function used tends to provide too large values for parameter α , which leads to over prediction of soil moisture content.

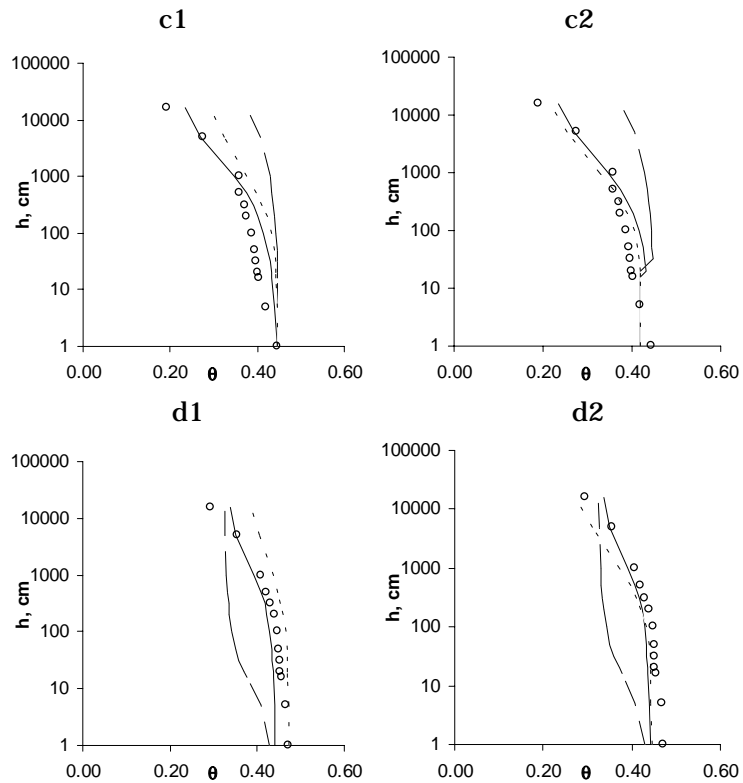


Figure 24/II. Semi-physical, Jonasson's and van Genuchten's predictions of the WRC from the PSDC, Swedish agricultural subsoils, c1 = clay content 31-35 % (θ_r and θ_s given), c2 = (θ_r and θ_s estimated) and d1 = clay content 51-55 % (θ_r and θ_s given) and d2 = (θ_r and θ_s estimated).

4.6 Prediction of hydraulic conductivity from the WRC using modification of Andersson's method and van Genuchten's method

In the study, a modification of Andersson's method for estimating the relative hydraulic conductivity function from WRC was proposed (see Eq. (3-18) in Chapter 3.3.3). Moreover, the van Genuchten-type relative hydraulic conductivity function given in Eq. (3-31) was used as another method to predict $K_r(h)$. Twenty Central European soils were selected for testing the methods based on the criteria that samples resemble Finnish forest soils. Horizon, texture, bulk density and organic matter content of the selected UNSODA samples are introduced in App. 5. Soil water retention curve, saturated hydraulic conductivity K_s and unsaturated hydraulic conductivity $K(h)$ were available as measured values.

The saturated hydraulic conductivity was estimated using Andersson's method given in Eq. (3-11) and van Genuchten-type function given in Eq. (3-31). The results of the prediction of the saturated hydraulic conductivity function are shown in App. 8/I. In Andersson's method the integration in Eq. (3-11) was carried out from small pipe diameter D_{min} corresponding to pressure head value 15 000 cm up to the pipe diameter D_{max} corresponding to the bubbling pressure h_B . The bubbling pressure was determined using the method suggested by Mualem (1976a). The results obtained using this method (see column K_s , h_B in App. 8/I) gave too low values compared to measured K_s -value. The average value predicted by Eq. (3-11) was 1.67 cm d^{-1} compared to average measured value 189 cm d^{-1} . The biggest difficulty was the estimation of the bubbling pressure, which defines the upper limit for integration in Eq. (3-11). The method proposed by Mualem (1976a) gave in this case too low values for h_B (average value -7.3 cm) compared to optimum bubbling pressure $h_{B,opt}$ (average value -1.1 cm). $h_{B,opt}$ is the optimum bubbling pressure that gives accurate prediction of K_s in Andersson's method (found by trial-and-error method from Eq. (3-11)).

Van Genuchten-type equation (3-36) for predicting K_s -values gave much better results compared to Andersson's equation. Average predicted value was 131.9 cm d^{-1} (column $K_{s,vG}$ in App. 8/I), when the value suggested in the literature for coefficient c_{sat} ($108 \text{ cm}^3 \text{ s}^{-1}$) was used. Optimum value for coefficient c_{sat} is shown in App. 8/I (column $c_{sat,opt}$) indicating that the variation is very big between different samples.

The results of the prediction of the unsaturated hydraulic conductivity function $K(h)$ are shown in Figs. 25 and 26 and in App. 8/II. Saturated value K_s was given as input value in both methods and relative hydraulic conductivity $K_R(h)$ was calculated in the extension of the Andersson's method using Eq. (3-18) and in van Genuchten's method from Eq. (3-31). $K(h)$ was calculated as $K(h) = K_s K_R(h)$. Average error, E_{aver} , shown in App. 8/II is given for the whole range (all measurements) and for three different pressure head ranges representing wet ($0 < h < 100 \text{ cm}$), medium ($100 < h < 500 \text{ cm}$), and dry ($h > 500 \text{ cm}$) ranges. E_{aver} is the absolute value of the average logarithmic error:

$$E_{aver} = \frac{\sum_{i=1}^M |\log(K_{i,m}) - \log(K_{i,c})|}{M_1} \quad (4-3)$$

where $K_{i,m}$ is measured and $K_{i,c}$ is calculated value and M_1 is the number of measurements in the soil sample. According to the results given in App. 8/II, modified Andersson's method gave slightly smaller error for the whole range, $E_{aver} =$

0.75, compared to van Genuchten's method, $E_{aver} = 1.02$. Andersson's method worked better in dry range ($E_{aver} = 0.59$) compared to van Genuchten's method ($E_{aver} = 1.07$). In wet range both methods gave almost the same average error: $E_{aver} = 1.1$ in Andersson's method and $E_{aver} = 1.19$ in van Genuchten's method.

Andersson's method was also tested in the case that the optimum value for the bubbling pressure $h_{B,opt}$ given in App. 8/I was used. The average error, $E_{aver}/h_{B,opt}$, was in this case 0.42 compared $E_{aver} = 0.75$ when Mualem's method (1976) was used to estimate h_B . In van Genuchten's method exponent λ in Eq. (3-29) is 0.5 according to the original theory, but it is also possible to take λ as a parameter. The optimized λ -values are shown in App. 8/II (average optimized value was 1.24) and the average error, E_{aver}/λ_{opt} was 0.61 compared to 1.02 when standard value for λ was used.

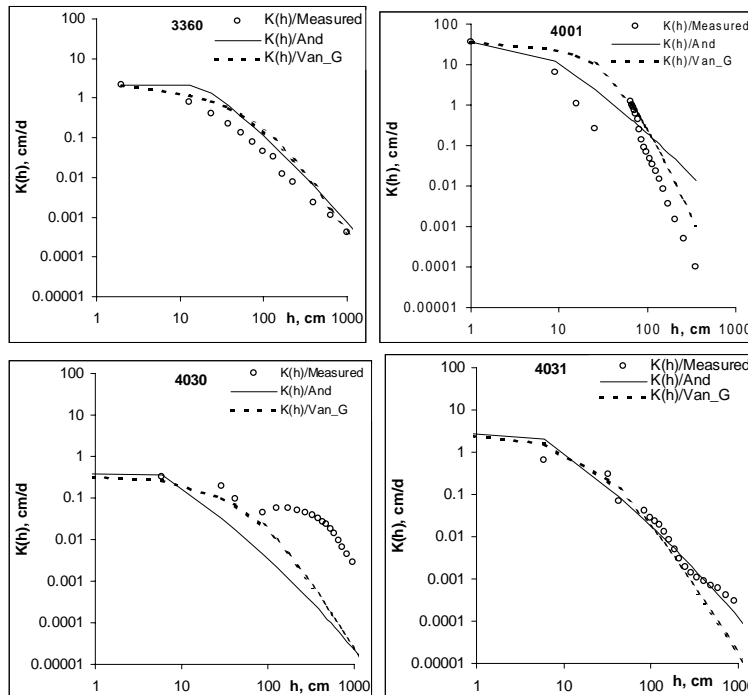


Figure 25. Predictions of hydraulic conductivity function of van Genuchten's and Andersson's equations, a = Hoffmeister Schlag (3360) silt loam soil, b = Lille (4001) sand soil, c = Helecine I (4030) silt loam soil and d = Helecine II (4031) silt loam soil.

Both van Genuchten's and the modified Andersson's method predicted accurately the whole range of the curve of Hoffmeister Schlag's sand soil and Helecine II's silt loam soil (Fig. 25a and d) but gave too large conductivity values in the dry range of the curve of Lille's sand soil (Fig. 25 b).

Hydraulic conductivity functions of Helecline silt loam soils (Fig. 25c and d) resembled each other. Observations of hydraulic conductivity were similar, but both Andersson's and van Genuchten's equations had difficulties in giving reasonable predictions in the dry of the Helecline I soil (4030).

The hydraulic conductivity prediction of Retie I sand soil (Fig. 26a) was successful when Andersson's or van Genuchten's method was used. Only one observation point was difficult to follow in the wet range of the curve. Berse podzol sand soil (Fig. 26b) and Endingen I (Fig. 26d) were problematic for both methods since the measured curves were constantly lower than the predicted curves. The same type of overprediction of conductivity values could be seen also for soils 4052, 4081, 4082, 4091, 4092, 4102 and 4110 (graphs not shown).

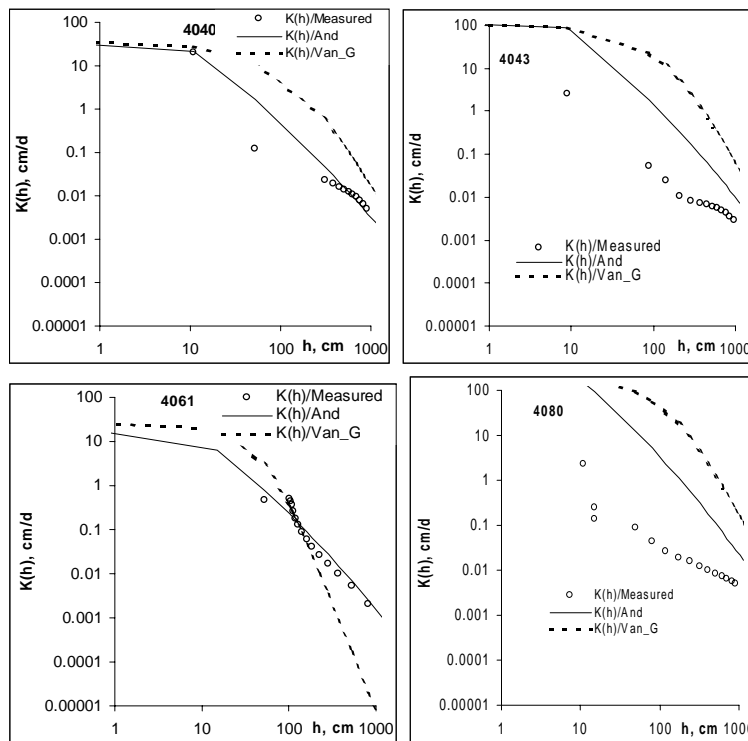


Figure 26. Predictions of hydraulic conductivity function of van Genuchten's and Andersson's equations, a = Retie (4040) sand soil b = Lubbeek II (4043) silt loam soil, c = Berse (4061) podzol sand soil and d = Endingen I (4080) silt loam soil.

4.6 Sensitivity analysis of the water retention characteristics

To examine the relative importance of the four parameters of the models, a one-dimensional sensitivity analysis is performed on various water retention characteristics (Fig. 27).

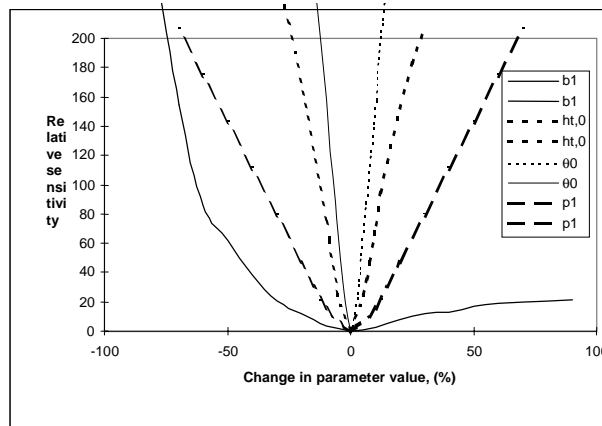


Figure 27. Variation of the relative sensitivity as a function of the percentage of change in parameter value for the four parameters (b , $h_{t,0}$, θ_0 and p) of Andersson's model (Eq. 3-2) for one horizon, plot 1, pit 1.

From the analysis it was concluded that $h_{t,0}$ and θ_0 of Andersson's function were the most sensitive parameters. The least sensitive parameter was b . Parameters p , $h_{t,0}$, and θ_0 showed rather a symmetric linear pattern. Determining the relative importance of $h_{t,0}$ and θ_0 requires accurate estimates of these parameters. The parameter b exhibited a non-symmetric sensitivity. Relative insensitivity for positive perturbation of the parameter value and a strong non-linear sensitivity for negative perturbation were observed. Underestimating these parameter values will result in poorer performance of the model than overestimating them.

Aim of this Chapter is 1) to estimate soil water retention curve $\theta(h)$ and unsaturated hydraulic conductivity curve $K(h)$ from particle size distribution curve and compare the estimated water retention curve with the measured one, and 2) to check the usefulness of the estimation procedures by comparing calculated water balance components with measured values of soil matric potential (pressure head) in forested areas. For agricultural hillslope additional measurements available for comparison are depth to water table, drainage flow and surface runoff. The water balance comparisons are carried out using three different methods to estimate the soil hydraulic properties: 1) estimate $\theta(h)$ and $K(h)$ from PSDC, 2) fit Andersson function to measured $\theta(h)$ -curve and estimate $K(h)$ using Andersson's method, 3) use van Genuchten's function (3-31) to estimate $K(h)$ from $\theta(h)$ -curve. In the method 1) measured soil water retention curve is not utilized at all.

The PSDCs and measured soil water retention curves used in this Chapter were not utilized in the development of the estimation procedures described earlier in Chapter 3 and therefore, in all applications the comparison of estimated water retention curves with the measured curves are shown and used as independent validation data sets for the procedures. Moreover, in water balance calculations the unsaturated hydraulic conductivity curve plays an important role and $K(h)$ -curves from the three methods described above in 1-3 are also shown in order to get a better idea on the influence of the $\theta(h)$ - and $K(h)$ -curves on water balance components of forested and agricultural hillslopes.

5.1 Forested hillslope in Rudbäcken

5.1.1 Estimation of the WRC from the PSDC

The particle size distribution curves were available at depths of 0-0.1 m, 0.1-0.2 m, 0.2-0.3 m and 0.3 m below the humus layer. In the estimation procedure, the PSDCs were used to estimate the WRCs separately for the four depths. In the CROPWATN-model, the humus layer was assumed to be 0.1 m thick. The soil water retention curve of the humus layer was the same than in the experiment carried out in Mämmilampi in Hyytiälä (measured curve). In Section 4.4 it was seen that WRCs of the humus layers do not have large variation. $K_r(h)$ was calculated using the modified

Andersson's method given in Eq. (3-18) and van Genuchten's method given in Eq. (3-31). $K_r(\theta)$ is obtained by replacing the corresponding h with θ obtained from WRC. K_s -value of the humus layer was calibrated and the value was 1.0 m d^{-1} (see Section 5.1.2). In calculations the relative value is multiplied by the saturated hydraulic conductivity K_s to get the value used in the model for calculating the water balance, i.e. $K(h) = K_s K_r(h)$ or $K(\theta) = K_s K_r(\theta)$. The WRC and $K_r(\theta)$ -curves for the humus are shown in Fig. 28. The same curves were used as input data for humus layer in the forested soil profile in Mämmilampi (see Section 5.2).

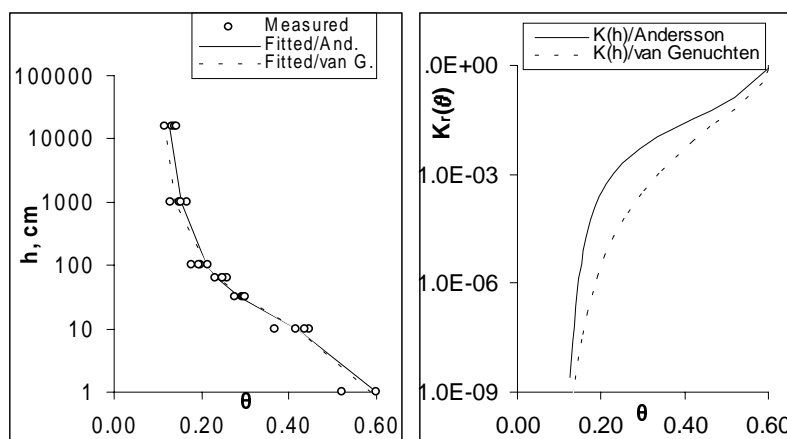


Figure 28. Measured water retention characteristics and estimated curves for the humus layer using Andersson's and van Genuchten's functions and estimated relative hydraulic conductivity, $K_r(\theta)$, of forested hillslope in Mämmilampi.

In this case, the saturated values, θ_s , of the mineral soil were defined as the average of measured saturated water contents; residual water content values, θ_r , were assumed to be 0.02, 0.05, 0.02 and 0.01 for the layers 0-10, 10-20, 20-30 and 30-45 cm, respectively.

The curves estimated from the PSDCs using the modified Andersson's method do not differ very much from the measured curves and generally the agreement with the measured curves is very good. The WRCs estimated from the PSDCs for the four different depths are shown in Figs. 29 - 31, together with the measured data and Andersson's (Eq. 3-25) and van Genuchten-type (Eq. 3-40) functions fitted to them.

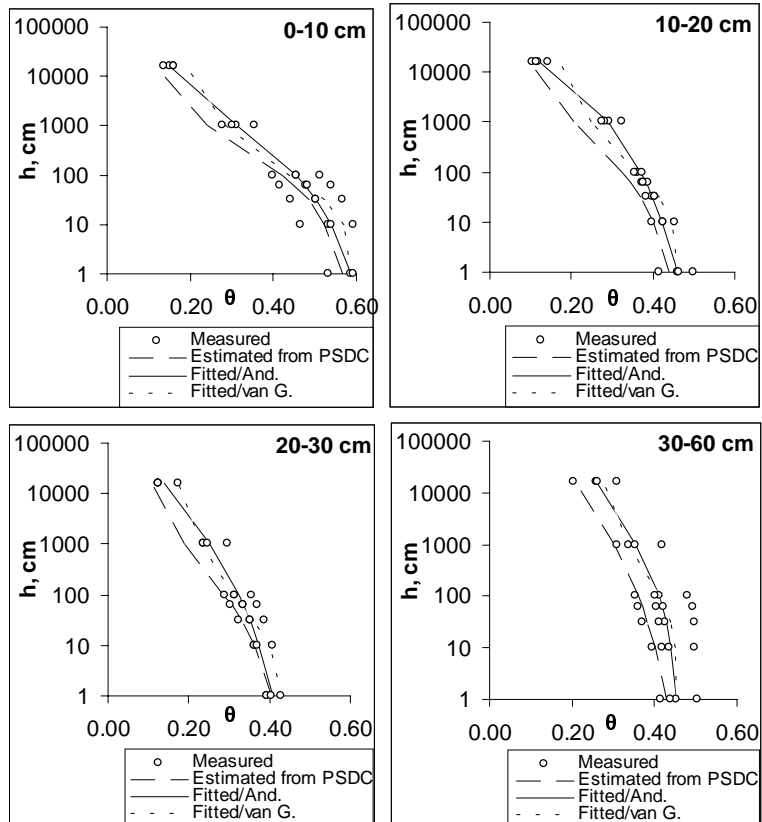


Figure 29. Measured water retention characteristics and curve estimated from the PSDC for the lower part of the forested hillslope in Siuntio. Fitted curves using the Andersson's and van Genuchten's functions are also shown.

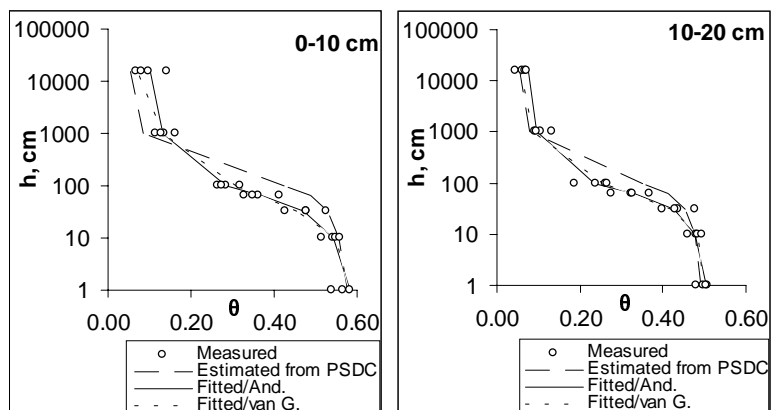


Figure 30/I. Measured water retention characteristics and curve estimated from the PSDC. Fitted curves using the Andersson's and van Genuchten's functions are also shown (middle part of the forested hillslope in Siuntio).

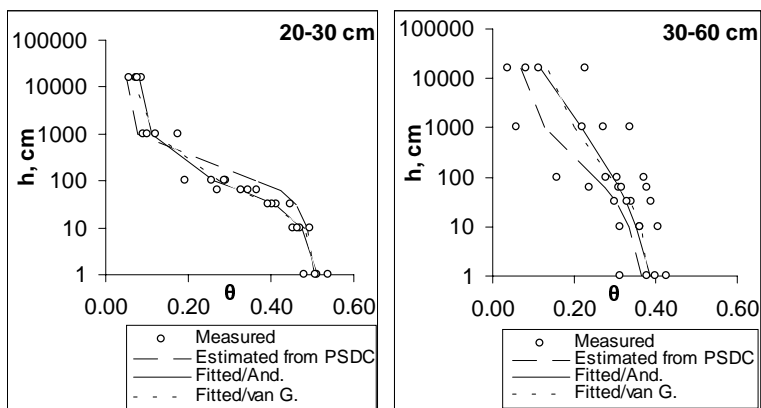


Figure 30/II. Measured water retention characteristics and curve estimated from the PSDC. Fitted curves using the Andersson's and van Genuchten's functions are also shown (middle part of the forested hillslope in Siuntio).

5.1.2 Comparison of unsaturated hydraulic conductivity

Measured values for unsaturated hydraulic conductivity were not available; three different curves for $K_r(\theta)$ -values were calculated (see Figs. 32 - 34). The calculations were carried out using three different options (Chapter 3.9) for the soil hydraulic properties. In option 1) the water retention curve was estimated from the particle size distribution curve and $K_r(h)$ was calculated using the modified Andersson's method given in Eq. (3-18).

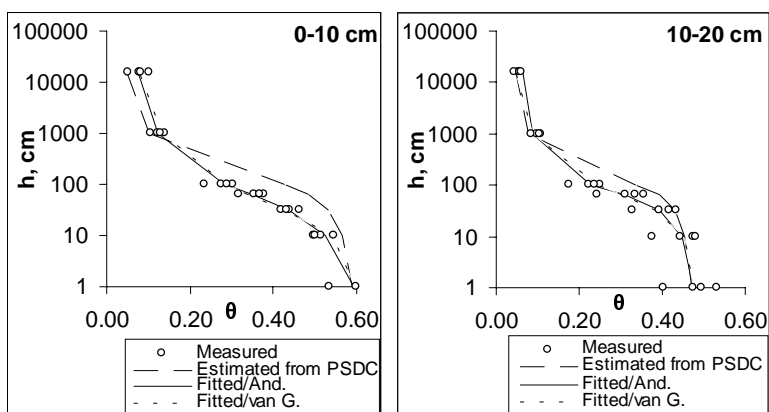


Figure 31/I. Measured water retention characteristics and curve estimated from the PSDC. Fitted curves using the Andersson's and van Genuchten's functions are also shown (upper part of the forested hillslope in Siuntio).

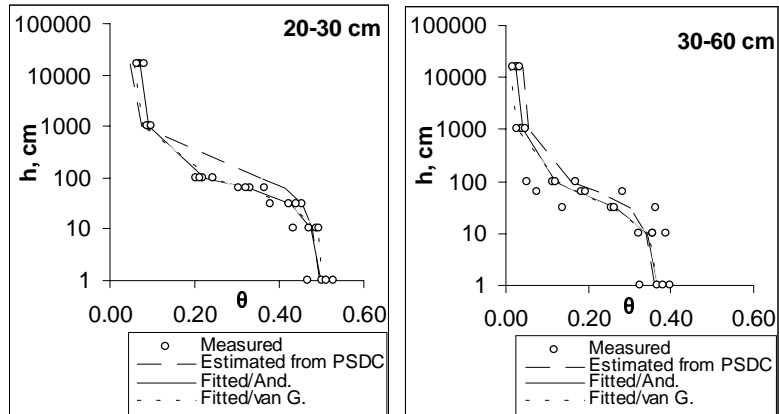


Figure 31/II. Measured water retention characteristics and curve estimated from the PSDC. Fitted curves using the Andersson's and van Genuchten's functions are also shown (upper part of the forested hillslope in Siuntio).

In methods 2) and 3) measured WRC was used and in method 2) $K_R(h)$ was estimated using Eq. (3-18) and in option 3) $K_R(h)$ was estimated using van Genuchten's function (3-31). K_S -values were calibrated both for the humus layer and the mineral soil.

For humus layer the value was 1.0 m d^{-1} , and K_S -values for the lower part of the hillslope were $0.2 - 0.5 \text{ m d}^{-1}$ and $0.5 - 0.6 \text{ m d}^{-1}$ for the middle and upper parts of the hillslope, respectively.

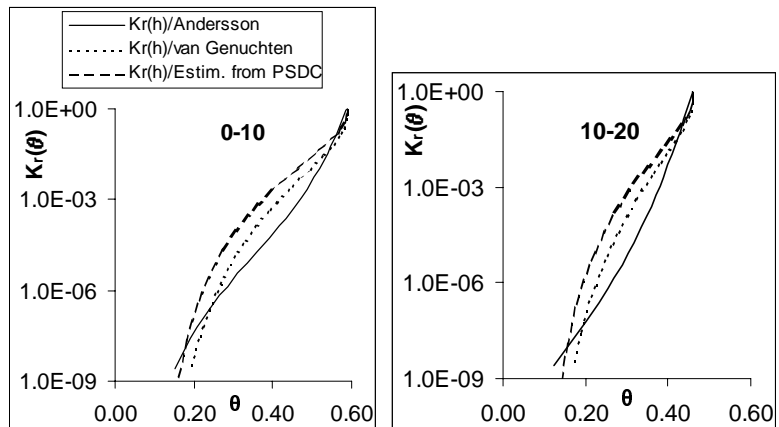


Figure 32/I. Estimated relative hydraulic conductivity curves for the lower part of the forested hillslope in Siuntio using $K(\theta)$ estimated from the PSDC, Andersson's and van Genuchten's functions.

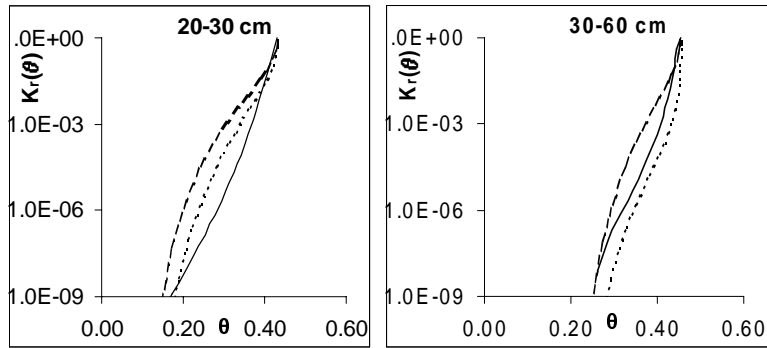


Figure 32/II. Estimated relative hydraulic conductivity curves for the lower part of the forested hillslope in Siuntio using $K(\theta)$ estimated from the PSDC, Andersson's and van Genuchten's functions.

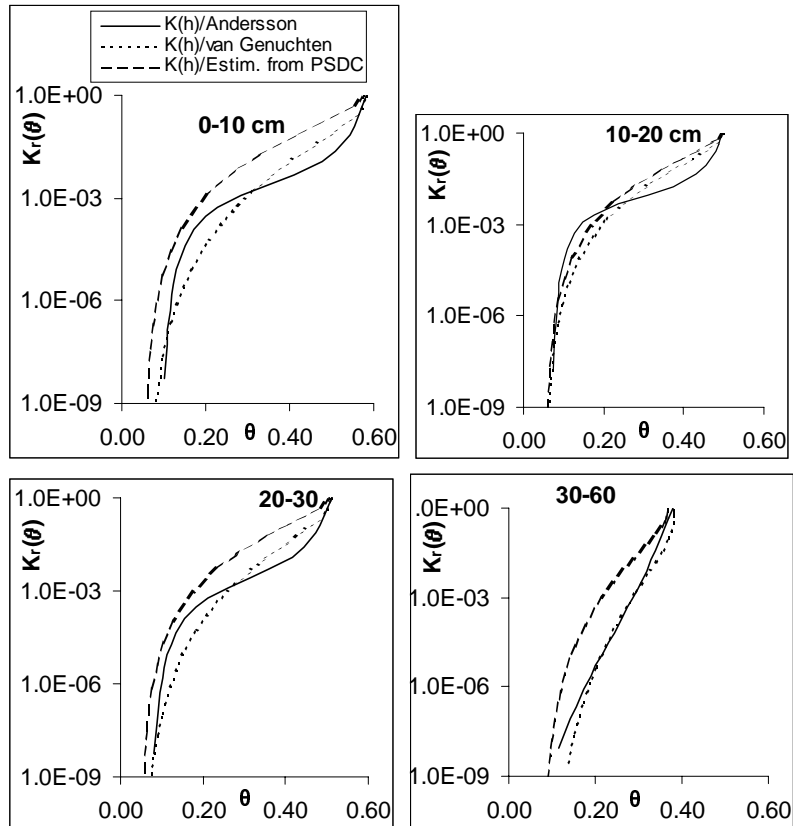


Figure 33. Estimated relative hydraulic conductivity curves for the middle part of the forested hillslope in Siuntio using $K(\theta)$ estimated from the PSDC, Andersson's and van Genuchten's functions.

The results indicate that the three estimated curves differ distinctly from each other. The curve estimated from the PSDC gave on the average bigger relative values compared to the two other curves. The two other curves based on the fitted WRCs differ from each other especially near the saturation part of the curves. The influence of the WRC and $K(\theta)$ -curves on the water balance of the hillslope will be discussed in Section 5.1.3.

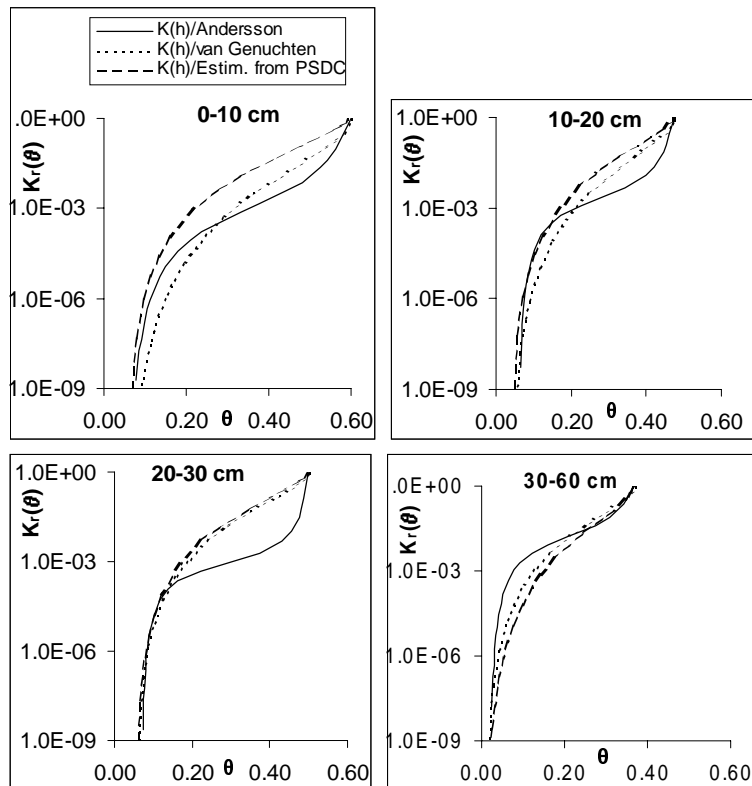


Figure 34. Estimated relative hydraulic conductivity curves for the upper part of the forested hillslope in Siuntio using $K(\theta)$ estimated from the PSDC, Andersson's and van Genuchten's functions.

5.1.3 Comparison of measured and estimated pressure heads in Rudbäcken hillslope

The next step in testing the estimation of the WRC and unsaturated hydraulic conductivity curves was to compare the calculated soil matric potential values using the CROPWATN-model with the measured values at depths of 0.05, 0.25 and 0.5 m below the humus layer.

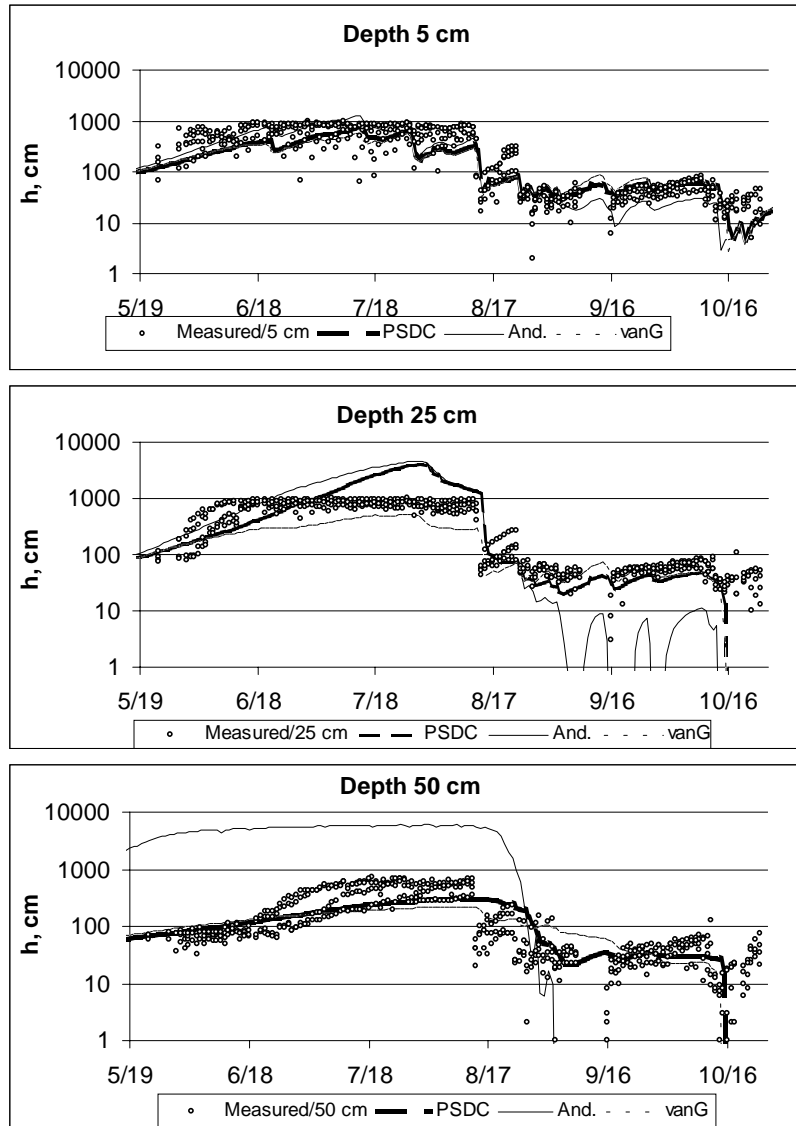


Figure 35/II. Measured and calculated pressure heads at three different depths in the lower part of the forested hillslope in Siuntio. Hydraulic properties estimated from a) the PSDC (WRC estimated from the PSDC) b) using Andersson's functions (WRC fitted to data) c) using van Genuchten's functions (WRC fitted to data).

Measured and calculated pressure head values for the lower part of the hillslope are shown in Fig. 35 for the options 1), 2) and 3) (Chapter 3.6.1). The best overall results were obtained using options 1) and 3). In option 2), the prediction failed for depth 0.5 m, indicating that the $K(h)$ -curve at some

depth was not properly estimated. It is not clear, however, which one of the curves shown in Fig. 32 is the reason for poor modelling results at the depth of 0.5 m. It can be seen that the soils are drier than the measured values because the reliable measurement range of the tensiometer is about 0 – 700 cm.

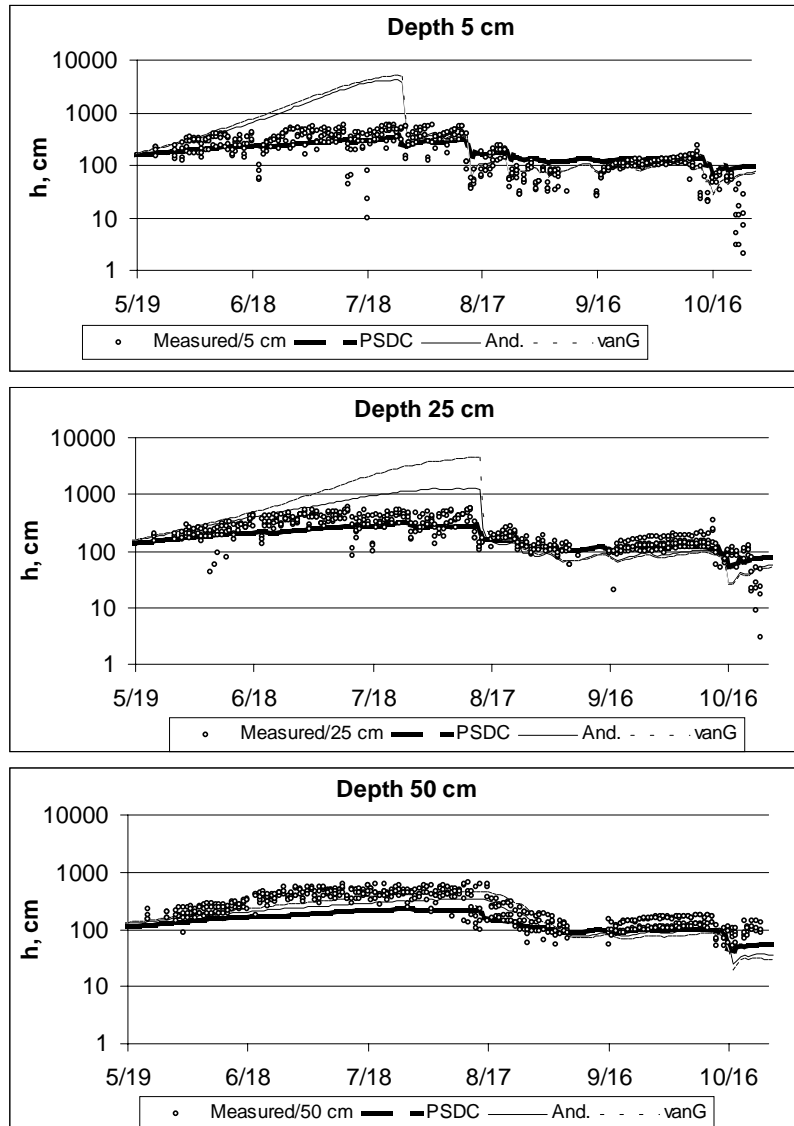


Figure 36. Measured and calculated pressure heads at three different depths in the middle part of the forested hillslope in Siuntio. Hydraulic properties estimated a) from the PSDC b) using Andersson's functions (WRC fitted to data) c) using van Genuchten's functions (WRC fitted to data).

Measured and calculated pressure head values for the middle part of the hillslope are shown in Fig. 36 for options 1), 2) and 3). The best results were obtained using option 1). Both option 2) and 3) predicted a profile that was too dry at depths of 0.05 and 0.25 m below the humus layer. Andersson's function fitted to the WRC data, option 2), was now successful in predicting the soil matric potential values properly at the depth of 0.5 m.

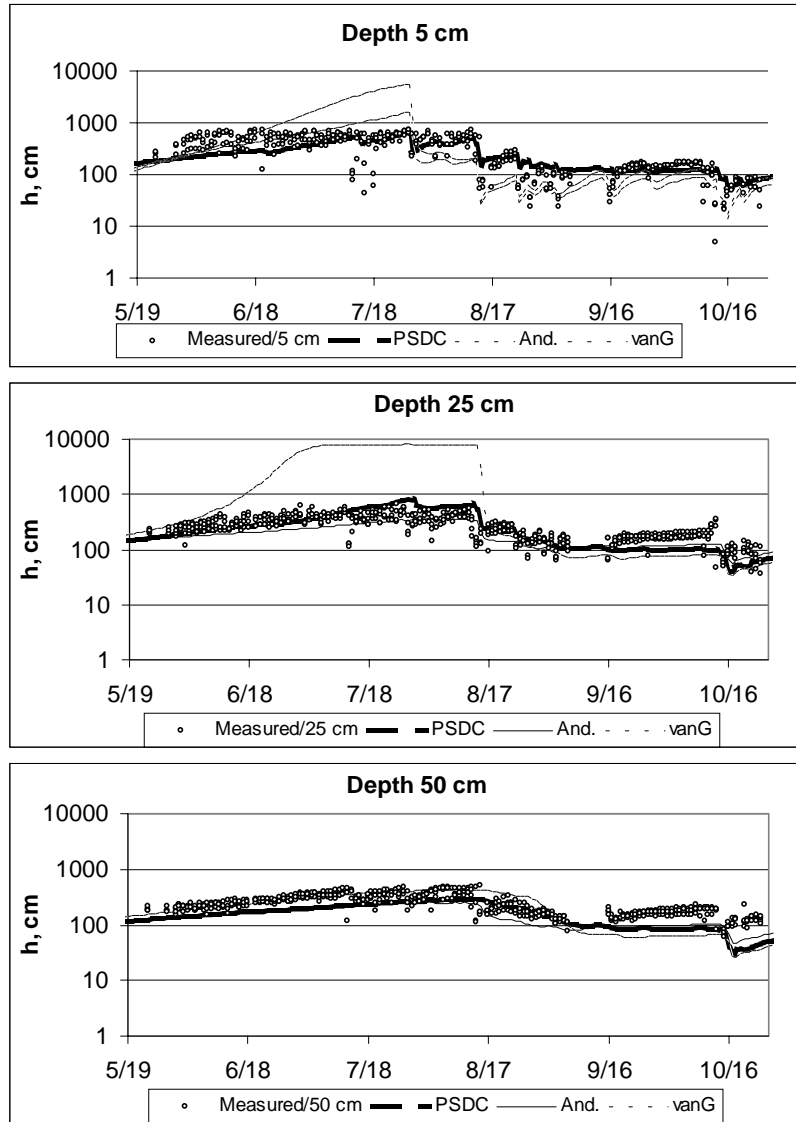


Figure 37. Measured and calculated pressure heads at three different depths in the upper part of the forested hillslope in Siuntio. Hydraulic properties estimated a) from the PSDC. b) using Andersson's functions (WRC fitted to data) c) using van Genuchten's functions (WRC fitted to data).

Measured and calculated pressure head values for the upper part of the hillslope are shown in Fig. 37 for the options 1), 2) and 3). Again, the best overall results were obtained using options 1), but option 2) also gave quite good results. On the contrary, option 3) gave a profile that was too dry especially at the depth of 0.25 m but the soil surface was also too dry (at the depth of 0.05 m). The main reason for this is the difference in the water retention curves. Moreover, in option 3) the relative hydraulic conductivity is about ten times smaller in the dry end of the WRC in the upper layers.

5.2 Forested soil profile in Mämmilampi, Hyytiälä

5.2.1 Setting up the model

The soil profile was taken to be 5.0 m thick and with an initial depth to groundwater level known to be around 3-5 m and 4.0 m was selected. The soil profile was divided into 20 layers. The thickness of the humus layer was assumed to be 0.1 m divided to three uniform layers, 0.02, 0.04 and 0.04 m. Below the humus layer, 0.05 m thick nodes were used to a depth of 0.6 m, while below that the thickness of the layer increased gradually from 0.1 m to 0.6 m so that the total thickness of the profile was 5.0 m. Measured PSDC and water retention curves were available from the mineral soil below the humus layer at depths of 0-0.1 m, 0.1-0.2 m, 0.2-0.3 m; the fourth curve was assumed to represent the profile below 0.3 m.

5.2.2 Estimation of soil hydraulic properties from the PSDC

The soil water retention curves estimated from the PSDC compared to the measured curves are shown in Fig. 38, indicating that it was possible to predict the WRCs from the particle size distribution curves. The curves estimated from the PSDC had a smaller $d\theta/dh$ near saturation, which has importance in water balance calculations. The $K(h)$ -curves estimated using the three methods (options described in Section 5.1.2) are shown in Fig. 39. A prominent feature with the curves is that van Genuchten's function, option 3), gave a considerably smaller relative value for unsaturated hydraulic conductivity, while the small value had a very clear effect on the water balance calculations described in Section 5.2.3.

For humus layer water retention curve and the hydraulic conductivity function were the same that were used in the Siuntio profile (see Fig. 28). For mineral soil the saturated hydraulic conductivity values were calibrated and value 1.4 m d^{-1} was used for depths smaller than 0.30 m and 0.7 m d^{-1} below that. As shown later on, the simulations with the above mentioned K_s -values were quite good for options 1) and 2), but failed for option 3) due to the fact that the relative values of $K_r(h)$ were very small compared to the $K(h)$ -curves estimated using Andersson's method.

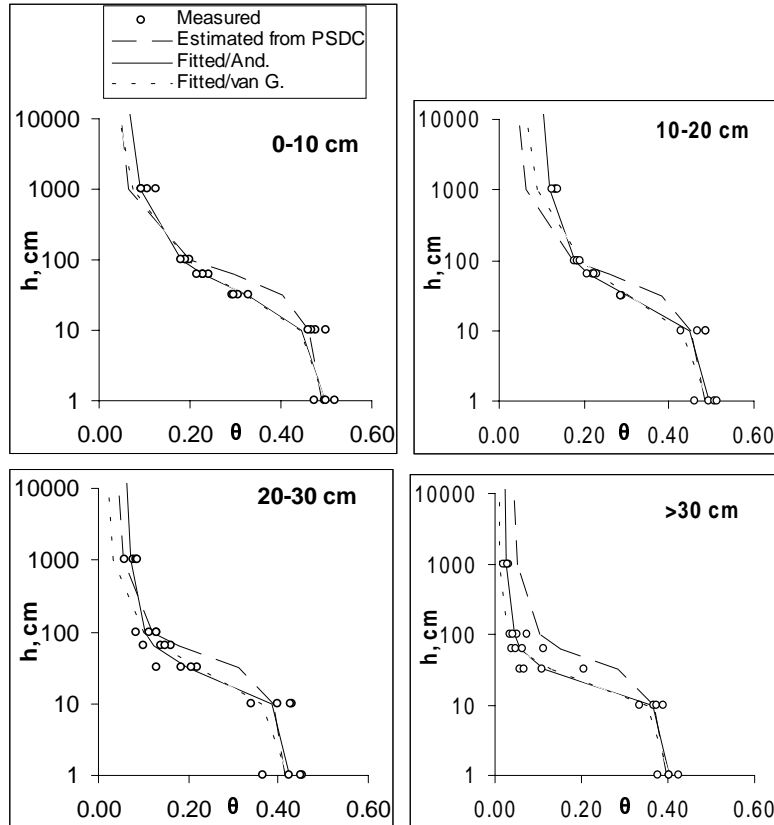


Figure 38. Measured water retention characteristics and curve estimated from the PSDC. Fitted curves using the Andersson's and van Genuchten's functions are also shown (forested profile in Hyttiälä).

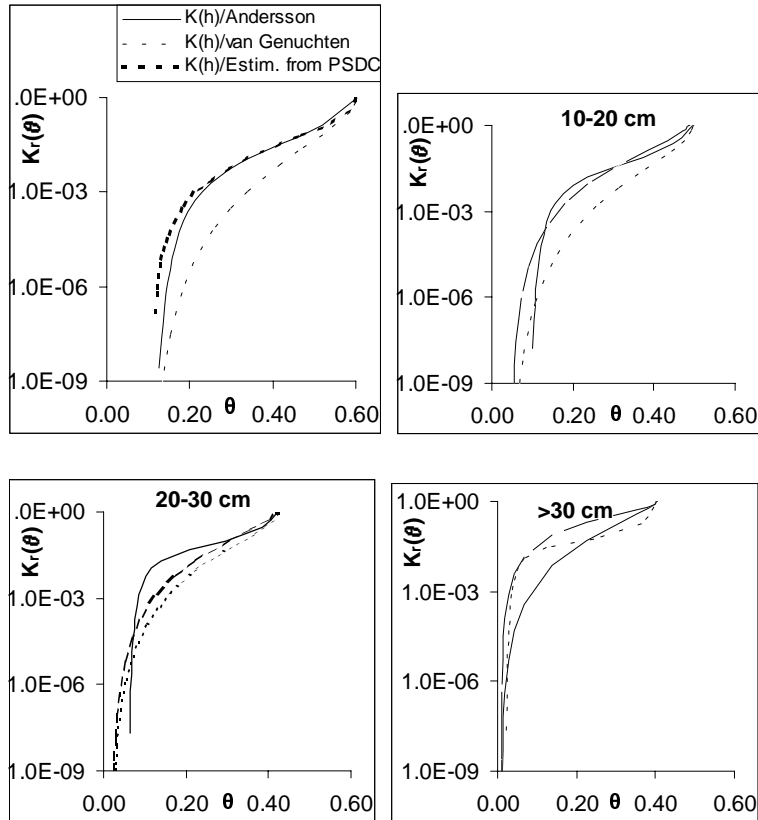


Figure 39. Estimated relative hydraulic conductivity curves for the soil profile in Hyytiälä using $K(\theta)$ estimated from the the PSDC, Andersson's and van Genuchten's functions.

5.2.2 Comparison of measured and calculated pressure heads

The results of the calculation of the soil matric potential for three different depths, immediately below and 0.2 and 0.4 m below the humus layer, are shown in Figs. 40 - 42 for the three different methods for estimating the soil hydraulic properties. In the profile, depth to groundwater level is around 4 m throughout the calculation period indicating that the profile is unsaturated all the time below the observation depths (0.4 m), showing that the shape of the unsaturated hydraulic conductivity function plays a key role in the calculation of the water balance.

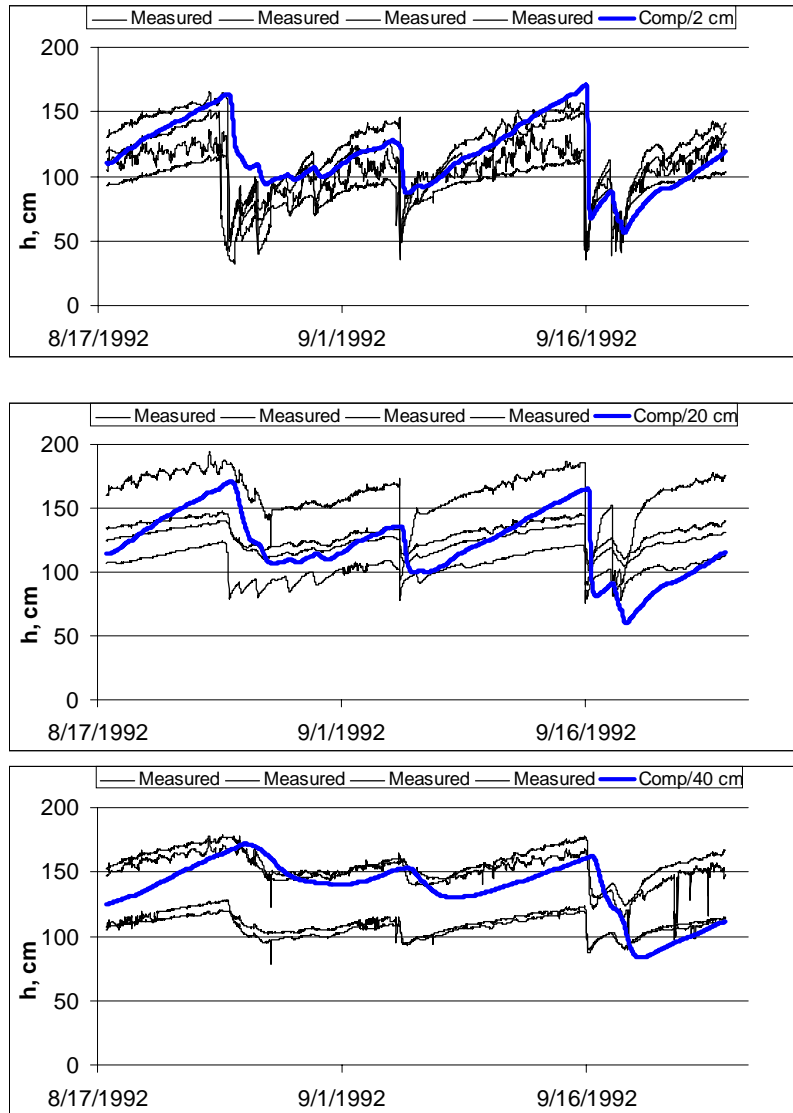


Figure 40. Four separately measured tensiometers and calculated pressure heads in Hyytiälä at three different depths using hydraulic properties estimated from the PSDC (option 1). Upper curve 2 cm below the humus layer, middle curve 20 cm below the humus layer and lower curve 40 cm below the humus layer.

The results obtained using option 1) (Fig. 40) were better than the results from option 2), shown in Fig. 41, which means that, in this case, the $K_r(h)$ -curve estimated from the predicted WRC proved to give better results. Several computer runs were made to find out if a change in K_s -value would improve the results obtained using option 2), but the results shown in Fig. 41 were the best.

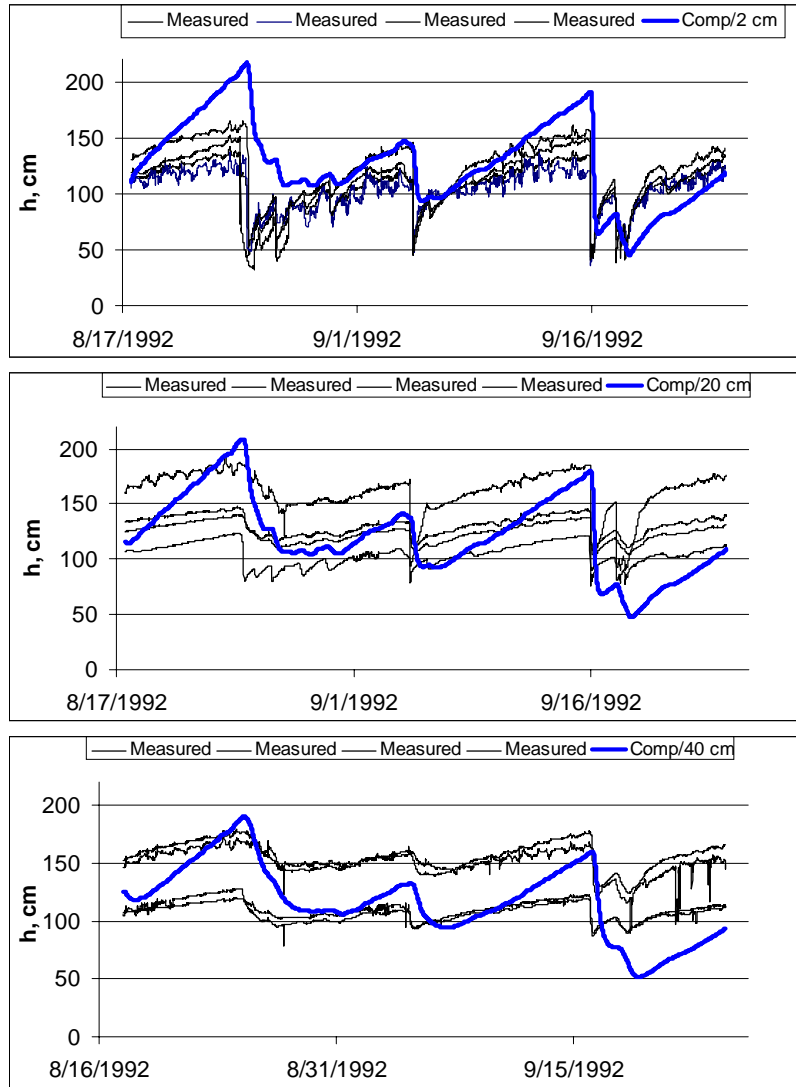


Figure 41. Four separately measured tensiometers and calculated pressure heads in Hyytiälä at three different depths using hydraulic properties estimated using Andersson’s method (option 2). Upper curve 2 cm below the humus layer, middle curve 20 cm below the humus layer and lower curve 40 cm below the humus layer.

The pressure head values calculated using option 3) shown in Fig. 42 were too high (i.e. pressure head values too close to zero) at depths 0.2 and 0.4 m after the heavy rains started at the end of August. The reason for this is that $K_r(h)$ was too low and the infiltrated water could not flow towards the groundwater level fast enough.

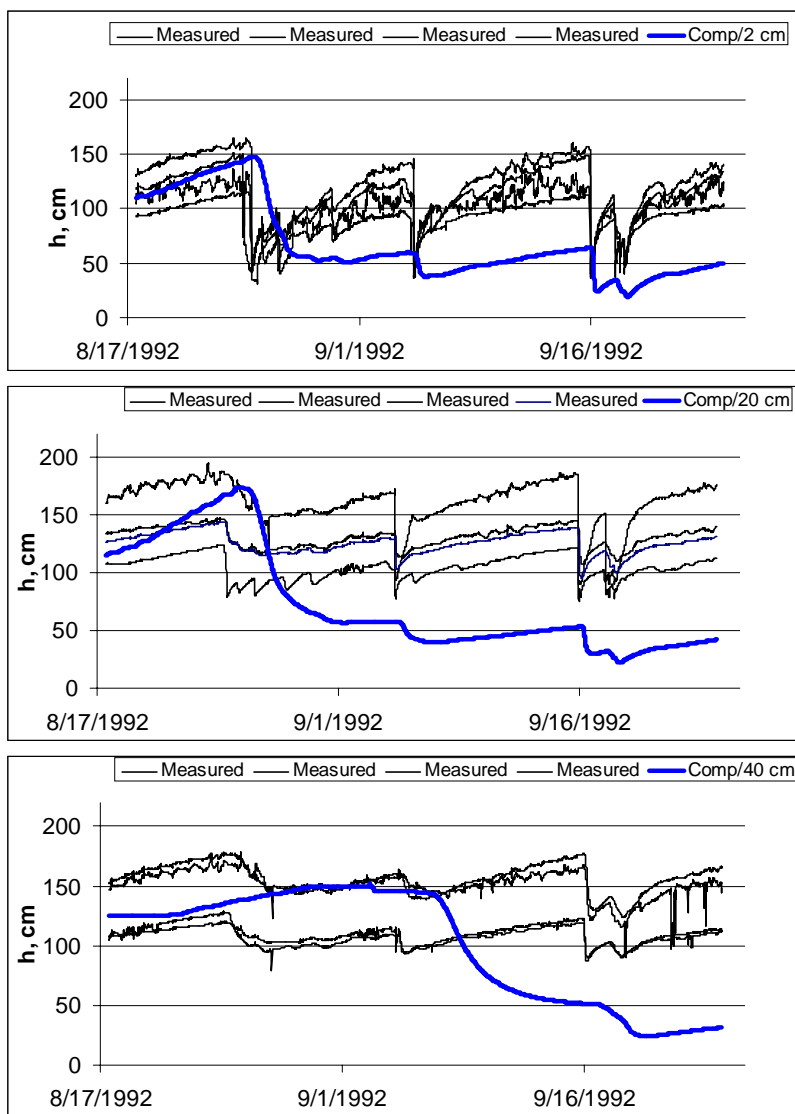


Figure 42. Four separately measured tensiometers and calculated pressure heads in Hyytiälä at three different depths using hydraulic properties estimated using van Genuchten's method (option 3). Upper curve 2 cm below the humus layer, middle curve 20 cm below the humus layer and lower curve 40 cm below the humus layer.

The results shown in Fig. 43 confirm the conclusion that the $K_r(h)$ -curve estimated using option 3) gave too small K_s -values since very good results could be obtained when unrealistically high K_s -values were selected. The pressure heads shown in Fig. 43 were calculated using K_s -value equal to $1\ 500\ \text{m d}^{-1}$ in mineral soil, which is definitely too high for this profile.

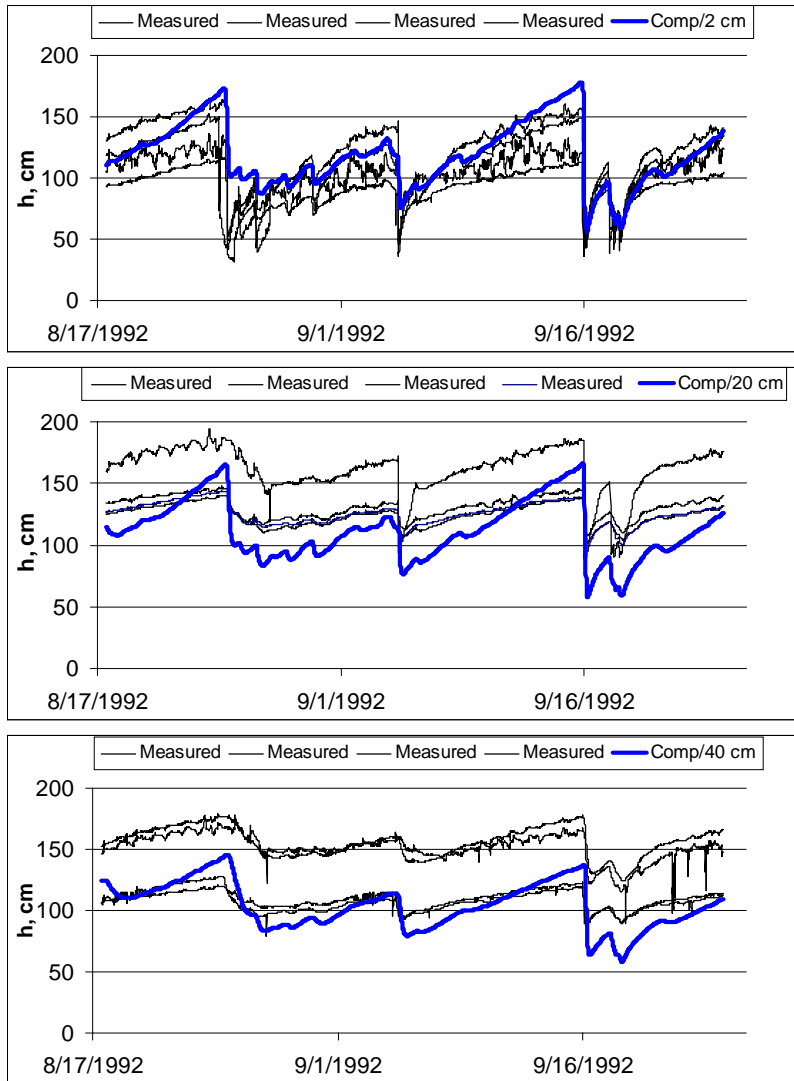


Figure 43. Four separately measured tensiometers and calculated pressure heads in Hyytiälä at three different depths using hydraulic properties estimated using van Genuchten's method (option 3 with very large K_s -value). Upper curve 2 cm below the humus layer, middle curve 20 cm below the humus layer and lower curve 40 cm below the humus layer.

5.3 Sjöckulla experimental field

5.3.1 Estimation of the WRC from the PSDC

The measured PSDCs are shown in Fig. 44 for four different depths indicating that the clay fraction is high both in topsoil, 38-44 %, and in subsoil, 40-50 %. Measured water retention curves were available from depths 0.05-0.1 m, 0.35-0.4 m and 0.65-0.7 m. In the estimation procedure, the PSDCs were used to estimate the WRCs separately for the three depths. In the CROPWATN-model, the first curve was used for the layer 0-0.3 m, the second curve for the layer 0.3-0.6 m and the third curve for the layer 0.6-2.85 m. In the estimation procedure described in Section 3.6.3, it is necessary to give as input data the saturated water content θ_s and residual water content θ_r . In this case, the saturated values were defined as the average values of measured saturated water content from 3-6 samples (Paasonen-Kivekäs 2000: $\theta_s = 0.50 \text{ (m}^3 \text{ m}^{-3})/0.05 - 0.1 \text{ m}$, $\theta_s = 0.425/0.35 - 0.4 \text{ m}$ and $\theta_s = 0.53/0.65 - 0.7 \text{ m}$.

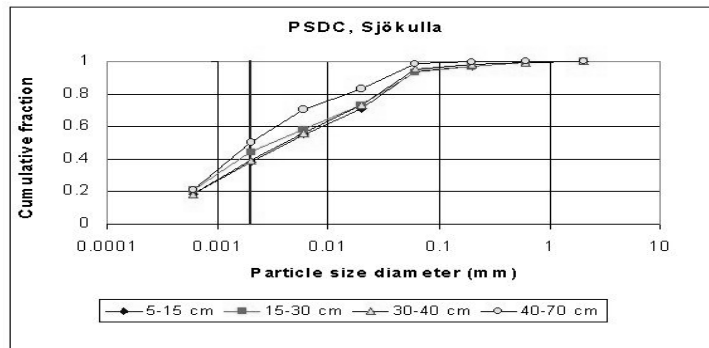


Figure 44. Measured particle size distribution curves at four different depths in the Sjöckulla experimental field.

The residual water content was estimated using regression equations given by Karvonen (1988): $\theta_r = 0.023 + 0.00434F_{CLAY}$ for topsoil and $\theta_r = 0.04 + 0.00423F_{CLAY}$ for subsoil, where F_{CLAY} is the amount of clay in the sample (%).

The values obtained for different layers were as follows: $\theta_r = 0.20 \text{ (m}^3 \text{ m}^{-3})/0.05 - 0.1 \text{ m}$, $\theta_r = 0.21/0.35 - 0.4 \text{ m}$ and $\theta_r = 0.25/0.65 - 0.7 \text{ m}$. The estimated WRCs for the three different depths are shown in Fig. 45 together with the measured values. Moreover, Andersson's function, Eq. (3-2), and van Genuchten-type water retention values, Eq. (3-28), were fitted to the measured data; the results are also shown in Fig. 45. The curves estimated from the PSDCs using the

modified Andersson's method deviate slightly from the measured curves at the dry end of the curve. The main reason for this deviation is that the estimated residual water content forces the curve to bend at high absolute values of the pressure head.

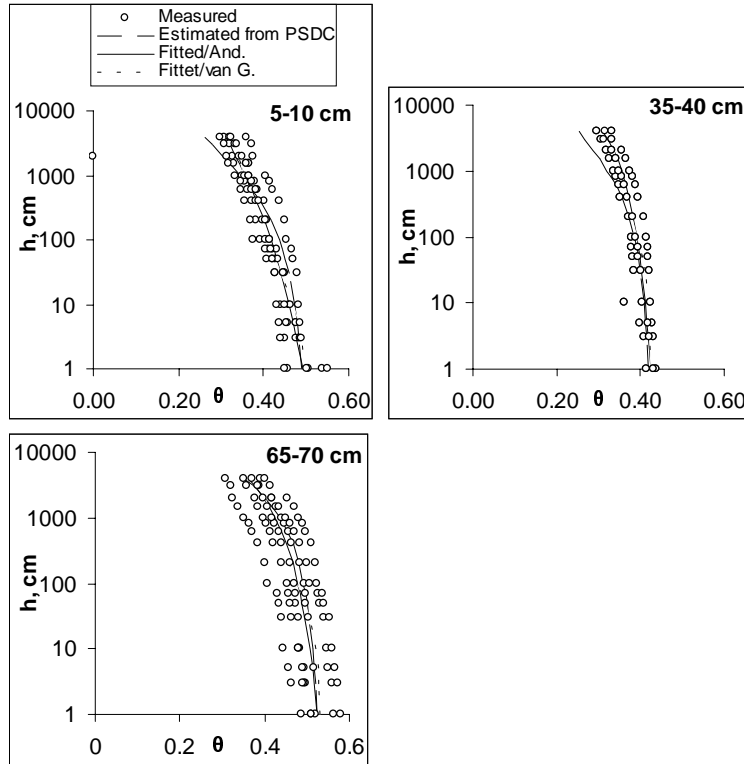


Figure 45. Measured water retention characteristics and estimated WRCs fitted to Sjøkulla experimental data, a) depth 5-10 cm, b) 35-40 cm and c) 65-70 cm.

5.3.2 Comparison of unsaturated hydraulic conductivity

Measured values for unsaturated hydraulic conductivity were not available and three different curves for relative $K_r(\theta)$ -values were calculated (see Fig. 46): 1) the first curve was calculated from the water retention curve estimated from the PSDC using Andersson's method (denoted as $K(\theta)$ /Estimated from the PSDC in Fig. 46), 2) the second curve was calculated from the WRC fitted to observed data using Andersson's method (denoted as $K(\theta)$ /Andersson in Fig. 46) and 3) the third curve was calculated using the van Genuchten-model (denoted as $K(\theta)$ /van Genuchten in Fig.

46). In calculations, the relative value is multiplied by the saturated hydraulic conductivity K_s to get the value used in the model for calculating the water balance, i.e. $K(\theta) = K_s K_r(\theta)$.

The results indicate that the three estimated curves differ distinctly from each other. The curve estimated from the PSDC gave on average relative values at least 10 times greater than the other two curves. The other two, based on the fitted WRCs, differ from each other especially near the saturation part of the curves. Moreover, the curves at depth of 0.05-0.1 m are at different levels over the whole water content range.

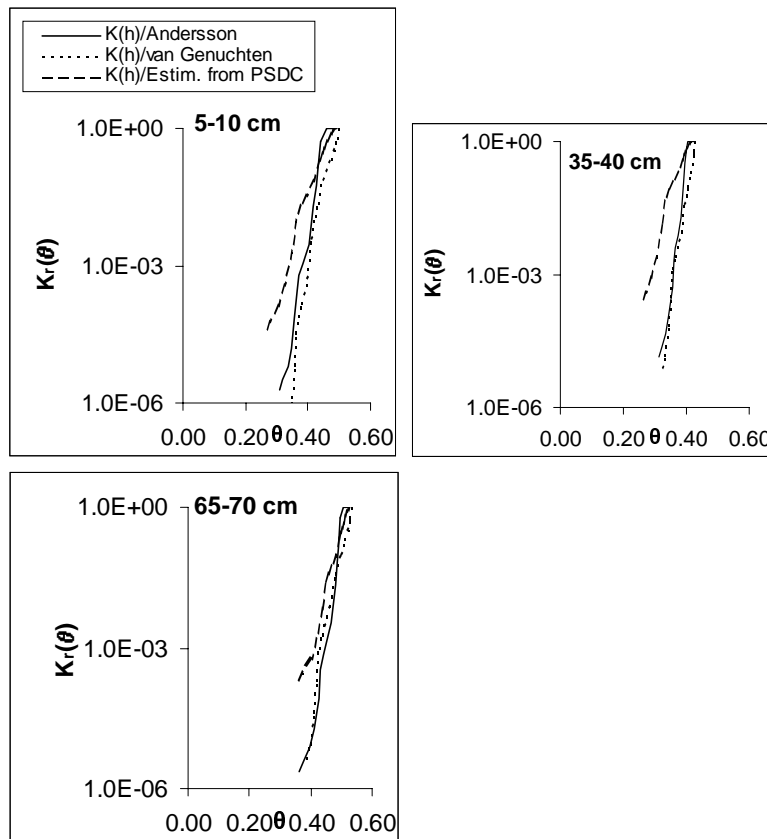


Figure 46. Estimated relative unsaturated hydraulic conductivity curves: 1) using the modified Andersson's method (solid line) 2) using the van Genuchten-type function (dotted line), and 3) estimated from particle size distribution curve at Sjökulla (dashed line), a) depth 5-10 cm, b) 35-40 cm and c) 65-70cm.

In Andersson's method, the relative value $K_r(h)$ equals the saturated value for soil matric potential values greater than

the bubbling pressure h_b discussed in Chapter 3.3.3. In the curves estimated for the Sjökkulla profile, the following values for the bubbling pressure were obtained: $h_b = 0.16$ m, $h_b = 0.50$ m and $h_b = 0.18$ m. The van Genuchten-type function gave a very fast decrease for $K(h)$ near saturation. For example, for the curve at a depth of 0.65-0.7 m, the relative value of $K_r(h = 0.01$ m) was 0.158 and $K_r(h = 0.03$ m) was 0.087, i.e. less than 9 % of the saturated value in near-saturated conditions (with soil matric potential value close to zero tension). This type of behaviour in near-saturated conditions is quite typical for the van Genuchten-type equation when parameter α is small. The implications of the shape of the $K_r(h)$ -curve for water balance calculations will be discussed in Section 5.4.4.

5.3.3 Calculation of the water balance components of an agricultural hillslope

The next step in testing the estimation of the WRC and unsaturated hydraulic conductivity curves was to calculate the water balance of the Sjökkulla agricultural hillslope using the CROPWATN-model (Chapter 3.9). The WRC and relative hydraulic conductivity curves corresponding to options 1 - 3 are shown in Figs. 45 and 46.

The calculations were done both with and without the macropore sub model. In the case when macropores were included, the saturated hydraulic conductivity of the soil matrix was assumed to be 0.003 m h⁻¹ (7.2 cm d⁻¹) in the topsoil layer (0-0.30 m), 0.001 m h⁻¹ (2.4 cm d⁻¹) in the layer between 0.3 and 0.6 m and 0.0005 m h⁻¹ (1.2 cm d⁻¹) below 0.6 m (Mecke and Ilvesniemi 1999). When macropores were not included in the calculations, it was necessary to use much higher values for the saturated hydraulic conductivity of the soil matrix since in the single-porosity model the only way to handle the influence of macropores is to increase the saturated value for the hydraulic conductivity. Otherwise, too much surface runoff would be produced. The K_s -values in the single-porosity option were as follows: 0.03 m h⁻¹ (72 cm d⁻¹) at layer 0-0.3 m, 0.02 m h⁻¹ (48 cm d⁻¹) at layer 0.30-0.6 m and 0.001 m h⁻¹ (2.4 cm d⁻¹) at layer 0.60-3.0 m. The influence of the macropores was small, below the depth of 0.6 m, which is compatible with the decrease of the hydraulic conductivity of the macropores with increased depth (see Eqs. (3-40) and (3-41)).

5.3.3.1 Lower part of the hillslope, macropore model included

The measured and calculated depths of the water table are shown in Fig. 47 for the three different parameterisations of the soil hydraulic properties. The first option, which used only the PSDC gave the best fit between measured and computed values. The results obtained using the other two options based on fitting the water retention curve to measured data showed that variation of groundwater level as a function of time could not be reproduced by the model. The main reason for this was that the unsaturated hydraulic conductivity values from the curves in options 2) and 3) were around ten percent of $K(\theta)$ -values estimated using option 1) and therefore, the upward flux from the water table is reduced very fast when θ decreases. The results given by options 2) and 3) did not differ very much from each other.

The main reason for the difference between the $K(\theta)$ -curves of option 1) and options 2) and 3) is that measured water retention curves implicitly include the influence of macropores; therefore the slope of the curve near saturation is different from the curve obtained from option 1) and the estimated $K(\theta)$ decreases too fast compared to option 1). In option 1), the PSDC is used and the influence of macropores is not included in the estimation of the water retention curve. In this case, it can be claimed that the curve estimated from the PSDC more closely describes the WRC of the soil matrix.

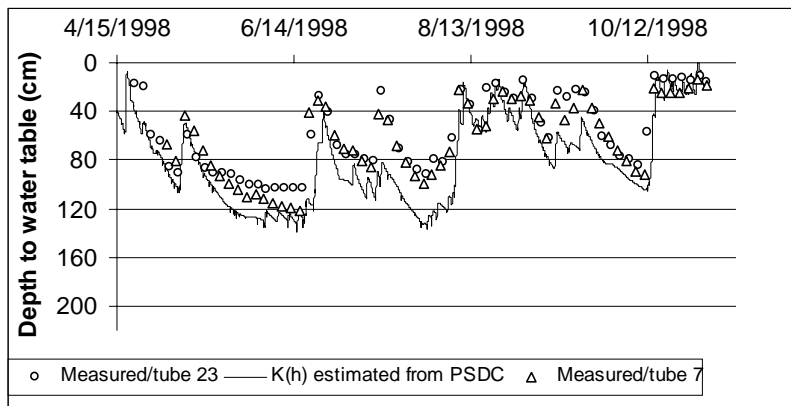


Figure 47/I. Measured and computed depth to water table using three different options of modelling unsaturated hydraulic conductivity (Sjökulla, lower part of the agricultural hillslope, macropores included in the model).

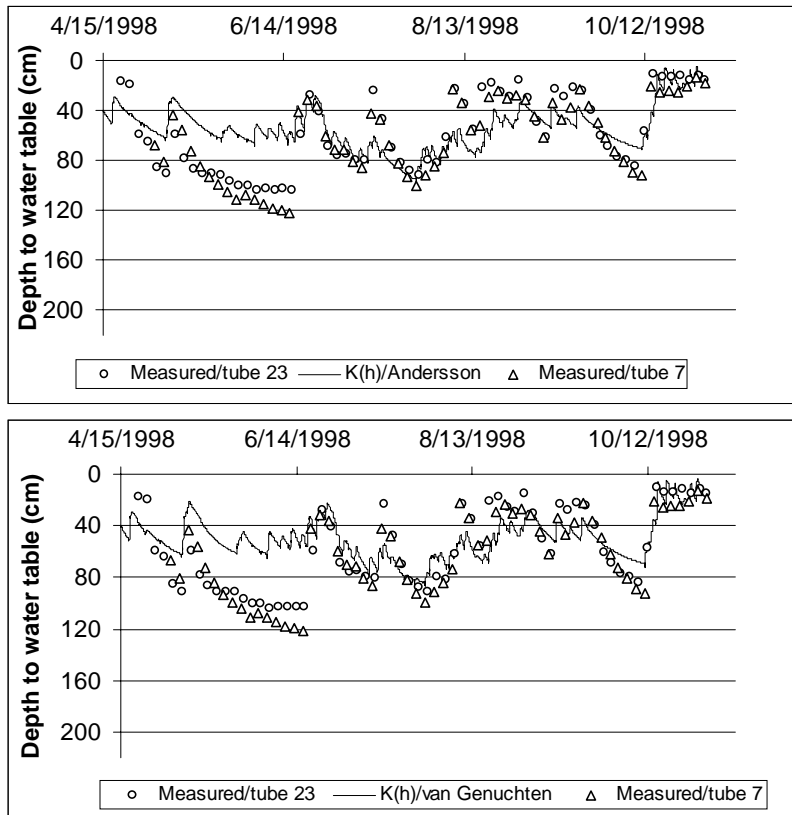


Figure 47/II. Measured and computed depth to water table using three different options of modelling unsaturated hydraulic conductivity (Sjökulla, lower part of the agricultural hillslope, macropores included in the model).

The comparison of calculated values of drainage flux and surface runoff with measured values are shown in Figs. 48 and 49. The simulated cumulative drainage flux using option 1), $K(h)$ estimated from the PSDC, is very close to the measured value and cumulative surface runoff is also calculated quite well with this option.

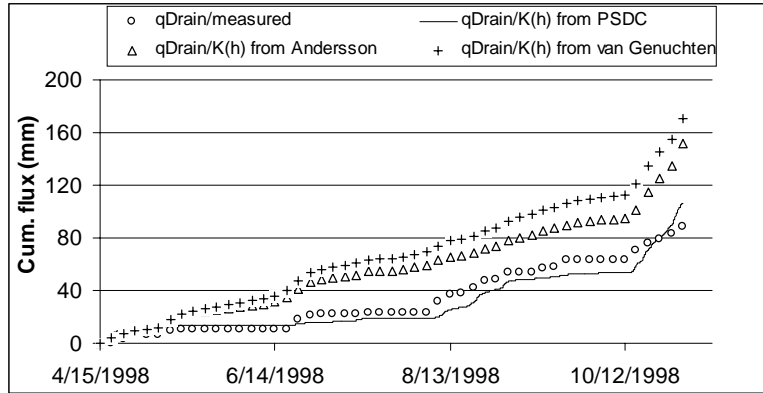


Figure 48. Measured and computed cumulative drainage flux using three different options of modelling unsaturated hydraulic conductivity (Sjökulla, lower part of the agricultural hillslope, macropores included in the model).

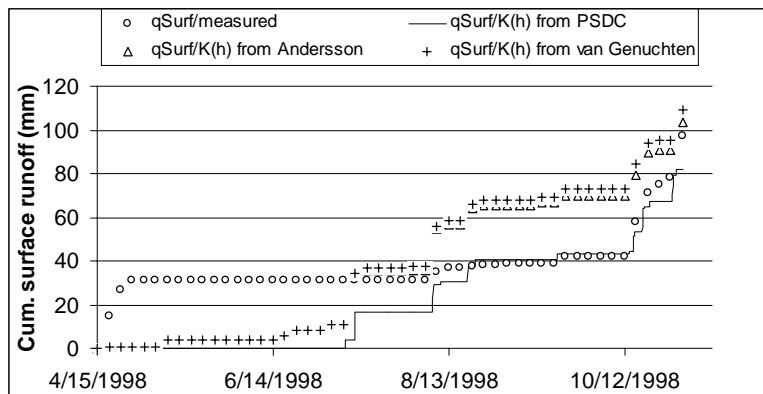


Figure 49. Measured and computed cumulative surface runoff using three different options of modelling unsaturated hydraulic conductivity (Sjökulla, lower part of the agricultural hillslope, macropores included in the model).

The two other methods overestimated both drainage flux and surface runoff considerably due to the fact that the groundwater table stays closer to the soil surface throughout the season.

The calculated values of the other water balance components are shown in Table 5. The most prominent feature is that option 1) gave quite a good fit for both drainage flux, but options 2) and 3) overestimated drainage flux and, correspondingly, gave considerably lower estimates for the actual evapotranspiration rate as compared to method 1). The calculation period was wetter than average indicating that actual evapotranspiration should be quite close to potential value. The water balance components

support the conclusion that option 1), where the water retention curve and the unsaturated hydraulic conductivity curve are estimated solely from the particle size distribution curve, gave the best overall fit to measured results.

Table 5. Measured and calculated cumulative water balance components (mm) of the lower part of the Sjøkulla agricultural hillslope. Total precipitation during the period between 15.05 - 31.10.1998 was 608 mm and potential evapotranspiration was 420 mm. ΔW is the change (mm) in total water content of the profile. Macropore model is included in calculations.

	Drainage	Surface runoff	Deep flow	Actual ET	ΔW
Measured	89	97			
Option 1)	106	82	21	394	5
Option 2)	151	104	34	310	9
Option 3)	171	108	36	286	7

5.3.3.2 Lower part of the hillslope, macropore model not included

Simulations were carried out using all the three options when macropores were not included in the model. In this case, the saturated hydraulic conductivity values of the soil matrix were higher compared to the situation when macropores were included in the model. The results of measured and computed depth to water table are shown in Fig. 50. Even in this case, the first option proved to be better compared to cases when measured water retention curves were used (options 2 and 3). None of the three methods performed very well during the whole computation period when macropores were not included in the model. The computed water table depth using option 1) was at too low a level in June and July, but the method was successful in simulating the rise of the water table during the heavy rains in mid August. Computed water level using options 2) and 3) was at the correct level in June. In July, water table depth fell to a depth of 1.20 m and mid August rains could not raise the water level close to the soil surface as indicated by the measured values.

The simulated cumulative water balance components are shown in Figs. 50 and 51 and in Table 6. Cumulative drainage flux and surface runoff were predicted very well using option 1), but as shown in Fig. 50, water table depth was not correctly simulated and therefore, the option with macropores included proved to be better. Calculated cumulative drainage flux was very close to measured values for options 2) and 3), but the timing of drainage flux was not correctly simulated. Cumulative surface runoff components

were very much overestimated using options 2) and 3). The conclusion is that for options 2) and 3) slightly better results with respect to cumulative values were obtained when macropores were not included in the model, but the difference made when the macropore sub model was used, was quite small.

Table 6. Measured and calculated cumulative water balance components (mm) of the lower part of the Sjökulla agricultural hillslope. Total precipitation during 15.05 - 31.10.1998 was 608 mm and potential evapotranspiration was 420 mm. ΔW is the change (mm) in total water content of the profile. Macropore model was not included in calculations.

	Drainage	Surface runoff	Deep flow	Actual ET	ΔW
Measured	89	97			
Option 1)	96	86	15	412	9
Option 2)	82	144	19	355	8
Option 3)	98	161	22	319	8

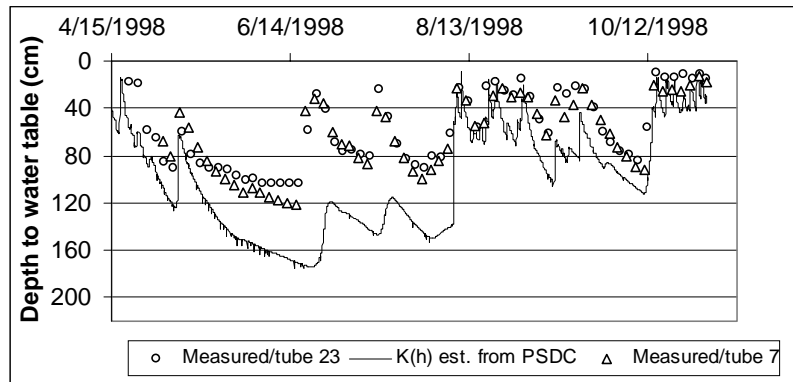


Figure 50/I. Measured and computed depth to water table using three different options of modelling unsaturated hydraulic conductivity (Sjökulla, lower part of the agricultural hillslope, macropores not included in the model).

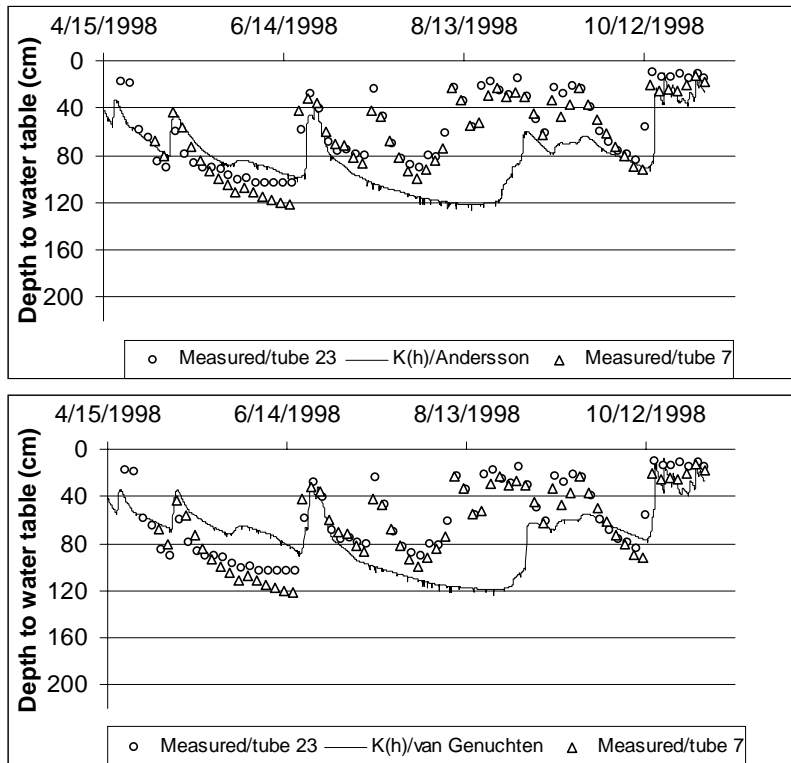


Figure 50/II. Measured and computed depth to water table using three different options of modelling unsaturated hydraulic conductivity (Sjökulla, lower part of the agricultural hillslope, macropores not included in the model).

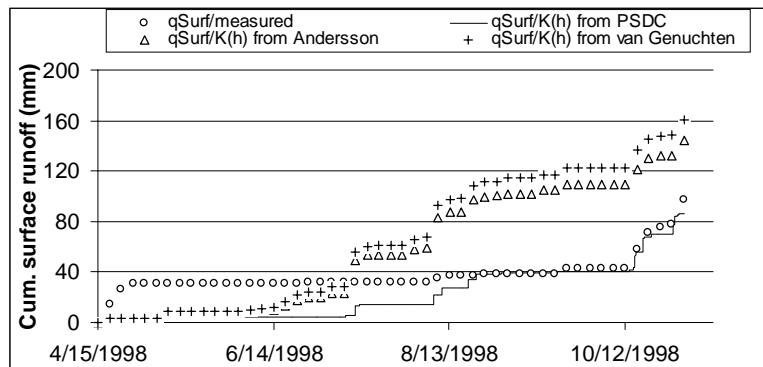


Figure 51. Measured and computed cumulative surface runoff using three different options of modelling unsaturated hydraulic conductivity (Sjökulla, lower part of the agricultural hillslope, macropores not included in the model).

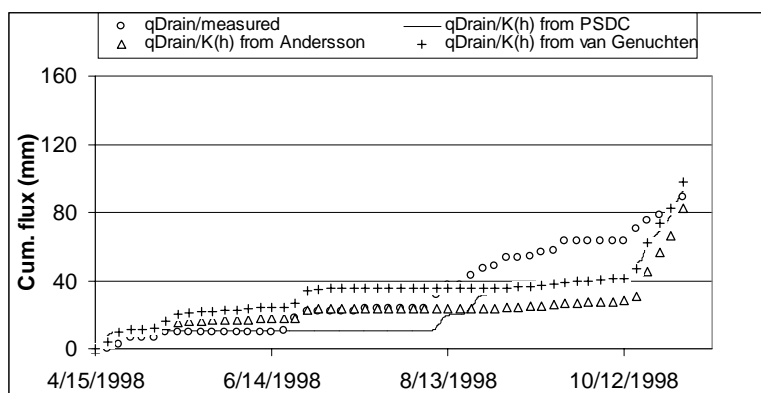


Figure 52. Measured and computed cumulative drainage flux using three different options of modelling unsaturated hydraulic conductivity (Sjökulla, lower part of the agricultural hillslope, macropores not included in the model).

5.3.3.3 Upper part of the hillslope, macropore model included

The measured and calculated depths to the water table in the upper part of the hillslope are shown in Fig. 53 for the three different parameterisations of the soil hydraulic properties. Separate measurements of the water balance components were not available from the upper part of the hillslope and therefore calculated values can be compared only to measurements of the water table depth. The first option, which used only the PSDC, also gave the best fit between measured and computed values for the upper part of the hillslope. The results obtained using the other two options based on fitting the water retention curve to measured data showed that the sharp increase in water table depth in June could not be reproduced by the model. The reason for this was the same as in the lower part of the hillslope: smaller relative values for $K(h)$ reduced the calculated upward fluxes in options 2) and 3) compared to option 1). In the upper part, the results given by options 2) and 3) did not differ very much from each other.

The calculated cumulative water balance components are shown in Table 7. The biggest difference compared to the results for the lower part (see Table 5) was the smaller surface runoff and increase in deep subsurface flow towards the secondary drainage system.

Table 7. Calculated cumulative water balance components (mm) of the upper part of the Sjöckulla agricultural hillslope. Total precipitation during 15.05 - 31.10.1998 was 608 mm and potential evapotranspiration was 420 mm. ΔW is the change (mm) in total water content of the profile. Macropore model was included in calculations.

	Drainage	Surface runoff	Deep flow	Actual ET	ΔW
Option 1)	87	35	81	393	12
Option 2)	122	53	109	317	7
Option 3)	136	57	112	285	8

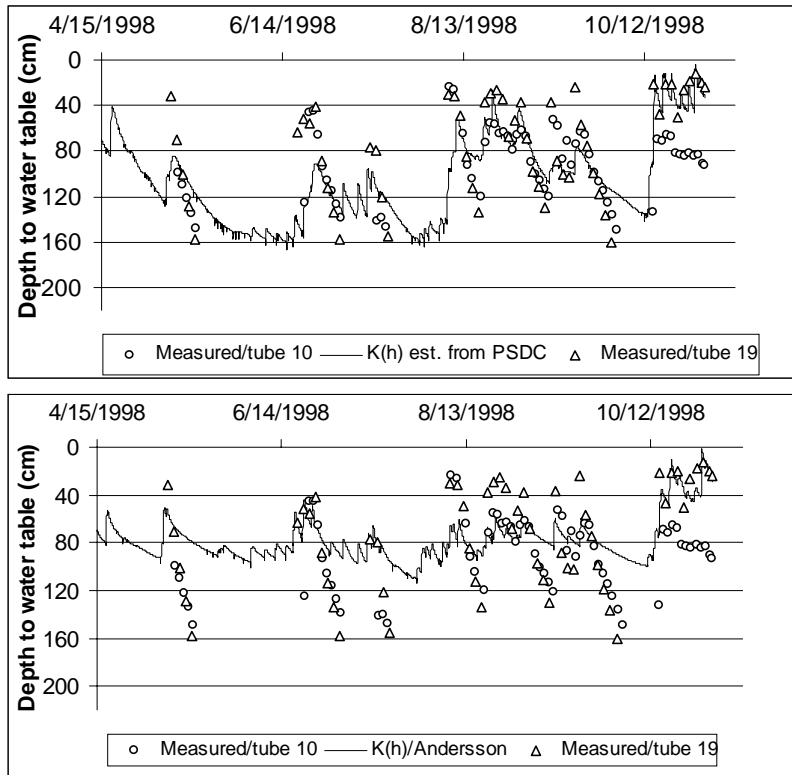


Figure 53/I. Measured and computed depth to water table using three different options of modelling unsaturated hydraulic conductivity (Sjöckulla, upper part of the agricultural hillslope, macropores included in the model).

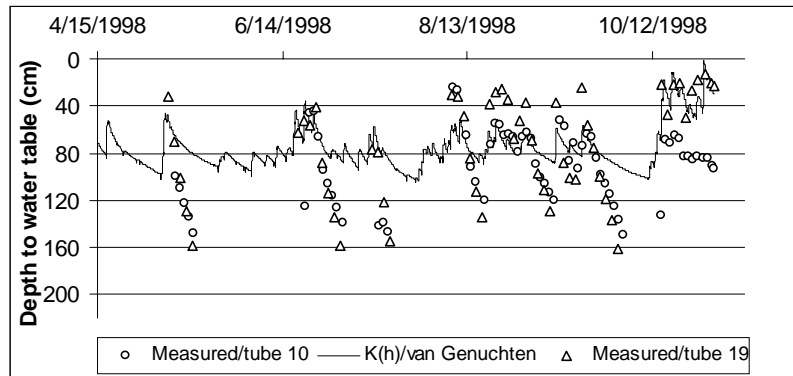


Figure 53/II. Measured and computed depth to water table using three different options of modelling unsaturated hydraulic conductivity (Sjökulla, upper part of the agricultural hillslope, macropores included in the model).

5.3.3.4 Upper part of the hillslope, macropore model not included

The water balance components of the upper part of the hillslope were also calculated by neglecting the explicit influence of the macropores and correspondingly, the saturated water content values of the soil matrix had to be greater than in the case when macroporosity was included. The soil matrix hydraulic conductivity values were the same used in the lower part of the hillslope except at depths below 0.6 m where the greater estimated depth of macropores (2.0 m in the upper parts and 1.1 m in the lower part) was compensated by using K_s -value 0.005 m h^{-1} (12 cm d^{-1}). The calculated and measured depths to the water table are shown in Fig. 54. The measured water table depths are in quite good agreement with values calculated using option 1) and the results are almost equally good compared to the case when macropores were included (see Fig. 53). The computed depth to the water table could not follow the measured curves when hydraulic properties were estimated from the measured water retention curves (options 2) and 3)), i.e. the results are in agreement with the results obtained from the lower part of the hillslope.

The calculated cumulative values for the case where macropores were not included are shown in Table 8. For option 1), the results were not very different from the values shown in Table 7 for macropore-case. For options 2) and 3), the cumulative drainage flux is much smaller than in Table 7 and the surface runoff was correspondingly much larger than in calculations where macroporosity was included.

Table 8. Calculated cumulative water balance components (mm) of the upper part of the Sjökulla agricultural hillslope. Total precipitation during 15.05 - 31.10.1998 was 608 mm and potential evapotranspiration was 420 mm. ΔW is the change (mm) in total water content of the profile. Macropore model was not included in calculations.

	Drainage	Surface runoff	Deep flow	Actual ET	ΔW
Option 1)	89	39	58	414	8
Option 2)	48	136	65	344	5
Option 3)	56	153	68	315	6

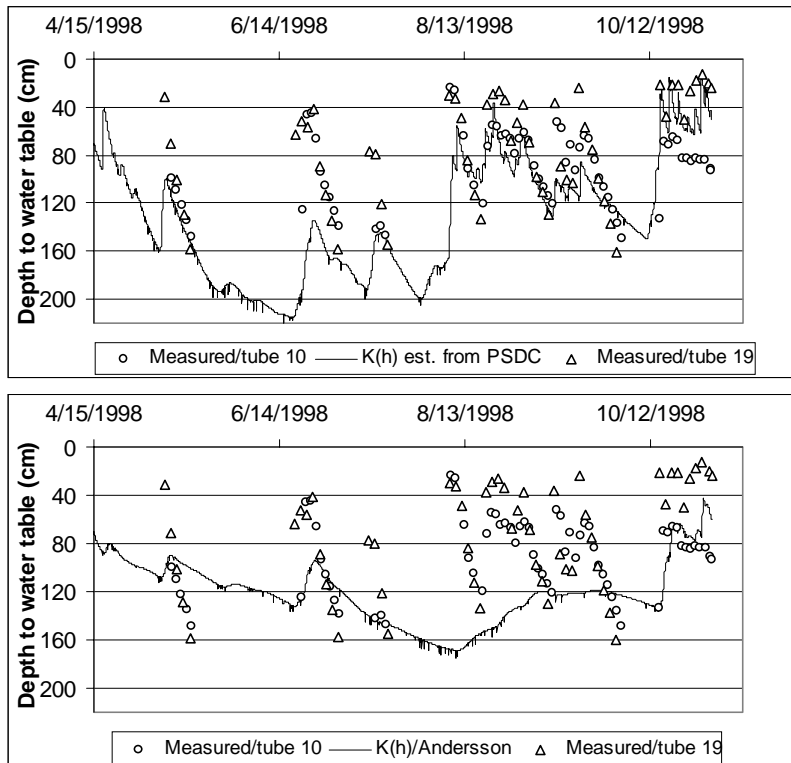


Figure 54/I. Measured and computed depth to water table using three different options of modelling unsaturated hydraulic conductivity (Sjökulla, lower part of the agricultural

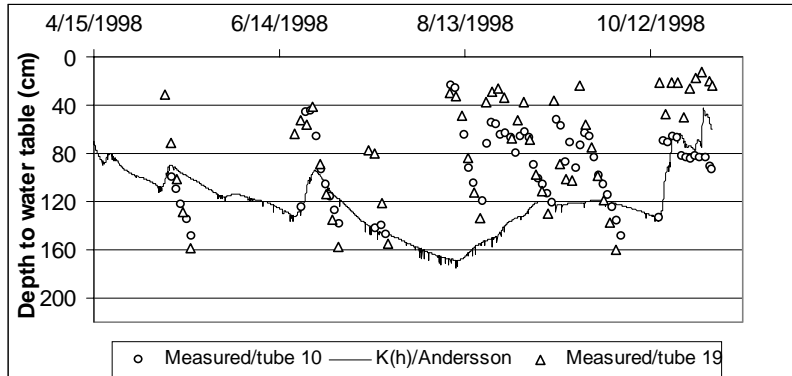


Figure 54/II. Measured and computed depth to water table using three different options of modelling unsaturated hydraulic conductivity (Sjökulla, lower part of the agricultural hillslope, macropores not included in the model).

Essential part of the study is the determination of soil water retention curves for different forest sites. The measured curves for 108 samples are shown in App. 2. Determining the WRC in the laboratory has certain weaknesses. Laboratory method for determining the WRC, which was used, cannot take into consideration the macropores of the soil sample. Hysteresis also is neglected in the laboratory method because only the desorption was used. Hence the actual WRC is not achieved when this laboratory method was used. For sandy soils it is almost impossible to characterize the water content at or near saturation in the laboratory without destroying the natural aggregate structure (Deurer et al. 2000). Anisotropy of the samples can be caused by the vertical variation in physical properties. The eluvial layer sample having a thickness of 5 cm is composed of both eluvial and illuvial layers. Hence the sample can represent in some cases in fact two podzol horizons.

The Finnish forest site type theory, developed by Cajander (1926), is based on the indicator plants in the field layer. Cajander (1926) suggested that there is not a clear relationship between the soil type and the forest site type. In the present study, the WRC of the C-horizon of the most fertile forest site type showed that the amount of plant-available water ($\theta_{2.0} - \theta_{4.2}$) is greatest in OMT and MT forest site types (see the average curves shown in Chapter 4.1 and in App. 3/layer C). The amount of plant-available water was smallest in the poorest forest site type (CT). Earlier studies support the results obtained in this work. Westman (1988) found that in Finnish forest soils site fertility was primarily related to the fine fraction ($\phi < 0.06$ mm) content in the C-horizon and the related properties (i.e. CEC). Heiskanen (1988) proposed that MT forest site type has more plant-available water in subsoil than other site types. The reason for this was that MT sites had the greatest amounts of fine fraction. The sites of the study were chosen from the same district as the sites of the present study.

It could be seen that there was a plain difference in the plant-available water between the virgin subsoil and the horizons above it (see Chapter 4.1 and App. 3). This was the case in every four forest site types of the study. Smallest variation (standard deviation) was obtained in dry part ($\log h$ from 1.5 to 4.2) of the WRC of the subsoil samples taken from CT. The largest variation of this range was in MT samples. Difference between the WRCs of forest site types was smallest in bottom half of illuvial layer (B_2). In the wet end of the WRC of eluvial layer VT type had smallest average water content values and in the dry end MT had the largest average water content values. The WRCs of MT and OMT

resembled strongly each other in three lower horizons. The increasing clay content could be seen in the shape of WRC curves. When there was a lot of clay in the soil sample, the shape resembled a gentle S-type. The water retention characteristic curve is strongly affected by soil texture. The amount of clay is an important factor in determining the shape of the curve. Urvas and Erviö (1974) and Penttinen (2000) showed in their studies of Finnish forest site types that clay content increased from the layers of the top soil to the subsoil in the most productive site types. In the poorest forest site types the subsoil did not contain clay. Aaltonen (1928) found that the coarse fraction of soil increases from the top layer to the subsoil.

Comparison with the results of Heiskanen (1988) of WRCs showed that the average curves of various site types obtained in this study resembled the corresponding curves given by Heiskanen. Heiskanen (1988) noticed also that MT sites had most plant-available water in eluvial and illuvial layers.

Selected WRCs of four different forest site types for podzolic soil horizons were shown in this study (see Chapter 4.2). These curves differ from the average curves, which are calculated from a large number of curves. In this study, there was no division made between the graded and till soils. Hence, difficulties can arise in using the selected WRCs, especially in VT site type, because, in this type, the soils can belong to both the graded and till soils. However, if the particle size distribution curve of the profile has been determined, the results of this study can be used in two different ways to determine WRC for water balance calculations. The first choice is to compare the measured PSDC with the curves shown in App. 1 for different forest types and select the sample that resembles the measured one. The corresponding WRC can be obtained from App. 2 and parameters of Andersson's function from App. 4 and parameters of van Genuchten's function from App. 6. The second choice is to utilize the semi-physical method described in Chapter 3.4 and determine the parameters of the WRC from measured PSDC.

The results of the study showed that both Andersson's and van Genuchten's functions were in most cases successful in fitting computed WRC to measured curve (see Chapter 4.3). The weakness of Andersson's function in fitting was that in some cases it could not follow the measured curve at pressure head value $h = 10$ cm (see Figs. 11a, 13c, 13d and 14d) as well as van Genuchten's function. One drawback of Andersson's function shown in Eq. (3-2) is that saturated water content is not included as a parameter and therefore the method can give too high values for water content at saturation (see Fig. 14b).

The WRCs of the humus layers of VT and OMT forest site types seemed to be of V-type (see Chapter 4.4). There was no

difference in WRCs between the site types. Laurén and Mannerkoski (2001) found that, at the pressure head values studied, the water retention in the mor layers was higher on the MT sites than on the CT sites. The water retention characteristics of humus layers studied here were of similar magnitude to those presented earlier for other forest floor data and peat (Sharratt 1997, Heiskanen 1988, Weiss et al. 1998 and Laurén and Mannerkoski 2001) with the exceptions of the two VT pits shown in Figs. 16a and 16b, where saturated water content values are erroneous. Humus layer samples did not show any biporous structure, which is typical for many mineral soils (Messing 1993 and Durner 1994). Laboratory measurements of the WRC of humus samples proved to be less reliable than the measurements of mineral soil samples. This is caused by the swelling and cracking of the samples during wetting and drying. The determination of saturated water content of humus samples proved to be inaccurate, because water flows more easily from the frame of the humus sample than of the mineral soil sample. The same difficulty was stated earlier by Heiskanen (1988).

In the present study, a new semi-physical method was introduced to predict the WRC from the PSDC (see Chapter 3.4). Moreover, WRC was predicted from PSDC using van Genuchten's (see Chapter 3.5.3) and Jonasson's (see Eqs. (3-27a) and (3-27b)) methods. The comparison of the results given by the three methods is given for Finnish forest soil samples in Chapter 4.5.1 in Table 2 and 3. Totally 108 samples were used to predict the WRC from the PSDC. In most cases, the WRC prediction was good at relative saturation rates around 0.5 (see Figs. 21 and 22), but in some cases the calculation of the relative water content at low moisture content and/or high moisture content was not successful. The results showed that the semi-physical method predicted the WRC better than the other methods both in the case that saturated and residual water content values were estimated from PSDC and bulk density, and in the case that θ_s and θ_r were given as input data. When saturated water content, θ_s , and residual water content, θ_r , were estimated, the semi-physical method was most successful ($R^2 = 0.823$). Nearly as good coefficient of determination ($R^2 = 0.809$) was obtained when q_s and θ_r were given in the semi physical method. The reason for this is that in the semi-physical method saturated and residual water content are indirectly included in the WRC equation (3-2) through parameters p_i and θ_0 that are determined from Eqs. (3-23) and (3-24). Therefore, coefficient of determination was not improved even though θ_s and θ_r were given as input data. van Genuchten's method behaved in opposite way giving larger values for R^2 when θ_s and θ_r were given ($R^2 = 0.636$ in Table 2 and $R^2 = 0.740$ in Table 3).

Jonasson's method underestimated soil moisture content over the whole range both when θ_s and θ_r were estimated ($R^2 = 0.588$) and when they were given as input data ($R^2 = 0.621$). Jonasson's functions given in Eqs. (3-27) were developed from agricultural data (Andersson and Wiklert 1972) and this is the most probable reason for too low predictions.

Van Genuchten's method gave too large water content values over the whole range both in the case that θ_s and θ_r were estimated ($R^2 = 0.636$) and when they were given as input data ($R^2 = 0.74$) (see Figs. 19 and 20). Both in the semi-physical and in van Genuchten's method a transfer function is needed to convert grain diameter to equivalent pore diameter. The transfer function given in Eq. (3-25) was originally developed for the semi-physical method to relate the inflection point of the PSDC, x_p , and the inflection point of the WRC, $h_{i,0}$. The same transfer function was used in van Genuchten's method to calculate parameters h_g and α from D_g (see Eqs. (3-35a) and (3-35b)). However, it seems that the transfer function was not suitable to be used in van Genuchten's method. Therefore, it would be necessary to develop a different transfer function to predict h_g and α from D_g .

The results from the prediction of the WRC from PSDC for Swedish agricultural data are given in Chapter 4.5.2 and App. 7. The semi-physical method gave the best results both when saturated water content and residual water content were estimated and when they were given as input values. The semi-physical method and van Genuchten's method were capable of predicting the WRC from PSDC for the whole clay content range (0-30 for topsoil and 0-55 for subsoil). Jonasson's method failed when topsoil clay content was larger than 25 % and subsoil clay content was greater than 30 %. Haverkamp and Parlange's (1986) used the semi-physical method developed for van Genuchten function for predicting the WRC from the PSDC. The method was successful only in the coarse textured soils with no organic matter (see Chapter 1.2.1.3).

The method for predicting unsaturated hydraulic conductivity from water retention characteristics is an alternative for the laboratory or in situ measurements. By using it, the water balance calculations can be made without any laborious and expensive determination technique. In the present study, neither laboratory nor in situ measurements for $K(h)$ were accomplished. The extension of Andersson's original function developed in this study and van Genuchten's function were tested against data given in the UNSODA database (20 soil samples). The results are given in Chapter 4.6 and App. 8/I for saturated hydraulic conductivity K_s and in App. 8/II for the unsaturated part of the samples.

The van Genuchten-type equation (3-36) for predicting saturated hydraulic conductivity from WRC gave much better results than Andersson's method given in Eq. (3-11). In Andersson's method it is possible to find the optimum value for the bubbling pressure, $h_{B,opt}$, which gives accurate prediction of K using Eq. (3-11). Unfortunately there does not exist any reliable method to estimate $h_{B,opt}$ from soil texture. The results of prediction of K_s show that in most cases it is not possible to estimate K_s accurately from soil texture since the structure of the soil sample (aggregates, macropores etc.) may be a more important factor.

The prediction of unsaturated hydraulic conductivity was carried out for the 20 soils in such a way that saturated hydraulic conductivity was assumed to be known, i.e. the measured value in each sample was given as input data for the extension of the Andersson's method and van Genuchten's method. Average error, E_{ave} , shown in App. 8/II is given for the whole range (all measurements) and for three different pressure head ranges representing wet, medium and dry ranges, respectively: $0 < h < 100$ cm, $100 < h < 500$ cm, and $h > 500$ cm. E_{ave} is the absolute value of the average logarithmic error. Andersson's method gave slightly better results if the whole measurement range is considered. E_{ave} was in this case 0.75 in Andersson's method and 1.02 in van Genuchten's method. The wet end of the curve is more interesting with respect to water balance calculations than the dry range. In this part of the curve the two methods worked equally well. Average error in the wet range was 1.1 in Andersson's method and 1.19 in van Genuchten's method. The reason for quite big average error in the wet range in approximately half of the samples is that saturated hydraulic conductivity was very big and unsaturated values decreased much faster than the methods predicted. This type of behaviour can be seen e.g. in Figs. 26b and 26d. Soils 4052, 4081, 4082, 4091, 4092, 4102 and 4110 were of the same type. The high K_s -value of these samples may be caused e.g. by macropores and in these type of soils the unsaturated $K(h)$ decreases very fast when h decreases. Since K_s was defined as input value, both methods overestimated $K(h)$ at wet range considerably in these type of samples. The slope of the WRC near saturation is the most important property in determining the shape of the estimated conductivity function as pointed out by Durner (1994). Future developments of the $K(h)$ -prediction models should better take into account this part of the curve.

In this study, the K_s of the humus layer (Chapter 5.2) was calibrated to be 1.0 m d^{-1} . van Genuchten calculations gave $K(h)$ values from $1.0 * 10^{-4}$ to $1.0 * 10^{-6} \text{ m d}^{-1}$ when the pressure head changed from 40 to 600 cm. Andersson calculations gave $K(h)$ values from $1.0 * 10^{-2}$ to $1.0 * 10^{-4} \text{ m d}^{-1}$. Andersson values were almost two orders of magnitude

greater than van Genuchten's values at the dry end of the curve. Laurén and Mannerkoski (2001) obtained values, which are quite close to the values calculated by van Genuchten's method. The mean $K(h)$ of the mor was slightly lower at the CT sites than at the MT sites through the pressure head range studied (Laurén and Mannerkoski 2001). The mean $K(h)$ on the MT sites decreased from $8.8 * 10^{-3}$ to $1.4 * 10^{-6}$ m d⁻¹ when the pressure head changed from 40 to 600 cm. The decrease on the CT sites was from $6.9 * 10^{-3}$ to $4.9 * 10^{-7}$ m d⁻¹ (Laurén and Mannerkoski 2001). Based on the results shown above it can be concluded that Andersson's method gives too high values for $K(h)$ for humus layers. Mecke and Ilvesniemi (1999) extrapolated saturated conductivity of two coarse podzol profiles of Mämmilampi to be from 4.0 to 25.7 m d⁻¹ in subsoil and from 0.17 to 0.31 m d⁻¹ in the two top mineral soil horizons of the profiles.

The developed procedures for estimating the water retention curve and unsaturated hydraulic conductivity curve from the PSDC were tested against the measured WRCs and against soil matric potential values in forested hillslopes and measured water balance components of an agricultural hillslope. The quasi-two-dimensional hillslope model simulated well in 1991 and 1992 the seasonal variation in the ground water table in the upper part of the hillslope, but failed to reproduce the measured water table depth in the lower part. The sharp increase of the water table in June could have been reproduced by the model better if a larger infiltration capacity of macropores had been used. Because the mor layers usually have high macroporosity, Laurén (1999) used ACIDIC (Kareinen et al. 1998) with the volume of macropores calculated by subtracting the water content at matric potential -1 kPa from the total porosity of the layer. Koivusalo et al. (1999) concluded that the quasi-two-dimensional model for clay soils has to include a description for the macropore flow. In the study carried out by Koivusalo et al. (1999) it was noticed that the water balance model performed well during the wet periods, but failed to follow the water table observations during the dry season.

In Chapter 5 water balance calculations were carried out with three different options for WRC. In option 1) $\theta(h)$ and $K(h)$ were estimated from PSDC and measured soil water retention curve was not utilized at all. In option 2) Andersson's function was fitted to measured $\theta(h)$ -curve and $K(h)$ was estimated using Andersson's method shown in Eq. (3-18). In option 3) van Genuchten's function was fitted to measured WRC and (3-31) was used to estimate $K(h)$ from $\theta(h)$ -curve.

The best overall fit between measured and calculated values was obtained in the case where the water retention curve was estimated from the particle size distribution curve

and the unsaturated hydraulic conductivity was estimated using the semi-physical method. The results were much poorer when measured water retention curves were used as the basis of estimation of the relative unsaturated hydraulic conductivity curve due to the fact that, in this case, the unsaturated value was underestimated compared to the case where $K(h)$ was estimated from the PSDC; the small relative values for the unsaturated hydraulic conductivity reduce upward flux from the water table and the dynamics of the water table depth as a function of time cannot be reproduced. The inclusion of macropore option of the CROPWATN-model for agricultural hillslopes produced better results than in cases where single-porosity option was used.

The study was undertaken with the primary objective of developing two methods: one that links the particle size distribution curve with water retention characteristics and the other that links water retention characteristics with the hydraulic conductivity function.

Chapter 3 presents Andersson's method and the semi-physical method for the estimation of water retention characteristics from the particle size distribution curve, and for the calculation of the unsaturated hydraulic conductivity function from the water retention characteristics.

In Chapter 4.1 average, and in Chapter 4.2, selected water retention characteristics curves of four forest site types, *Calluna* (CT), *Vaccinium* (VT), *Myrtillus* (MT) and *Oxalis-Myrtillus* (OMT) and four podsollic soil layers (A, B1, B2 and C) are presented. The first part of the results presents the average water retention characteristics of the four horizons based on 360 samples taken from the four different Finnish forest site types. The results show that subsoil data can be used as base data, which describes in a realistic way the different forest site types; the larger amount of plant-available water, the better the site type.

Chapter 4.3 and 4.4 (humus) describe the results of the methods of fitting Andersson's and van Genuchten's functions to the WRC data that were collected from four different Finnish forest site types. The fittings of the proposed equations to Finnish forest mineral soil data were successful. Both methods were also used in humus layer samples and the fittings of equations to sample data were very accurate.

The results from predicting water retention characteristics from the particle size distribution curve were presented in Chapter 4.5 both for forest samples and Swedish agricultural soils. Estimation of WRC from the PSDC was accomplished using the semi-physical method, which was developed in this study, van Genuchten's and Jonasson's methods. Observations of these comparisons were taken from 108 Finnish forest site samples and 7 Swedish agricultural soil samples. The models presented gave realistic estimations in the Finnish forest site samples. Semi-physical method was the most accurate of three methods in predicting WRC of average Finnish forest soil samples both when θ_s and θ_r were estimated and when they were given as input data. Van Genuchten's method gave good shape for the curve but all the water content values were too large indicating that the transfer function developed originally for the semi-physical method was not suitable in van Genuchten's method. Jonasson's method gave the poorest result. Arable soil sample estimations were realistic in the semi-physical and

van Genuchten's methods. Jonassons method failed to follow the observed WRC of topsoil when the clay content was 26-30 % and when the clay content was greater than 30 % in the subsoil.

Chapter 4.6 discusses the simulation results of the UNSODA data, which were coarse soil samples from fields of Central Europe. The simulation was accomplished for predicting the unsaturated hydraulic conductivity from the PSDC. The van Genuchten-type equation for predicting saturated hydraulic conductivity from WRC gave much better results than Andersson's method. However, the results of prediction of K_s show that in most cases it is not possible to estimate K_s accurately from soil texture since the structure of the soil sample (aggregates, macropores etc.) may be a more important factor. Andersson's method gave slightly better results in the prediction of unsaturated hydraulic conductivity if the whole measurement range is considered. In the wet end of the curve the two methods worked equally well.

Chapter 4.7 is devoted to the sensitiveness of the parameters of water retention characteristics. To examine the relative importance of the four parameters of the Andersson's semi-physical method of the WRC, a one-dimensional sensitivity analysis was performed on various water retention characteristic curves. From the analysis, it was concluded that $h_{t,0}$ and θ_0 of Andersson's function were the most sensitive parameters. The least sensitive parameter was b_1 .

Chapter 5 introduces the implications of soil hydraulic properties on the water balance of forested and agricultural hillslopes (Chapters 5.2 - 5.4). The purpose of the simulations was to find out if the WRC and unsaturated hydraulic conductivity function predicted from the PSDC using the methods developed in this study can be used in existing models to provide realistic results in terms of soil water balance components. A forested hillslope of Rudbäcken was used as the test case of the CROPWATN-model. Agricultural hydraulic field measurements were taken from Sjöckulla. The results were better in both applications when water retention curves were estimated from the PSDC using the semi-physical method developed in this study. In this option measured soil water retention curve was not used. The two other options used measured WRC and estimated curve for unsaturated hydraulic conductivity (Andersson's function in option 2) and van Genuchten's function in option 3)). The inclusion of the macropore option of the CROPWATN-model for agricultural hillslopes produced better results than cases in which the single-porosity option was used.

- Aaltonen, V. T. 1928. Über den Einfluss des Waldes auf die Kornzusammensetzung des Erdsbodens in Sandböden. Summary: The Effect of the Forest upon the Mechanical Composition of Soil in Sandy Soils. *Metsätieteellisen laitoksen julk.*, 13(5), 1-24.
- Al-Soufi, R. 1983. Unsaturated hydraulic conductivity. "Evaluation research study". Thesis of licenciate in Technology. Helsinki University of Technology, Laboratory of Hydrology and Water Resources Engineering.
- Andersson, S. 1969. Theoretical relationships in capillary systems between capillary conductivity, pore size distribution, tension and water content (in Swedish). *Grundförbättring*, 22(4), 143-154.
- Andersson, S. 1990a. Markfysikaliska undersökningar i odlad jord, XXVI. Om mineraljordens och mullens rumsutfyllande egenskaper. En teoretisk studie. (In Swedish), Swedish University of agricultural sciences, Uppsala, 70 p.
- Andersson, S. 1990b. Markfysikaliska undersökningar i odlad jord, XXVII. Kornkurvor. Teoretiska exempel, analys och kommentarer. (In Swedish), Swedish University of agricultural sciences, Uppsala, 155 p.
- Andersson, S. 1990c. Markfysikaliska undersökningar i odlad jord, XXVIII Bindningskurvor, por- och kornkurvor, En matematiskt strukturerad model. (In Swedish), Swedish University of agricultural sciences, Uppsala, 155 p.
- Andersson, S. and P. Wiklert, 1972. Markfysikaliska undersökningar i odlad jord, XXIII. Om de vattenhållande egenskaperna hos svenska jordarter. (In Swedish), Swedish University of agricultural sciences, Uppsala, 53 p.
- Arya, L.M. and J.F. Paris. 1981. A physico-empirical model to predict the soil moisture characteristic from particle-size distribution and bulk density data. *Soil Sci. Soc. Am. J.*, 45, 1023-1030.
- Assouline, T., D. Tessier and A. Bruand. 1998. A conceptual model of the soil water retention curve. *Water Resour. Res.*, 34(2), 223-231.
- Averjanov, S.F. 1950. About permeability of subsurface soils in case of incomplete saturation. p. 19-21 in English Collection, Vol. 7, (1950), as quoted by P.Ya. Palubarinova, 1962, *The theory of ground water movement* (English translation by I.M. Roger DeWiest, Princeton University Press).
- Bear, J. 1972. *Dynamics of fluids in porous media*. Elsevier. New York.

- Bloemen, G.W. 1980. Calculation of hydraulic conductivities of soils from texture and organic matter content. *Z. Pflanzenernährung und Bodenkunde*, 143(5), 581-615.
- Bonell, M. 1993. Progress in understanding runoff generation dynamics in forests. *J. Hydrol.*, 150, 217-275.
- Brooks, R.H. and C.T. Corey, 1964. Hydraulic Properties of Porous Media. Hydrol. Paper, 3. Colorado State University, Fort Collins.
- Bruce, R. R. and A. Klute. 1956. The measurement of soil moisture diffusivity. *Soil Sci. Soc. Am. Proc.*, 35, 458-462.
- Burden, D.S. and H.M. Selim. 1989. Correlation of spatially variable soil water retention for a surface soil. *Soil Sci.*, 149, 436-447.
- Burdine, N.T. 1953. Relative permeability calculations from pore-size distribution data. *Petrol Trans., AIME*. 198, 71-77.
- Buttle, J.M. and D.A. House. 1997. Spatial variability of saturated hydraulic conductivity in shallow macroporous soils in a forested basin. *J. Hydrol.*, 203, 127-142.
- Cajander, A.K. 1926. The theory of forest types. *Acta Forestalia Fennica*, 29, 108 p.
- Campbell, G. 1974. A simple method for determining unsaturated conductivity from moisture retention data. *Soil Sci.*, 117, 311-314.
- Childs, E.C. and G.N. Collis-George. 1950. The permeability of porous materials. *Proc. Roy. Soc. London, Ser. A.*, 201, 392-405.
- Clapp, R.B. and G.M. Hornberger. 1978. Empirical equations for some hydraulic properties. *Water Resour. Res.*, 14, 601-604.
- Climatological statistics in Finland 1961-1991. 1991. Supplement to the meteorological yearbook of Finland, 90(1), 125 p.
- Clothier, B.E. and I. White. 1981. Measurement of sorptivity and soil water diffusivity in the field. *Soil Sci. Soc. Am. J.*, 45, 241-245.
- Dane, J.H. and S. Hruska. 1983. In-situ determination of soil hydraulic properties during drainage. *Soil Sci. Soc. Am. J.*, 47, 19-624.
- Delleur J.W. (ed.) 1999, The handbook of ground water engineering. CRC Press.
- Deurer, M., W. H. Duijnsveld and J. Böttcher. 2000. Spatial analysis of water characteristic functions in a sandy podzol under pine forest. *Water Resour. Res.*, 36, 2925-2935.
- de Vos, J.E. 1997. Water flow and nutrient transport in a layered silt loam soil. Ph D-thesis, Wageningen University, 284 pp.

- Dirksen, C. 1975. Determination of soil water diffusivity by sorptivity measurements. *Soil Sci. Soc. Am. Proc.*, 39, 22-27.
- Dullien, F. A. L. 1979. *Porous Media Fluid Transport and Pore Structure*, Academic Press, New York, NY.
- Durner, W. 1994. Hydraulic conductivity estimation for soils with heterogeneous pore structure. *Water Resour. Res.*, 30, 211-223.
- Elonen, P. 1971. Particle-size analysis of soil. *Acta Agr. Fenn.*, 122, 1-122 .
- Fatt, I. and H. Dykstra. 1951. Relative permeability studies. *Trans. Am. Inst. Min., Metall. Pet. Eng.*, 192, 249-255.
- Fuentes, C., R. Haverkamp and J.-Y. Parlange. 1992. Parameter constraints on closed form soil water relationships. *J. Hydrol.*, 134, 117-142.
- Gardner, W.R. 1958. Some steady-state solutions of the unsaturated moisture flow equation with application to evaporation to from a water table. *Soil Sci.*, 85, 228-232.
- Giménez, D., R.R. Allmaras, D.R. Huggins and E.A. Nater, 1997. Prediction of the saturated hydraulic conductivity-porosity dependence using fractals. *Soil Sci. Soc. Am. J.*, 61, 1285-1292.
- Green, R.E., L. R. Ahuja and S. K. Chong. 1986. Hydraulic conductivity, diffusivity, and sorptivity of unsaturated soils: field methods, p. 771-798. In A. Klute (ed.) *Methods of Soil Analysis. Part 1. 2nd ed. Agronomy Monogra. 9.* ASA and SSSA, Madison, WI.
- Greminger, P. J., Y.K. Sud and D.R. Nielsen. 1985. Spatial variability of field-measured soil water characteristics. *Soil Sci. Soc. Am. J.*, 49 (5), 1075-1082.
- Gupta S.C. and W.E. Larson, 1979. Estimating soil water retention characteristics from particle size distribution, organic matter percent and bulk density. *Water Resour. Res.*, 15, 1633-1635.
- Gupta, S.C. and R.P. Ewing. 1992. Modeling water retention characteristics and surface roughness of tilled soils, p. 379-388. In van Genuchten, M. Th., F.J. Leij and L.J. Lund. (eds.). *Proc. Int. Workshop, Indirect methods for estimating the hydraulic properties of unsaturated soils.* University of California, Riverside, CA.
- Gärdenes, A. 1998. Soil organic matter in European forest floors in relation to stand characteristics and environmental factors. *Scand. J. For. Res.*, 13, 274-283.
- Haverkamp, R. and J.-Y. Parlange. 1986. Predicting the water retention curve from particle-size distribution: I. Sandy soils without organic matter. *Soil Sci.*, 142, 325-339.
- Haverkamp, R., F. Bouraoui , C. Zammit and R. Angulo-Jaramillo. 1999. Soil properties and moisture movement in the unsaturated zone. In J. W. Delleur (ed.), *The handbook of ground water engineering.* CRC Press.

- Heiskanen, J. 1988. Metsämaan vedenpidätyskyvystä ja sen suhteista eräisiin kasvupaikasta mitattuihin tunnuksiin. Lic.For. Thesis. Univ. Helsinki, Dept. Silviculture. 92 p. (In Finnish)
- Heiskanen, J. 1993. Variation in water retention characteristics of peat growth media used in tree nurseries. *Silva Fennica*, 27, 77-97.
- Hillel, D. 1971. Soil and water. Physical principles and processes. 288 pp. Academic Press, Orlando.
- Jauhiainen, M. and A. Nissinen. 1994. Calibration of the SOIL model with autumn and summer data of forest soil water tension. Nordic hydrological programme, NHP-Report 36, 17-30.
- Jauhiainen, M. 2000. Hydraulic properties of Finnish forest soils. Lic.For. Thesis. Univ. Helsinki, Dept. Forest Ecology. 88 p.
- Jarvis, N., and I. Messing. 1995. Near-saturated hydraulic conductivity in soils of contrasting texture measured by tension infiltrometers. *Soil Sci. Soc. Am. J.*, 59, 27-34.
- Jonasson, S. 1991. Estimation of soil water retention for natural sediments from grain size distribution and bulk density. Institute of Geology. Publ. A 62. Gothenburg, Sweden, 161 p.
- Kareinen, T., A. Nissinen and H. Ilvesniemi. 1998. Analysis of forest chemistry and hydrology with a dynamic model ACIDIC. *Acta Forestalia Fennica*, 262. 42 p.
- Karvonen, T. 1988. A model for predicting the effect of drainage of soil moisture, soil temperature and crop yield. Thesis for the degree of doctor of technology, Helsinki University of Technology, Laboratory of hydrology and water resources management, Otaniemi, Finland, 215 p.
- Karvonen, T. and J. Kleemola 1995. CROPWATN: Prediction of water and nitrogen limited crop production. Modelling and Parameterization of the Soil-Plant-Atmosphere System: A Comparison of Potato Growth Models (Eds. Kabat, P., Marshall, B., van den Broek, B.J., Vos., J. and van Keulen, H.). Wageningen Pers, Wageningen, The Netherlands. p. 335-369.
- Karvonen, T., H. Koivusalo and T. Kokkonen. 2001. Modeling runoff from hydrologically similar areas. User interface and brief description of the latest model version. Laboratory of Water Resources Helsinki University of Technology, Research report, 38 p.
- Karvonen, T. 2002. Modeling of crop growth as influenced by water, nitrogen and heat balance: Description of CROPWATN 6.0-model. Laboratory of Water Resources Helsinki University of Technology, Research report, 50 p.

- Klute, A., and C. Dirksen. 1986. Hydraulic conductivity and diffusivity: Laboratory methods. p. 687-734. In A. Klute (ed.) *Methods of Soil Analysis. Part 1.* 2nd ed. Agronomy Monograph 9. ASA and SSSA, Madison, WI.
- Kool, J.B. and J.C. Parker. 1987. Development and evaluation of closed-form expressions for hysteretic soil hydraulic properties. *Water Resour. Res.*, 24, 817-830.
- Kool, J.B. and J.C. Parker. 1988. Analysis of the inverse problem for transient unsaturated flow. *Water Resour. Res.*, 24, 817-830.
- Kool, J.B., J.C. Parker and M.Th. van Genuchten. 1987. Parameter estimation for unsaturated flow and transport models - A review. *J. Hydrol.*, 91, 255-293.
- Kosugi, K. 1994. Three-parameter lognormal distribution model for soil water retention. *Water Resour. Res.*, 30, 891-901.
- Kosugi, K. 1996. Lognormal distribution model for unsaturated soil hydraulic properties. *Water Resour. Res.*, 32, 2697-2703.
- Krenn, A. 1999. Estimation of soil water retention using two models based on regression analysis and an artificial neural network, p. 1261-1268. In M. Th. van Genuchten, F. J. Leij, and L. Wu.(eds.), *Characterization and measurement of the hydraulic properties of unsaturated porous media.* University of California, Riverside, CA.
- Kutilek, M. and D.R. Nielsen. 1983. *Soil hydrology.* 370 pp. Catena Verlag, Gremlingen-Destedt.
- Laurén, A. and J. Heiskanen. 1997. Physical properties of the mor layer in a Scots pine stand. I. Hydraulic conductivity. *Can. J. Soil Sci.*, 77, 627-634.
- Laurén, A. and H. Mannerkoski. 2001. Hydraulic properties of mor layers in Finland. *Scand. J. For. Res.*, 16, 429-441.
- Leij, F.J., W.J. Alves, M.Th. Van Genuchten and J.R. Williams. 1999. The UNSODA unsaturated soil hydraulic database. p. 1269-1281. In M. Th. van Genuchten, F. J. Leij and L. Wu.(eds.), *Characterization and measurement of the hydraulic properties of unsaturated porous media,* University of California, Riverside, CA.
- Mannerkoski, H. and V. Möttönen. 1990. Maan vesitalous ja ilmatila metsäaurausalueilla. *Silva Fennica*, 24(3), 279-301. (In Finnish with English summary: Soil water conditions and air-filled porosity on ploughed reforestation areas).
- Marshall, T.J. 1958. A relation between permeability and size distribution of pores. *J. Soil Sci.*, 9, 1-8.

- Mecke, M. and H. Ilvesniemi. 1999. Near-saturated hydraulic conductivity and water retention in coarse podzol profiles. *Scand. For. Res.*, 14, 391-401.
- Messing, I. 1993. Saturated and near-saturated hydraulic conductivity in clay soils. Measurement and prediction in field and laboratory. Department of Soil Sciences, Reports and dissertations, 12. Uppsala.
- Millington, R.J. and J.P. Quirk. 1961. Permeability of porous solids. *Trans. Faraday Soc.*, 5, 1200-1206.
- Mishra, S. and J.C. Parker. 1989. Estimation of soil hydraulic properties and their uncertainty from particle size distribution data. *J. Hydrol.*, 108, 1-18.
- Mishra, S. and J.C. Parker. 1990. On the relation between saturated hydraulic conductivity and capillary retention characteristics. *Ground Water*, 28, 775-777.
- Mualem, Y. 1976a. A new model for predicting the hydraulic conductivity of unsaturated porous media. *Water Resour. Res.*, 12, 513-522.
- Mualem, Y. 1976b. Hysteretical models for prediction of the hydraulic conductivity of unsaturated porous media. *Water Resour. Res.*, 12, 1248-1254.
- Mualem, Y. 1992. Modeling the hydraulic conductivity of unsaturated porous media, p. 15-36. In van Genuchten, M.Th., F.J. Leij and L.J. Lund. (eds.). *Proc. Int. Workshop, Indirect methods for estimating the hydraulic properties of unsaturated soils*. University of California, Riverside, CA.
- Mulla, D.J. 1988. Estimating spatial patterns in water content, matric suction and hydraulic conductivity. *Soil Sci. Soc. Am. J.*, 52, 1547-1553.
- Nemes, A., M.G. Schaap, F.J. Leij and J.H.M. Wösten. 2001. Description of the unsaturated hydraulic database UNSODA version 2.0. *J Hydrol.*, 251, 151-162.
- Neuman, S.P. 1973. Calibration of distributed parameter groundwater flow models viewed as a multiple-objective decision process under uncertainty. *Water Resour Res.*, 9, 1006-1021.
- Nielsen, D.R., J.W. Biggar and K.T. Erh. 1973. Spatial variability of field-measured soil water properties. *Hilgardia*, 42, 215-260.
- Nimmo, J.R. 1991. Comment on the treatment of residual water content in "A consistent set of parameter models for the two phase flow immiscible fluids in the subsurface." by L. Luckner et al., *Water Resour Res.*, 27, 661-662.
- Nordén, L.-G. 1989. Water use by Norway spruce - a study of two stands using field measurements and soil water modelling. Dissertation. Swedish university of agricultural sciences, Department of forest site research, Umeå, Sweden. 34 p.

- Paasonen-Kivekäs, M., H. Koivusalo, T. Karvonen, P. Vakkilainen and J. Virtanen. 1999. Nitrogen transport via surface and subsurface flow in agricultural field. Impact of Land-Use Change on Nutrient Loads from Diffuse Sources (Proc. Of IUGG Symposium HS3, Birmingham, July 1999) IAHS Publ., no. 257, 163-170.
- Paasonen-Kivekäs M. (2000). Influence of water management control on nutrient leaching (in Finnish). *Salaojituksen tutkimusyhdistys ry:n tiedote*, 25, 8-40.
- Pachepsky, Y.A., T.A. Polubesova, M. Hajnos, Z. Sokolowska and K. Jozefaciuk. 1995a. Fractal parameters of pore surface area as influenced by simulated soil degradation. *Soil Sci. Soc. Am. J.*, 59, 99-104.
- Pachepsky, Y.A., R.A. Shcherbakov and L.P. Korsunskaya. 1995b. Scaling of soil water retention using a fractal model. *Soil Sci.*, 159(2), 99-104.
- Päivänen, J. 1973. Hydraulic conductivity and water retention in peat soils. *Acta For. Fenn.*, 129, 70 p.
- Parlange, J.-Y. 1976. Capillary hysteresis and relationship between drying and wetting curves. *Water Resour. Res.*, 12(2), 224-228.
- Penttinen, S. 2000. Electrical and hydraulic classification of forest till soils in Central Lapland, Finland. *Geological Survey of Finland, Bulletin 398*, 88 p.
- Perfect, E., N. McLaughlin, B. Kay and G. Topp. 1996. An improved fractal equation for the soil water retention curve. *Water Resour. Res.*, 33, 281-287.
- Perrier, E., M. Rieu, G. Sposito and G. de Marsily. 1996. Models of the water retention curve for soils with a fractal pore size distribution. *Water Resour. Res.*, 32, 3025-3031.
- Priestley, C.H.B. and R.J. Taylor. 1972. On the assessment of surface heat flux and evaporation using large-scale parameters. *Monthly Weather Rev.*, 100, 81-92.
- Purcell, W.R. 1949. Capillary pressures – their measurement using mercury and the calculation of permeability there from. *J. Pet. Tech.*, 1, 39-46.
- Raats, P.A.C. 1992. A superclass of soils, p. 45-51. In van Genuchten, M.Th., F.J. Leij and L.J. Lund. (eds.). *Proc. Int. Workshop, Indirect methods for estimating the hydraulic properties of unsaturated soils*. University of California, Riverside, CA.
- Rajkai, K., S. Kabos, M.Th. van Genuchten and P.-E. Jansson. 1996. Estimation of water retention characteristics from the bulk density and particle-size distribution of Swedish soils, *Soil Sci.*, 161, 832-845.
- Rawls, W.J., D.L. Brakensiek and K.E. Saxton. 1982. Estimation of soil water properties. *Trans. ASAE*, 25, 1316-1320.

- Rawls, W.J. and D.L. Brakensiek. 1982. Estimating soil water retention from soil properties. *J. Irrig. and Drain. Div., ASCE*, 108 (IR2), 166-171.
- Reynolds, W.D. and D.E. Elrick. 1985. In situ measurement of field-saturated hydraulic conductivity, sorptivity and the α parameter using the Guelph Permeameter. *Soil Sci.*, 140, 292-296.
- Richards, L.A. 1931. Capillary conduction of liquids through porous media. *Physics*, 1, 318-333.
- Rieu, M. and G. Sposito. 1991a. Fractal fragmentation, soil porosity, and soil water properties: I. Theory. *Soil Sci Soc. Am. J.*, 55, 1231-1238.
- Rieu, M. and G. Sposito. 1991b. Fractal fragmentation, soil porosity, and soil water properties: II. Applications. *Soil Sci Soc. Am. J.*, 55, 1239-1242.
- Rogowski, A.S. 1971. Watershed physics: model of the soil moisture characteristic. *Water Resour. Res.*, 7, 1575-1582.
- Rose, C.W., W.R. Stern and J.E. Drummond. 1965. Determination of hydraulic conductivity as a function of depth and water content for soil in situ. *Water Resour. Res.*, 3, 1-9.
- Ross, P.J., J. Williams and K.L. Bristow. 1991. Equations for extending water retention curves to dryness. *Soil Sci. Soc. Am. J.*, 55, 923-927.
- Russo, D. 1988. Determining soil hydraulic properties by parameter estimation: On the selection of a model for the hydraulic properties. *Water Resour. Res.*, 24 (3), 453-459.
- Russo, D., E. Bresler., U. Shani and J.C. Parker. 1991. Analyses of infiltration events in relation to determining soil hydraulic properties by inverse methodology. *Water Resour. Res.*, 27, 1361-1373.
- Sahlberg, S. 1992. Metsämaan orgaaninen aine ja sen vaikutus maan huokoisuuteen (in Finnish). Manuscript. M. Sc. Thesis. Univ. Helsinki, Dept. Forest Ecology. 51 p.
- Schaap, M., F., Leij and M. van Genuchten. 1999. A bootstrap-neural network approach to predict soil hydraulic parameters, p. 1237-1250. In M.Th. van Genuchten, F.J. Leij, and L. Wu.(eds.), *Characterization and measurement of the hydraulic properties of unsaturated porous media*. University of California, Riverside, CA.
- Schuh, W.M. and R.L. Cline. 1990. Effect of soil properties on unsaturated hydraulic conductivity pore-interaction factors. *Soil Sci. Soc. Am. J.*, 54, 1509-1519.
- Shouse, P.J., Russel, W.B., Burden, D.S., Selim, H.M., Sisson, J. B. and M. Th. van Genuchten. 1995. Spatial variability of soil water retention functions in a silt loam soil. *Soil Sci.*, 159, 1-12.

- Tamari, S. and J. Wösten. 1999. Using artificial bootstrap-neural networks to develop pedotransfer functions of soil hydraulic properties, p. 1251-1260. In M.Th. van Genuchten, F.J. Leij, and L. Wu.(eds.), Characterization and measurement of the hydraulic properties of unsaturated porous media. University of California, Riverside, CA.
- Tani. M. 1982. The properties of a water-table rise produces by a one-dimensional, vertical, unsaturated flow. (in Japanese with English summary), J. Jpn. For. Soc., 64, 409-418.
- Torres, R., W.E. Dietrich, D.R. Montgomery, S.P. Anderson and K. Loague. 1998. Unsaturated zone processes and the hydrologic response of a steep, unchanneled catchment. Water Resour. Res., 34, 1865-1879.
- Tyler, S. and S. Wheatcraft. 1989. Application of fractal mathematics to soil water retention estimation. Soil Sci. Soc. Am. J., 53, 987-996.
- van Dam, J.C., J. N.M. Stricker and A. Verhoef. 1992. An evaluation of the one-step outflow method, p. 633-644. In M.Th. Van Genuchten, F.J. Leij and L.J. Lund (eds.) Proc. Int. Workshop, Indirect methods for estimating the hydraulic properties of unsaturated soils. University of California, Riverside, CA.
- van Dam, J.C. and R.A. Feddes. 2000. Numerical simulation of infiltration, evaporation and shallow groundwater levels with Richards' equation. J. Hydrol., 233, 72-85.
- van Genuchten, M.Th.. 1980. A closed form equation for predicting the hydraulic conductivity of unsaturated soils. Soil Sci. Soc. Am. J., 44, 892-898.
- van Genuchten, M.Th. and D. R. Nielsen. 1985. On describing and predicting the hydraulic properties of unsaturated soils. Ann. Geophys., 3, 615-628.
- van Genuchten, M.Th. and F.J. Leij. 1992. On estimating the hydraulic properties of unsaturated soils, p. 1-14. In van Genuchten, M. Th., Leij, F. J. and L.J. Lund (eds.). Proc. Int. Workshop, Indirect methods for estimating the hydraulic properties of unsaturated soils. University of California, Riverside, CA.
- van Genuchten, M.Th., F.J. Leij and L. Wu (eds.). 1999. Proc. Int. Workshop, Characterization and Measurement of the Hydraulic Properties of Unsaturated Porous Media. Parts 1 and 2, University of California, Riverside, CA. 1602 p.
- Vereecken, H. 1992. Derivation and validation of pedotransfer functions for soil hydraulic properties, p. 473-488. In van Genuchten, M. Th., Leij, F. J. and L.J. Lund (eds.). Proc. Int. Workshop, Indirect methods for estimating the hydraulic properties of unsaturated soils. University of California, Riverside, CA

- Vereecken, H., J. Maes, J. Feyen and P. Darius. 1989. Estimating the soil moisture retention characteristic from texture, bulk density and carbon content. *Soil Sci.*, 148, 389-403.
- Visser, W.C. 1968. An empirical expression for the desorption curve, p. 329-335. In P.E. Rijtema and H. Wassink (ed.) *Water in the Unsaturated Zone. Vol. I. Proc. Wageningen Symposium. IASH/AIHS, UNESCO, Paris.*
- Watson, K.K. 1966. An instantaneous profile method for determining the hydraulic conductivity of unsaturated porous materials. *Water Resour. Res.*, 1, 577-586.
- Weiss, R., J. Alm, R. Laiho and J. Laine. 1998. Modeling moisture retention in peat soils. *Soil Sci. Soc. Am. J.*, 62, 305-313.
- Westman, C.-J. 1983. Taimitarhamaiden fysikaalisia ja kemiallisia ominaisuuksia sekä niiden suhde orgaanisen aineksen määrään. Summary: physical and physico-chemical properties of forest tree nursery soils and their relation to organic matter content. *Acta For. Fenn.*, 184, 34 p.
- Westman, C.-J. 1988. Metsämaan fysikaalis-kemialliset ominaisuudet CT-OmaT kasvupaikkasarjassa. Summary: Soil physical and physico-chemical properties of Finnish upland forest sites. *Silva Fennica*, 24, 141-158.
- Williams, R., L. Ahuja and J. Naney. 1992. Comparison of methods to estimate soil water characteristics from soil texture, bulk density and limited data. *Soil Sci.*, 153, 172-184.
- Wösten, J.H.M. and M.Th. van Genuchten. 1988. Using texture and other soil properties to predict the unsaturated soil hydraulic functions. *Soil Sci. Soc. Am. J.*, 52, 1762-1770.
- Wu, L., J.A. Vomocil and S.W. Childs. 1990. Pore size, particle size, aggregate size and water retention. *Soil Sci. Soc. Am. J.*, 54, 952-956.
- Wu, L. and J.A. Vomocil. 1992. Predicting the soil water characteristic from the aggregate size distribution, p. 139-145. In van Genuchten, M.Th., Leij, F.J. and L.J. Lund (eds.). *Proc. Int. Workshop, Indirect methods for estimating the hydraulic properties of unsaturated soils. University of California, Riverside, CA.*
- Yeh, W. W.-G. 1986. Review of parameter identification procedures in groundwater hydrology: The inverse problem. *Water Resour. Res.*, 22, 95-108.
- Zavarotto, L., N. Jarvis, and L. Persson. 1999. Use of similar media scaling to characterize spatial dependence of near-saturated hydraulic conductivity. *Soil Sci. Soc. Am. J.* 64, 486-492.

Zhang, R. and M.Th. van Genuchten. 1994. New models for unsaturated soil hydraulic properties. *Soil Sci.*, 158, 77-85.

Appendix 1. Particle size distributions of the mineral soil samples and bulk densities ρ_b (kg dm⁻³) and loss of ignition (%) (108 samples from four forest types and from four different layers).

Plot	Pit	Type	Layer	<2	2-6	6-20	20-60	60- 200	200-600	600-2000	>2000	ρ_b	LOI (%)
1	1	CT	A	2.1	1.2	3.0	4.8	8.2	55.3	25.4	0	1.06	4.7
1	1	CT	B1	0.7	0.9	3.3	6.5	10.0	53.4	25.2	0	1.11	2.1
1	1	CT	B2	1.1	1.3	3.0	6.1	10.1	55.4	23.0	0	1.26	4.7
1	1	CT	C	0.6	0.1	0.3	1.0	9.1	77.0	12.0	0	1.37	0.8
2	1	VT	A	10.6	1.6	0.2	10.4	48.5	27.5	1.1	0.0	1.32	5.6
2	1	VT	B1	11.0	0.0	2.2	7.0	47.9	30.2	1.6	0.1	1.22	4.1
2	1	VT	B2	7.3	2.0	1.7	6.9	55.3	26.5	0.2	0.0	1.46	2.5
2	1	VT	C	5.2	0.3	1.8	3.1	46.8	42.3	0.4	0.0	1.59	0.6
2	2	VT	A	16.7	0.0	6.5	8.7	40.0	24.5	3.0	0.6	1.05	5.6
2	2	VT	B1	11.2	2.1	2.4	8.7	49.4	25.8	0.4	0.0	1.35	4.1
2	2	VT	B2	8.1	2.0	0.2	8.7	49.8	30.9	0.3	0.0	1.31	2.5
2	2	VT	C	5.6	0.0	5.6	5.1	47.8	35.4	0.4	0.0	1.51	0.6
2	3	VT	A	17.8	0.0	0.0	5.6	44.1	29.7	2.5	0.3	1.26	5.6
2	3	VT	B1	9.3	1.5	4.2	8.3	44.9	31.0	0.7	0.1	1.26	4.1
2	3	VT	B2	8.7	0.0	4.3	6.8	48.8	30.6	0.7	0.1	1.22	2.5
2	3	VT	C	7.5	0.3	0.0	1.8	49.1	41.0	0.4	0.0	1.58	0.6
3	1	OMT	A	10.1	1.3	11.3	8.7	23.5	26.4	12.6	6.0	1.32	3.4
3	1	OMT	B1	9.0	2.9	6.3	11.4	24.6	25.1	12.3	8.3	1.17	3.0
3	1	OMT	B2	7.9	0.0	3.9	6.9	23.1	30.0	16.8	11.4	1.44	2.5
3	1	OMT	C	7.9	1.6	7.7	16.4	22.5	25.2	13.5	5.1	1.66	1.0
3	2	OMT	A	8.8	0.0	6.4	9.7	24.0	29.2	17.1	4.8	1.13	3.4
3	2	OMT	B1	10.5	0.3	5.4	9.8	18.1	27.7	22.4	5.8	1.53	3.0
3	2	OMT	B2	6.4	0.0	4.0	9.1	27.5	34.2	16.0	2.8	1.43	2.5
3	2	OMT	C	6.3	0.0	4.0	9.2	28.4	30.9	16.3	4.9	1.77	1.0
3	3	OMT	A	7.9	1.6	7.2	12.6	24.4	25.8	15.4	5.1	1.26	3.4
3	3	OMT	B1	9.9	1.6	5.4	11.9	20.9	24.1	15.6	10.6	1.32	3.0
3	3	OMT	B2	7.5	0.0	3.7	7.5	24.1	29.0	18.9	9.3	1.44	2.5
3	3	OMT	C	7.7	3.3	13.4	13.7	15.5	15.0	13.1	18.3	1.62	1.0
4	1	MT	A	3.5	3.5	11.5	23.9	24.5	20.2	12.9	0	1.12	5.8
4	1	MT	B1	4.9	3.8	12.4	24.2	23.5	19.0	12.2	0	1.14	4.5
4	1	MT	B2	3.2	3.5	12.1	25.7	24.4	19.2	11.8	0	1.32	3.4
4	1	MT	C	4.7	4.7	13.4	25.0	22.9	16.8	12.4	0	1.53	2.6
7	1	CT	A	2.2	1.6	3.3	6.7	15.1	36.7	34.4	0	1.05	3.8
7	1	CT	B1	1.7	1.5	3.4	7.3	17.9	36.7	31.5	0	1.18	4.4
7	1	CT	B2	0.6	1.1	3.2	8.9	17.9	34.6	33.6	0	1.37	2.8
7	1	CT	C	0.4	0.3	0.3	0.8	10.9	55.1	32.2	0	1.57	0.7
8	1	MT	A	1.5	1.6	3.7	9.2	34.5	38.4	11.1	0	1.23	2.4
8	1	MT	B1	1.9	1.0	2.6	8.0	36.9	39.3	10.4	0	1.15	5.5
8	1	MT	B2	0.5	0.3	1.1	4.3	34.2	48.8	10.8	0	1.40	1.6
8	1	MT	C	1.1	1.5	3.3	12.0	54.0	23.2	4.9	0	1.50	0.7
9	1	VT	A	7.2	0.3	5.5	5.2	17.2	40.4	21.8	2.3	1.31	3.3
9	1	VT	B1	8.4	1.1	1.8	1.8	10.8	36.8	30.2	9.1	1.25	3.3
9	1	VT	B2	5.2	0.3	1.6	0.1	6.7	43.5	32.3	10.3	1.48	1.2
9	1	VT	C	5.0	0.0	0.0	2.0	15.4	46.4	20.4	10.9	1.59	0.6
9	2	VT	A	7.0	0.0	1.8	1.0	16.1	48.6	24.8	0.7	1.20	3.3
9	2	VT	B1	7.2	0.3	0.0	2.7	12.2	43.5	31.4	2.6	1.26	3.3
9	2	VT	B2	5.2	0.3	1.8	0.5	10.0	35.6	34.4	12.2	1.50	1.2
9	2	VT	C	5.5	0.0	1.8	6.3	45.4	27.0	10.1	3.9	1.52	0.6
9	3	VT	A	7.2	0.3	3.2	5.1	17.5	44.1	22.0	0.5	1.14	3.3
9	3	VT	B1	6.4	1.1	3.7	3.3	17.2	37.7	23.2	7.4	1.27	3.3
9	3	VT	B2	7.5	0.0	1.8	6.3	17.5	35.7	24.8	6.4	1.55	1.2
9	3	VT	C	5.2	2.0	4.0	7.0	17.3	40.4	21.8	2.3	1.51	0.6
11	1	MT	A	1.5	1.3	2.1	4.3	11.5	53.6	25.7	0	1.17	3.1

Plot	Pit	Type	Layer	<2	2-6	6-20	20-60	60-200	200-600	600-2000	>2000	ρ_b	LOI (%)
11	1	MT	B1	1.6	1.1	1.9	4.1	11.8	54.0	25.5	0	1.28	2.5
11	1	MT	B2	0.8	0.8	1.7	3.3	12.1	55.0	26.4	0	1.35	1.6
11	1	MT	C	0.4	0.5	1.2	3.0	12.7	57.0	25.1	0	1.47	1.1
12	1	MT	A	1.9	1.3	4.2	12.0	37.2	42.8	0.6	0	1.22	2.1
12	1	MT	B1	0.4	0.6	3.2	12.1	36.1	47.2	0.4	0	1.29	2.5
12	1	MT	B2	0.4	0.9	3.9	11.1	31.8	51.5	0.4	0	1.43	1.4
12	1	MT	C	0.6	1.1	5.3	15.4	27.4	49.2	1.0	0	1.53	0.6
13	1	MT	A	2.9	3.4	13.6	33.0	30.7	15.6	0.7	0	1.16	3.8
13	1	MT	B1	0.7	2.2	14.1	38.3	30.7	13.1	0.7	0	1.06	3.9
13	1	MT	B2	1.1	3.7	18.0	39.9	28.5	8.3	0.5	0	1.27	1.8
13	1	MT	C	3.1	6.0	24.3	46.1	16.3	4.1	0.2	0	1.62	1.0
15	1	MT	A	3.1	3.1	7.2	19.3	24.1	27.8	15.4	0	1.17	3.3
15	1	MT	B1	2.4	1.8	5.8	20.9	25.6	27.8	15.6	0	1.24	4.1
15	1	MT	B2	1.5	2.3	6.6	20.9	26.0	28.0	14.7	0	1.38	2.3
15	1	MT	C	4.3	4.2	11.0	23.9	23.9	25.4	7.4	0	1.65	1.2
16	1	MT	A	2.1	2.0	5.6	13.9	14.4	33.2	28.7	0	1.20	2.8
16	1	MT	B1	2.5	1.4	4.3	11.3	10.9	29.8	39.8	0	1.25	3.6
16	1	MT	B2	1.3	0.6	1.9	6.2	8.8	35.1	46.1	0	1.46	3.9
16	1	MT	C	1.3	1.5	4.6	18.7	22.8	17.5	33.7	0	1.60	1.3
18	1	MT	A	7.8	10.7	21.6	25.2	16.0	10.3	8.5	0	1.18	6.1
18	1	MT	B1	9.8	11.3	21.5	25.8	15.3	9.0	7.2	0	1.12	3.9
18	1	MT	B2	9.0	10.7	21.5	25.3	19.0	8.8	5.7	0	1.26	2.6
18	1	MT	C	13.7	16.5	32.9	24.4	8.1	2.9	1.5	0	1.60	1.1
19	1	MT	A	1.4	2.0	6.3	20.6	54.3	13.8	1.6	0	1.20	1.3
19	1	MT	B1	1.8	1.8	5.4	19.0	53.8	15.8	2.3	0	1.09	3.7
19	1	MT	B2	0.3	1.5	5.5	20.3	52.5	17.3	2.7	0	1.30	1.3
19	1	MT	C	0.6	0.8	2.2	19.7	65.2	10.8	0.7	0	1.52	0.5
21	1	CT	A	2.4	1.5	1.9	3.6	30.7	51.9	7.9	0	1.22	2.8
21	1	CT	B1	1.1	0.9	1.3	2.3	36.6	50.2	7.7	0	1.38	2.8
21	1	CT	B2	0.9	0.6	0.8	2.1	36.0	51.7	7.9	0	1.52	1.6
21	1	CT	C	0.4	0.0	0.2	1.1	42.1	50.8	5.4	0	1.65	0.4
23	1	MT	A	3.6	3.9	5.5	13.1	19.3	30.5	24.1	0	1.20	3.9
23	1	MT	B1	2.2	3.6	5.4	12.8	20.4	31.9	23.8	0	1.23	4.1
23	1	MT	B2	1.7	4.0	4.8	12.2	19.9	30.7	26.7	0	1.40	2.5
23	1	MT	C	6.9	12.8	12.3	24.9	21.1	12.7	9.3	0	1.54	1.1
24	1	CT	A	2.3	2.4	6.8	15.2	25.1	32.9	15.2	0	1.35	2.8
24	1	CT	B1	0.9	1.9	6.5	15.7	23.5	34.2	17.2	0	1.14	7.4
24	1	CT	B2	0.2	2.0	7.0	11.8	17.8	34.8	26.4	0	1.51	4.0
24	1	CT	C	0.5	0.4	0.8	1.6	4.9	29.1	62.7	0	1.52	0.8
25	1	MT	A	5.7	5.7	15.4	11.8	29.0	20.3	12.0	0	1.23	3.7
25	1	MT	B1	4.3	4.4	10.8	27.1	24.3	17.6	11.5	0	1.12	4.9
25	1	MT	B2	2.5	4.3	12.4	31.0	25.6	15.1	9.2	0	1.25	3.2
25	1	MT	C	5.2	6.0	11.3	21.6	22.4	17.6	15.8	0	1.70	1.1
26	1	CT	A	2.9	2.2	4.8	9.4	9.8	23.2	47.7	0	1.16	10.0
26	1	CT	B1	2.1	2.0	4.9	11.9	10.9	22.6	45.7	0	1.27	7.0
26	1	CT	B2	0.8	1.2	3.1	6.1	5.5	19.1	64.2	0	1.63	6.4
26	1	CT	C	0.8	0.9	0.7	1.9	4.6	15.8	75.2	0	1.53	1.3
27	1	CT	A	2.2	1.3	2.3	4.7	10.1	40.3	39.0	0	1.21	4.5
27	1	CT	B1	1.1	0.8	1.6	3.2	9.4	42.5	41.5	0	1.34	5.6
27	1	CT	B2	0.3	0.1	1.0	2.4	4.7	37.6	53.9	0	1.63	1.7
27	1	CT	C	0.3	0.0	0.1	0.5	4.4	62.6	32.0	0	1.62	0.5
30	1	CT	A	1.8	1.4	2.7	5.4	11.6	33.0	44.1	0	1.13	4.7
30	1	CT	B1	0.6	0.8	1.8	4.6	9.5	28.7	54.1	0	1.31	4.7
30	1	CT	B2	0.3	0.1	0.9	2.0	6.3	36.2	54.1	0	1.59	0.9
30	1	CT	C	0.3	0.0	0.2	0.9	5.7	27.9	65.1	0	1.60	0.6

Appendix 2. Measured soil water retention curves as a function of pressure head h (cm) (108 samples from four forest types and from four different layers).

Plot	Pit	Type	Layer	$h = 1$	10	32	63	100	1000	16000
1	1	CT	A	0.524	0.411	0.224	0.221	0.153	0.094	0.031
1	1	CT	B1	0.486	0.391	0.242	0.24	0.177	0.111	0.044
1	1	CT	B2	0.44	0.297	0.198	0.195	0.137	0.087	0.038
1	1	CT	C	0.398	0.293	0.091	0.079	0.055	0.028	0.012
2	1	VT	A	0.49	0.483	0.421	0.297	0.242	0.189	0.159
2	1	VT	B1	0.525	0.503	0.445	0.268	0.211	0.127	0.071
2	1	VT	B2	0.438	0.425	0.402	0.256	0.193	0.137	0.074
2	1	VT	C	0.394	0.386	0.335	0.102	0.071	0.055	0.029
2	2	VT	A	0.622	0.581	0.466	0.328	0.275	0.153	0.125
2	2	VT	B1	0.481	0.469	0.395	0.236	0.191	0.13	0.119
2	2	VT	B2	0.505	0.486	0.429	0.215	0.163	0.119	0.11
2	2	VT	C	0.422	0.41	0.391	0.221	0.143	0.103	0.061
2	3	VT	A	0.508	0.478	0.391	0.251	0.22	0.087	0.07
2	3	VT	B1	0.504	0.499	0.428	0.241	0.185	0.094	0.041
2	3	VT	B2	0.542	0.505	0.432	0.224	0.17	0.15	0.13
2	3	VT	C	0.399	0.393	0.359	0.109	0.073	0.06	0.038
3	1	OMT	A	0.472	0.437	0.337	0.301	0.258	0.153	0.097
3	1	OMT	B1	0.534	0.495	0.407	0.335	0.274	0.138	0.08
3	1	OMT	B2	0.432	0.408	0.291	0.221	0.175	0.07	0.043
3	1	OMT	C	0.367	0.324	0.281	0.252	0.221	0.066	0.038
3	2	OMT	A	0.523	0.422	0.361	0.275	0.242	0.123	0.028
3	2	OMT	B1	0.405	0.401	0.376	0.281	0.235	0.101	0.089
3	2	OMT	B2	0.449	0.425	0.378	0.243	0.193	0.071	0.067
3	2	OMT	C	0.32	0.316	0.295	0.213	0.164	0.044	0.041
3	3	OMT	A	0.494	0.424	0.338	0.289	0.232	0.125	0.069
3	3	OMT	B1	0.466	0.447	0.36	0.311	0.264	0.142	0.064
3	3	OMT	B2	0.433	0.422	0.316	0.26	0.211	0.098	0.077
3	3	OMT	C	0.376	0.365	0.339	0.307	0.287	0.13	0.065
4	1	MT	A	0.557	0.431	0.304	0.259	0.219	0.115	0.058
4	1	MT	B1	0.565	0.542	0.452	0.385	0.305	0.168	0.092
4	1	MT	B2	0.484	0.453	0.404	0.36	0.316	0.141	0.102
4	1	MT	C	0.306	0.281	0.246	0.208	0.172	0.05	0.025
7	1	CT	A	0.495	0.4	0.264	0.242	0.17	0.106	0.071
7	1	CT	B1	0.416	0.253	0.173	0.163	0.117	0.084	0.055
7	1	CT	B2	0.447	0.311	0.201	0.193	0.13	0.098	0.03
7	1	CT	C	0.352	0.175	0.091	0.064	0.041	0.032	0.026
8	1	MT	A	0.532	0.468	0.432	0.391	0.279	0.197	0.092
8	1	MT	B1	0.58	0.519	0.484	0.424	0.286	0.191	0.152
8	1	MT	B2	0.45	0.432	0.424	0.369	0.167	0.089	0.056
8	1	MT	C	0.483	0.455	0.447	0.429	0.267	0.068	0.033
9	1	VT	A	0.461	0.436	0.289	0.241	0.213	0.113	0.024
9	1	VT	B1	0.502	0.467	0.299	0.241	0.211	0.136	0.127
9	1	VT	B2	0.424	0.373	0.145	0.105	0.089	0.063	0.02
9	1	VT	C	0.384	0.359	0.183	0.111	0.075	0.056	0.024
9	2	VT	A	0.504	0.468	0.277	0.216	0.185	0.1	0.02
9	2	VT	B1	0.488	0.451	0.24	0.184	0.158	0.098	0.026
9	2	VT	B2	0.405	0.383	0.193	0.132	0.117	0.059	0.021
9	2	VT	C	0.42	0.398	0.369	0.259	0.174	0.051	0.048
9	3	VT	A	0.539	0.492	0.322	0.249	0.209	0.119	0.089
9	3	VT	B1	0.482	0.454	0.303	0.231	0.191	0.103	0.024
9	3	VT	B2	0.396	0.375	0.285	0.206	0.18	0.08	0.074
9	3	VT	C	0.432	0.402	0.386	0.332	0.306	0.08	0.071
11	1	MT	A	0.378	0.272	0.253	0.195	0.114	0.075	0.07

Plot	Pit	Type	Layer	$b = 1$	10	32	63	100	1000	16000
11	1	MT	B1	0.358	0.22	0.2	0.145	0.1	0.038	0.03
11	1	MT	B2	0.3	0.195	0.171	0.121	0.068	0.03	0.024
11	1	MT	C	0.262	0.102	0.08	0.047	0.025	0.013	0.01
12	1	MT	A	0.538	0.5	0.308	0.241	0.109	0.045	0.03
12	1	MT	B1	0.489	0.462	0.341	0.245	0.095	0.082	0.07
12	1	MT	B2	0.433	0.42	0.325	0.272	0.08	0.054	0.04
12	1	MT	C	0.418	0.411	0.337	0.283	0.074	0.048	0.035
13	1	MT	A	0.585	0.563	0.491	0.428	0.174	0.103	0.08
13	1	MT	B1	0.583	0.564	0.475	0.404	0.143	0.132	0.11
13	1	MT	B2	0.503	0.492	0.423	0.375	0.117	0.092	0.08
13	1	MT	C	0.44	0.431	0.39	0.357	0.141	0.108	0.08
15	1	MT	A	0.51	0.467	0.333	0.273	0.214	0.098	0.066
15	1	MT	B1	0.548	0.528	0.409	0.332	0.255	0.149	0.099
15	1	MT	B2	0.478	0.453	0.38	0.318	0.219	0.112	0.088
15	1	MT	C	0.41	0.385	0.339	0.307	0.248	0.086	0.056
16	1	MT	A	0.528	0.438	0.312	0.274	0.233	0.134	0.075
16	1	MT	B1	0.522	0.456	0.345	0.298	0.265	0.184	0.121
16	1	MT	B2	0.502	0.428	0.319	0.283	0.249	0.165	0.108
16	1	MT	C	0.358	0.329	0.244	0.189	0.11	0.052	0.041
18	1	MT	A	0.628	0.497	0.427	0.395	0.349	0.196	0.096
18	1	MT	B1	0.533	0.487	0.405	0.374	0.336	0.191	0.076
18	1	MT	B2	0.462	0.413	0.368	0.345	0.32	0.204	0.075
18	1	MT	C	0.36	0.332	0.315	0.308	0.301	0.254	0.128
19	1	MT	A	0.573	0.41	0.329	0.3	0.351	0.132	0.066
19	1	MT	B1	0.581	0.54	0.467	0.402	0.32	0.171	0.111
19	1	MT	B2	0.474	0.439	0.38	0.339	0.33	0.159	0.08
19	1	MT	C	0.469	0.414	0.381	0.356	0.34	0.15	0.052
21	1	CT	A	0.61	0.534	0.364	0.255	0.226	0.095	0.081
21	1	CT	B1	0.464	0.452	0.337	0.205	0.172	0.089	0.08
21	1	CT	B2	0.433	0.413	0.319	0.164	0.132	0.063	0.037
21	1	CT	C	0.418	0.377	0.3	0.116	0.063	0.021	0.017
23	1	MT	A	0.62	0.48	0.388	0.328	0.295	0.177	0.134
23	1	MT	B1	0.596	0.532	0.437	0.357	0.313	0.197	0.144
23	1	MT	B2	0.561	0.535	0.467	0.379	0.351	0.228	0.134
23	1	MT	C	0.436	0.383	0.371	0.339	0.3	0.117	0.065
24	1	CT	A	0.523	0.477	0.386	0.325	0.272	0.131	0.023
24	1	CT	B1	0.534	0.455	0.366	0.326	0.281	0.168	0.103
24	1	CT	B2	0.506	0.461	0.375	0.332	0.295	0.149	0.141
24	1	CT	C	0.264	0.127	0.061	0.049	0.039	0.028	0.019
25	1	MT	A	0.526	0.424	0.36	0.29	0.264	0.161	0.086
25	1	MT	B1	0.516	0.487	0.416	0.331	0.3	0.159	0.135
25	1	MT	B2	0.498	0.471	0.415	0.342	0.313	0.174	0.128
25	1	MT	C	0.419	0.393	0.364	0.319	0.299	0.208	0.122
26	1	CT	A	0.632	0.595	0.444	0.354	0.318	0.203	0.105
26	1	CT	B1	0.468	0.44	0.333	0.283	0.257	0.157	0.055
26	1	CT	B2	0.351	0.223	0.154	0.127	0.116	0.073	0.02
26	1	CT	C	0.27	0.104	0.058	0.047	0.041	0.032	0.013
27	1	CT	A	0.537	0.476	0.351	0.242	0.217	0.143	0.097
27	1	CT	B1	0.447	0.406	0.269	0.187	0.175	0.111	0.032
27	1	CT	B2	0.394	0.343	0.182	0.122	0.108	0.058	0.022
27	1	CT	C	0.341	0.273	0.135	0.058	0.062	0.03	0.014
30	1	CT	A	0.538	0.51	0.306	0.26	0.117	0.093	0.035
30	1	CT	B1	0.471	0.426	0.231	0.196	0.131	0.091	0.057
30	1	CT	B2	0.416	0.307	0.115	0.091	0.054	0.037	0.023
30	1	CT	C	0.388	0.262	0.056	0.044	0.027	0.018	0.011

Appendix 3/I. Average WRCs of four forest types from four different layers as a function of pressure head h (cm). Std is standard deviation ($\text{m}^3 \text{m}^{-3}$), max and min are maximum and minimum volumetric water content, respectively (data based on 360 samples).

Layer C		$h = 1$	10	32	63	100	1000	16000
CT	Average	0.357	0.246	0.123	0.068	0.048	0.026	0.017
	Std	0.057	0.098	0.081	0.025	0.015	0.008	0.007
	Max	0.418	0.377	0.300	0.123	0.088	0.050	0.039
	Min	0.247	0.089	0.048	0.037	0.024	0.015	0.011
VT	Average	0.404	0.334	0.248	0.170	0.117	0.043	0.027
	Std	0.029	0.105	0.150	0.126	0.088	0.022	0.017
	Max	0.458	0.434	0.414	0.395	0.308	0.103	0.071
	Min	0.350	0.112	0.047	0.036	0.030	0.017	0.011
MT	Average	0.413	0.362	0.312	0.274	0.217	0.107	0.055
	Std	0.050	0.086	0.114	0.115	0.118	0.081	0.040
	Max	0.498	0.460	0.447	0.429	0.376	0.327	0.163
	Min	0.262	0.102	0.068	0.047	0.019	0.012	0.010
OMT	Average	0.406	0.357	0.296	0.254	0.216	0.101	0.065
	Std	0.040	0.064	0.109	0.092	0.088	0.054	0.034
	Max	0.491	0.456	0.403	0.362	0.340	0.221	0.134
	Min	0.320	0.190	0.060	0.059	0.050	0.036	0.022

Layer B2		$h = 1$	10	32	63	100	1000	16000
CT	Average	0.412	0.328	0.215	0.166	0.131	0.075	0.040
	Std	0.049	0.079	0.087	0.069	0.060	0.033	0.030
	Max	0.506	0.461	0.375	0.332	0.295	0.149	0.141
	Min	0.289	0.110	0.075	0.066	0.054	0.037	0.014
VT	Average	0.431	0.391	0.293	0.224	0.167	0.085	0.051
	Std	0.043	0.070	0.118	0.098	0.060	0.034	0.033
	Max	0.542	0.505	0.444	0.436	0.276	0.150	0.130
	Min	0.368	0.205	0.082	0.070	0.057	0.037	0.015
MT	Average	0.462	0.413	0.345	0.286	0.222	0.112	0.070
	Std	0.062	0.095	0.119	0.111	0.114	0.061	0.035
	Max	0.575	0.552	0.525	0.463	0.409	0.257	0.161
	Min	0.300	0.150	0.097	0.068	0.029	0.018	0.010
OMT	Average	0.458	0.413	0.322	0.255	0.206	0.094	0.065
	Std	0.058	0.071	0.129	0.098	0.093	0.039	0.024
	Max	0.561	0.539	0.507	0.396	0.336	0.166	0.128
	Min	0.374	0.308	0.098	0.094	0.075	0.052	0.038

Appendix 3/II. Average WRCs of four forest types from four different layers as a function of pressure head h (cm). Std is standard deviation ($\text{m}^3 \text{m}^{-3}$), max and min are maximum and minimum volumetric water content, respectively (data based on 360 samples).

Layer B1		$h = 1$	10	32	63	100	1000	16000
CT	Average	0.498	0.436	0.313	0.248	0.203	0.123	0.072
	Std	0.040	0.058	0.073	0.064	0.067	0.038	0.033
	Max	0.584	0.554	0.503	0.415	0.396	0.222	0.153
	Min	0.416	0.253	0.173	0.163	0.117	0.063	0.032
VT	Average	0.514	0.475	0.364	0.283	0.215	0.130	0.071
	Std	0.049	0.067	0.109	0.094	0.051	0.032	0.035
	Max	0.626	0.611	0.542	0.494	0.300	0.196	0.127
	Min	0.421	0.267	0.117	0.102	0.083	0.052	0.018
MT	Average	0.526	0.477	0.397	0.323	0.246	0.141	0.089
	Std	0.064	0.091	0.108	0.095	0.089	0.053	0.039
	Max	0.641	0.607	0.557	0.449	0.383	0.242	0.158
	Min	0.358	0.220	0.184	0.141	0.082	0.029	0.020
OMT	Average	0.495	0.456	0.366	0.286	0.232	0.128	0.082
	Std	0.069	0.070	0.106	0.074	0.072	0.037	0.037
	Max	0.663	0.594	0.544	0.419	0.356	0.202	0.171
	Min	0.403	0.323	0.214	0.198	0.102	0.079	0.023

Layer A		$h = 1$	10	32	63	100	1000	16000
CT	Average	0.545	0.474	0.332	0.266	0.210	0.117	0.066
	Std	0.047	0.050	0.058	0.045	0.050	0.034	0.029
	Max	0.641	0.595	0.444	0.354	0.318	0.203	0.106
	Min	0.433	0.386	0.224	0.183	0.117	0.058	0.023
VT	Average	0.431	0.391	0.293	0.224	0.167	0.085	0.051
	Std	0.043	0.070	0.118	0.098	0.060	0.034	0.033
	Max	0.542	0.505	0.444	0.436	0.276	0.150	0.130
	Min	0.368	0.205	0.082	0.070	0.057	0.037	0.015
MT	Average	0.514	0.442	0.360	0.298	0.234	0.125	0.073
	Std	0.059	0.068	0.080	0.073	0.080	0.046	0.028
	Max	0.628	0.563	0.491	0.428	0.351	0.203	0.141
	Min	0.360	0.223	0.195	0.131	0.068	0.026	0.016
OMT	Average	0.497	0.439	0.342	0.273	0.217	0.112	0.065
	Std	0.036	0.042	0.090	0.068	0.071	0.030	0.023
	Max	0.567	0.492	0.470	0.396	0.326	0.158	0.104
	Min	0.425	0.322	0.176	0.166	0.088	0.046	0.028

Appendix 4. Parameters of Andersson's function ($b_{i,0}$, b_i , θ_0 and p_i , Equation 3-2) for 108 soils.

Plot	Pit	Type	Layer	$b_{i,0}$	b_i	θ_0	p_i
1	1	CT	A	19.6	0.720	0.315	0.634
1	1	CT	B1	22.8	0.958	0.302	0.621
1	1	CT	B2	8.8	1.269	0.302	0.682
1	1	CT	C	14.6	0.279	0.220	0.423
2	1	VT	A	52.8	0.238	0.336	0.353
2	1	VT	B1	55.4	0.253	0.316	0.475
2	1	VT	B2	60.8	0.209	0.276	0.367
2	1	VT	C	44.5	0.098	0.219	0.366
2	2	VT	A	49.1	0.402	0.384	0.571
2	2	VT	B1	47.5	0.209	0.307	0.390
2	2	VT	B2	47.6	0.141	0.310	0.410
2	2	VT	C	58.1	0.135	0.255	0.359
2	3	VT	A	54.0	0.391	0.298	0.506
2	3	VT	B1	55.1	0.243	0.294	0.491
2	3	VT	B2	42.6	0.150	0.336	0.420
2	3	VT	C	47.7	0.078	0.225	0.361
3	1	OMT	A	60.6	0.838	0.300	0.500
3	1	OMT	B1	70.8	0.619	0.319	0.555
3	1	OMT	B2	49.1	0.521	0.250	0.473
3	1	OMT	C	125.7	0.686	0.196	0.411
3	2	OMT	A	55.3	1.296	0.298	0.764
3	2	OMT	B1	84.2	0.310	0.253	0.361
3	2	OMT	B2	62.0	0.301	0.261	0.429
3	2	OMT	C	83.8	0.283	0.184	0.318
3	3	OMT	A	53.5	0.869	0.295	0.568
3	3	OMT	B1	89.5	0.818	0.281	0.530
3	3	OMT	B2	58.7	0.521	0.265	0.438
3	3	OMT	C	263.0	0.678	0.218	0.395
4	1	MT	A	23.3	1.047	0.345	0.733
4	1	MT	B1	80.1	0.565	0.346	0.564
4	1	MT	B2	122.4	0.582	0.292	0.463
4	1	MT	C	107.1	0.546	0.165	0.336
7	1	CT	A	25.0	0.734	0.305	0.555
7	1	CT	B1	5.8	1.015	0.296	0.587
7	1	CT	B2	11.5	1.109	0.293	0.641
7	1	CT	C	7.8	0.429	0.207	0.404
8	1	MT	A	101.0	0.950	0.324	0.589
8	1	MT	B1	76.8	0.234	0.360	0.425
8	1	MT	B2	82.5	0.093	0.258	0.387
8	1	MT	C	101.2	0.085	0.259	0.436
9	1	VT	A	47.8	0.838	0.274	0.579
9	1	VT	B1	28.7	0.407	0.330	0.443
9	1	VT	B2	20.4	0.242	0.244	0.421
9	1	VT	C	27.2	0.249	0.220	0.386
9	2	VT	A	33.1	0.580	0.299	0.582
9	2	VT	B1	26.7	0.431	0.294	0.521
9	2	VT	B2	26.6	0.336	0.239	0.426
9	2	VT	C	72.8	0.250	0.234	0.409
9	3	VT	A	32.6	0.491	0.334	0.539
9	3	VT	B1	42.3	0.603	0.283	0.555
9	3	VT	B2	48.9	0.461	0.242	0.389
9	3	VT	C	143.9	0.350	0.243	0.406
11	1	MT	A	35.9	0.666	0.219	0.384

Plot	Pit	Type	Layer	$b_{i,0}$	b_i	θ_0	p_i
11	1	MT	B1	11.6	1.293	0.230	0.566
11	1	MT	B2	19.6	0.943	0.174	0.402
11	1	MT	C	2.8	0.779	0.190	0.428
12	1	MT	A	37.9	0.401	0.295	0.601
12	1	MT	B1	46.0	0.266	0.278	0.467
12	1	MT	B2	68.2	0.106	0.223	0.385
12	1	MT	C	69.8	0.079	0.217	0.374
13	1	MT	A	74.2	0.103	0.325	0.495
13	1	MT	B1	68.2	0.068	0.332	0.451
13	1	MT	B2	70.9	0.061	0.281	0.410
13	1	MT	C	75.8	0.070	0.260	0.345
15	1	MT	A	46.5	0.601	0.302	0.554
15	1	MT	B1	56.7	0.480	0.340	0.528
15	1	MT	B2	70.4	0.351	0.285	0.435
15	1	MT	C	116.5	0.468	0.232	0.411
16	1	MT	A	31.0	0.974	0.330	0.639
16	1	MT	B1	35.3	0.873	0.346	0.538
16	1	MT	B2	32.4	0.974	0.331	0.553
16	1	MT	C	49.3	0.396	0.202	0.366
18	1	MT	A	60.4	2.064	0.384	1.060
18	1	MT	B1	174.6	1.447	0.301	0.750
18	1	MT	B2	658.6	2.006	0.226	0.784
18	1	MT	C	601.0	1.582	0.062	0.734
19	1	MT	A	65.2	0.288	0.346	0.543
19	1	MT	B1	83.2	0.554	0.355	0.557
19	1	MT	B2	187.9	1.022	0.272	0.559
19	1	MT	C	317.2	0.950	0.242	0.568
21	1	CT	A	33.9	0.519	0.360	0.646
21	1	CT	B1	42.8	0.299	0.282	0.435
21	1	CT	B2	44.3	0.259	0.246	0.427
21	1	CT	C	43.0	0.183	0.214	0.421
23	1	MT	A	23.2	1.176	0.412	0.754
23	1	MT	B1	50.8	0.700	0.385	0.569
23	1	MT	B2	88.2	0.839	0.367	0.562
23	1	MT	C	189.9	0.617	0.241	0.443
24	1	CT	A	95.7	1.054	0.289	0.713
24	1	CT	B1	50.7	1.135	0.337	0.636
24	1	CT	B2	66.5	0.694	0.323	0.475
24	1	CT	C	5.9	0.554	0.165	0.320
25	1	MT	A	39.4	1.338	0.333	0.697
25	1	MT	B1	69.5	0.536	0.331	0.463
25	1	MT	B2	87.7	0.627	0.321	0.457
25	1	MT	C	248.4	1.388	0.265	0.482
26	1	CT	A	47.9	0.687	0.402	0.656
26	1	CT	B1	72.4	1.197	0.285	0.621
26	1	CT	B2	3.9	1.515	0.273	0.661
26	1	CT	C	0.9	0.713	0.283	0.604
27	1	CT	A	34.9	0.465	0.334	0.506
27	1	CT	B1	33.7	0.557	0.270	0.485
27	1	CT	B2	24.6	0.394	0.228	0.419
27	1	CT	C	21.3	0.327	0.185	0.364
30	1	CT	A	35.7	0.408	0.311	0.580
30	1	CT	B1	25.7	0.392	0.286	0.474
30	1	CT	B2	15.2	0.312	0.232	0.442
30	1	CT	C	12.1	0.184	0.207	0.405

Appendix 5. Horizon, texture bulk density (ρ_b , g cm⁻³) and organic matter content (OM, %) of the selected UNSODA samples.

Number Series	Horizon	Texture	ρ_b	OM	
3360	Hoffmeister Schlag	Ap	silt loam	2.65*	1.08
3361	Hoffmeister Schlag	Ap	silt loam	2.65*	0.81
4001	Lille	B	sand	1.62	0.53
4030	Helecine	Ap	silt loam	1.49	1.46
4031	Helecine	AB	silt loam	1.48	1.42
4040	Retie	Ap	sand	1.58	1.58
4043	Lubbeek	C	silt loam	1.53	0.46
4052	Beerse podzol I	C	sand	1.6	0.18
4061	Beerse podzol II	A2	sand	1.68	0.36
4062	Beerse podzol II	Bh	loamy sand	1.68	0.32
4070	Humbeek	Ap	silt loam	1.51	1.49
4071	Humbeek	B2t	silt loam	1.47	0.42
4080	Edingen I	Ap	silt loam	1.44	1.6
4081	Edingen I	B2g	silt loam	1.51	0.5
4082	Edingen I	B3	silt loam	1.49	0.2
4091	Edingen II	A/B	silt loam	1.43	0.32
4092	Edingen II	B2g	silt loam	1.47	0.31
4102	BoZ polder I	C2	loam	1.53	0.44
4110	BoZ polder II	Ap	sandy loam	1.51	1.35
4111	BoZ polder II	C1	sandy loam	1.66	1.29

*Particle density

Appendix 6/I. Summary of the fitted parameters (α and n estimated, θ_s and θ_r given) of van Genuchten WRC equation to soil data (360 samples).

Plot	Pit	Type	Layer	α	n	θ_s	θ_r
1	1	CT	A	0.132	1.509	0.524	0.031
1	1	CT	B1	0.134	1.437	0.486	0.044
1	1	CT	B2	0.255	1.398	0.44	0.038
1	1	CT	C	0.097	2.127	0.398	0.012
1	2	CT	A	0.087	1.529	0.55	0.049
1	2	CT	B1	0.078	1.544	0.54	0.046
1	2	CT	B2	0.081	1.575	0.472	0.031
1	2	CT	C	0.081	2.141	0.408	0.012
1	3	CT	A	0.106	1.666	0.57	0.103
1	3	CT	B1	0.096	1.716	0.505	0.098
1	3	CT	B2	0.118	1.465	0.462	0.034
1	3	CT	C	0.077	2.276	0.414	0.012
2	1	VT	A	0.025	2.494	0.49	0.159
2	1	VT	B1	0.025	2.243	0.525	0.071
2	1	VT	B2	0.02	2.45	0.438	0.074
2	1	VT	C	0.024	4.367	0.394	0.029
2	2	VT	A	0.038	1.878	0.622	0.125
2	2	VT	B1	0.026	2.798	0.481	0.119
2	2	VT	B2	0.024	3.602	0.505	0.111
2	2	VT	C	0.019	3.312	0.422	0.061
2	3	VT	A	0.032	2.023	0.508	0.082
2	3	VT	B1	0.023	2.378	0.504	0.041
2	3	VT	B2	0.027	3.459	0.542	0.13
2	3	VT	C	0.022	5.028	0.399	0.038
3	1	OMT	A	0.055	1.487	0.472	0.097
3	1	OMT	B1	0.04	1.573	0.534	0.08
3	1	OMT	B2	0.043	1.722	0.432	0.043
3	1	OMT	C	0.031	1.564	0.367	0.038
3	2	OMT	A	0.087	1.387	0.523	0.028
3	2	OMT	B1	0.018	2.205	0.405	0.089
3	2	OMT	B2	0.024	2.254	0.449	0.067
3	2	OMT	C	0.017	2.365	0.32	0.041
3	3	OMT	A	0.07	1.469	0.494	0.069
3	3	OMT	B1	0.038	1.485	0.466	0.064
3	3	OMT	B2	0.036	1.746	0.433	0.077
3	3	OMT	C	0.014	1.594	0.376	0.065
4	1	MT	A	0.136	1.44	0.557	0.058
4	1	MT	B1	0.033	1.571	0.565	0.092
4	1	MT	B2	0.024	1.634	0.484	0.102
4	1	MT	C	0.025	1.654	0.306	0.025
4	2	MT	A	0.041	1.521	0.561	0.067
4	2	MT	B1	0.022	1.547	0.514	0.051
4	2	MT	B2	0.029	1.539	0.497	0.055
4	2	MT	C	0.032	1.598	0.453	0.163
4	3	MT	A	0.023	1.628	0.478	0.087
4	3	MT	B1	0.016	1.705	0.508	0.09
4	3	MT	B2	0.009	1.722	0.487	0.068
4	3	MT	C	0.01	1.682	0.466	0.071
5	1	VT	A	0.048	1.437	0.484	0.109
5	1	VT	B1	0.027	1.621	0.529	0.058

Appendix 6/II. Summary of the fitted parameters (α and n estimated, θ_s and θ_r given) of van Genuchten WRC equation to soil data (360 samples).

Plot	Pit	Type	Layer	α	n	θ_s	θ_r
5	1	VT	B2	0.02	1.717	0.406	0.04
5	1	VT	C	0.021	2.725	0.377	0.031
5	2	VT	A	0.036	1.568	0.51	0.042
5	2	VT	B1	0.022	1.764	0.503	0.048
5	2	VT	B2	0.014	2.884	0.421	0.06
5	2	VT	C	0.015	2.836	0.411	0.023
5	3	VT	A	0.036	1.615	0.571	0.064
5	3	VT	B1	0.027	1.729	0.626	0.08
5	3	VT	B2	0.017	2.03	0.446	0.023
5	3	VT	C	0.021	1.924	0.417	0.012
6	1	VT	A	0.014	1.639	0.491	0.042
6	1	VT	B1	0.011	5.138	0.551	0.066
6	1	VT	B2	0.016	1.944	0.474	0.03
6	1	VT	C	0.012	6.107	0.448	0.016
6	2	VT	A	0.02	2.104	0.508	0.122
6	2	VT	B1	0.022	1.685	0.537	0.036
6	2	VT	B2	0.022	1.804	0.397	0.016
6	2	VT	C	0.013	2.089	0.458	0.053
6	3	VT	A	0.017	1.962	0.552	0.084
6	3	VT	B1	0.012	3.836	0.566	0.09
6	3	VT	B2	0.011	5.515	0.473	0.039
6	3	VT	C	0.011	2.692	0.433	0.014
7	1	CT	A	0.106	1.553	0.495	0.071
7	1	CT	B1	0.34	1.45	0.416	0.055
7	1	CT	B2	0.237	1.395	0.447	0.03
7	1	CT	C	0.225	1.849	0.352	0.026
7	2	CT	A	0.087	1.514	0.532	0.046
7	2	CT	B1	0.091	1.422	0.474	0.049
7	2	CT	B2	0.078	1.566	0.415	0.073
7	2	CT	C	0.037	3.521	0.337	0.039
7	3	CT	A	0.076	1.517	0.503	0.106
7	3	CT	B1	0.053	1.517	0.506	0.066
7	3	CT	B2	0.083	1.518	0.469	0.06
7	3	CT	C	0.111	1.884	0.378	0.014
8	1	MT	A	0.044	1.434	0.532	0.092
8	1	MT	B1	0.028	1.807	0.58	0.152
8	1	MT	B2	0.013	5.166	0.45	0.056
8	1	MT	C	0.011	3.942	0.483	0.033
8	2	MT	A	0.025	1.769	0.503	0.092
8	2	MT	B1	0.025	1.791	0.593	0.116
8	2	MT	B2	0.03	2.207	0.418	0.065
8	2	MT	C	0.037	2.272	0.389	0.023
8	3	MT	A	0.012	3.74	0.444	0.044
8	3	MT	B1	0.013	4.381	0.547	0.114
8	3	MT	B2	0.021	2.526	0.475	0.073
8	3	MT	C	0.012	5.171	0.446	0.028
9	1	VT	A	0.065	1.451	0.461	0.024

Appendix 6/III. Summary of the fitted parameters (α and n estimated, θ_s and θ_r given) of van Genuchten WRC equation to soil data (360 samples).

Plot	Pit	Type	Layer	α	n	θ_s	θ_r
9	1	VT	B1	0.058	1.916	0.502	0.127
9	1	VT	B2	0.069	2.107	0.424	0.02
9	1	VT	C	0.051	2.223	0.384	0.024
9	2	VT	A	0.071	1.551	0.504	0.02
9	2	VT	B1	0.072	1.656	0.488	0.026
9	2	VT	B2	0.058	1.892	0.405	0.021
9	2	VT	C	0.019	2.466	0.42	0.048
9	3	VT	A	0.06	1.748	0.539	0.089
9	3	VT	B1	0.059	1.542	0.482	0.024
9	3	VT	B2	0.039	1.858	0.396	0.074
9	3	VT	C	0.014	1.942	0.432	0.071
10	1	OMT	A	0.035	1.727	0.459	0.076
10	1	OMT	B1	0.035	1.487	0.483	0.076
10	1	OMT	B2	0.025	1.702	0.545	0.128
10	1	OMT	C	0.042	1.394	0.491	0.128
10	2	OMT	A	0.057	1.539	0.478	0.046
10	2	OMT	B1	0.051	1.563	0.542	0.084
10	2	OMT	B2	0.054	1.594	0.476	0.078
10	2	OMT	C	0.021	1.433	0.45	0.092
10	3	OMT	A	0.032	1.688	0.557	0.086
10	3	OMT	B1	0.064	1.571	0.474	0.079
10	3	OMT	B2	0.046	1.513	0.519	0.061
10	3	OMT	C	0.049	1.5	0.467	0.062
11	1	MT	A	0.237	1.421	0.554	0.075
11	1	MT	B1	0.18	1.461	0.494	0.038
11	1	MT	B2	0.172	1.476	0.423	0.03
11	1	MT	C	0.132	1.936	0.411	0.013
11	2	MT	A	0.06	1.717	0.524	0.072
11	2	MT	B1	0.051	1.906	0.492	0.044
11	2	MT	B2	0.051	1.87	0.503	0.04
11	2	MT	C	0.053	2.032	0.393	0.04
11	3	MT	A	0.126	1.521	0.473	0.026
11	3	MT	B1	0.114	1.493	0.468	0.029
11	3	MT	B2	0.091	1.559	0.428	0.032
11	3	MT	C	0.074	1.664	0.412	0.025
12	1	MT	A	0.027	1.922	0.586	0.045
12	1	MT	B1	0.018	2.448	0.508	0.082
12	1	MT	B2	0.017	1.946	0.458	0.054
12	1	MT	C	0.013	2.025	0.433	0.048
12	2	MT	A	0.021	3.192	0.502	0.064
12	2	MT	B1	0.021	3.38	0.533	0.091
12	2	MT	B2	0.022	4.795	0.477	0.042
12	2	MT	C	0.024	4.648	0.431	0.015
12	3	MT	A	0.023	2.836	0.551	0.044
12	3	MT	B1	0.021	3.627	0.507	0.037
12	3	MT	B2	0.022	4.641	0.458	0.018
12	3	MT	C	0.024	5.114	0.439	0.012
13	1	MT	A	0.013	1.76	0.6	0.103
13	1	MT	B1	0.017	1.974	0.63	0.132
13	1	MT	B2	0.013	1.974	0.531	0.092

Appendix 6/IV. Summary of the fitted parameters (α and n estimated, θ_i and θ_r given) of van Genuchten WRC equation to soil data (360 samples).

Plot	Pit	Type	Layer	α	n	θ_i	θ_r
13	1	MT	C	0.013	1.836	0.471	0.108
13	2	MT	A	0.02	1.583	0.51	0.096
13	2	MT	B1	0.024	1.765	0.576	0.158
13	2	MT	B2	0.016	2.102	0.499	0.054
13	2	MT	C	0.012	1.876	0.417	0.082
13	3	MT	A	0.02	1.988	0.482	0.095
13	3	MT	B1	0.03	1.728	0.566	0.086
13	3	MT	B2	0.012	2.053	0.565	0.1
13	3	MT	C	0.011	1.632	0.389	0.096
14	1	OMT	A	0.034	2.178	0.455	0.091
14	1	OMT	B1	0.028	2.267	0.502	0.086
14	1	OMT	B2	0.025	1.844	0.437	0.093
14	1	OMT	C	0.023	1.423	0.44	0.083
14	2	OMT	A	0.034	1.91	0.519	0.05
14	2	OMT	B1	0.045	1.796	0.476	0.089
14	2	OMT	B2	0.024	1.496	0.431	0.075
14	2	OMT	C	0.025	1.831	0.443	0.08
14	3	OMT	A	0.034	1.873	0.528	0.104
14	3	OMT	B1	0.023	1.915	0.456	0.111
14	3	OMT	B2	0.045	1.61	0.374	0.046
14	3	OMT	C	0.048	1.441	0.406	0.042
15	1	MT	A	0.052	1.647	0.51	0.066
15	1	MT	B1	0.038	1.701	0.548	0.099
15	1	MT	B2	0.027	1.887	0.478	0.088
15	1	MT	C	0.021	1.719	0.41	0.056
15	2	MT	A	0.022	1.5	0.476	0.016
15	2	MT	B1	0.024	1.89	0.566	0.152
15	2	MT	B2	0.02	1.61	0.484	0.079
15	2	MT	C	0.034	1.448	0.399	0.044
15	3	MT	A	0.057	1.652	0.551	0.064
15	3	MT	B1	0.038	1.648	0.473	0.053
15	3	MT	B2	0.04	1.614	0.376	0.036
15	3	MT	C	0.034	1.498	0.383	0.027
16	1	MT	A	0.106	1.449	0.528	0.075
16	1	MT	B1	0.092	1.456	0.522	0.121
16	1	MT	B2	0.104	1.44	0.502	0.108
16	1	MT	C	0.038	1.942	0.358	0.041
16	2	MT	A	0.056	1.48	0.467	0.059
16	2	MT	B1	0.046	1.489	0.464	0.088
16	2	MT	B2	0.348	1.426	0.378	0.062
16	2	MT	C	0.007	1.813	0.429	0.033
16	3	MT	A	0.134	1.4	0.477	0.055
16	3	MT	B1	0.162	1.384	0.416	0.045
16	3	MT	B2	0.708	1.46	0.325	0.031
16	3	MT	C	0.496	1.717	0.416	0.02
17	1	OMT	A	0.091	1.753	0.477	0.042
17	1	OMT	B1	0.08	1.636	0.455	0.053
17	1	OMT	B2	0.094	2.29	0.408	0.04
17	1	OMT	C	0.121	1.859	0.393	0.03
17	2	OMT	A	0.075	1.661	0.499	0.045

Appendix 6/V. Summary of the fitted parameters (α and n estimated, θ_s and θ_r given) of van Genuchten WRC equation to soil data (360 samples).

Plot	Pit	Type	Layer	α	n	θ_s	θ_r
17	2	OMT	B1	0.064	1.895	0.515	0.052
17	2	OMT	B2	0.071	2.827	0.443	0.038
17	2	OMT	C	0.07	2.139	0.411	0.036
17	3	OMT	A	0.089	1.643	0.495	0.039
17	3	OMT	B1	0.074	1.585	0.447	0.05
17	3	OMT	B2	0.082	1.943	0.411	0.05
17	3	OMT	C	0.179	2.046	0.368	0.022
18	1	MT	A	0.115	1.334	0.628	0.096
18	1	MT	B1	0.045	1.387	0.533	0.076
18	1	MT	B2	0.041	1.341	0.462	0.075
18	1	MT	C	0.027	1.285	0.36	0.128
18	2	MT	A	0.219	1.3	0.578	0.067
18	2	MT	B1	0.082	1.325	0.54	0.066
18	2	MT	B2	0.028	1.358	0.465	0.068
18	2	MT	C	0.009	1.314	0.417	0.08
18	3	MT	A	0.203	1.346	0.574	0.064
18	3	MT	B1	0.035	1.557	0.582	0.104
18	3	MT	B2	0.034	1.463	0.477	0.079
18	3	MT	C	0.024	1.443	0.468	0.055
19	1	MT	A	0.203	1.348	0.573	0.066
19	1	MT	B1	0.033	1.596	0.581	0.111
19	1	MT	B2	0.031	1.453	0.474	0.08
19	1	MT	C	0.025	1.446	0.469	0.052
19	2	MT	A	0.044	1.511	0.508	0.085
19	2	MT	B1	0.037	1.646	0.602	0.075
19	2	MT	B2	0.018	2.152	0.502	0.067
19	2	MT	C	0.012	4.033	0.459	0.016
19	3	MT	A	0.022	2.15	0.483	0.059
19	3	MT	B1	0.023	2.037	0.542	0.043
19	3	MT	B2	0.021	2.181	0.468	0.031
19	3	MT	C	0.017	2.668	0.459	0.018
20	1	VT	A	0.112	1.64	0.517	0.084
20	1	VT	B1	0.179	1.67	0.421	0.018
20	1	VT	B2	0.23	1.752	0.393	0.015
20	1	VT	C	0.428	1.872	0.353	0.019
20	2	VT	A	0.078	1.585	0.512	0.068
20	2	VT	B1	0.082	1.568	0.517	0.05
20	2	VT	B2	0.135	1.731	0.381	0.017
20	2	VT	C	0.53	1.683	0.402	0.016
20	3	VT	A	0.084	1.466	0.474	0.068
20	3	VT	B1	0.142	1.456	0.52	0.122
20	3	VT	B2	0.207	1.337	0.417	0.045
20	3	VT	C	0.318	1.982	0.35	0.02
21	1	CT	A	0.062	1.752	0.61	0.081
21	1	CT	B1	0.033	2.27	0.464	0.08
21	1	CT	B2	0.031	2.347	0.433	0.037
21	1	CT	C	0.029	3.099	0.418	0.017
21	2	CT	A	0.036	2.156	0.55	0.051
21	2	CT	B1	0.025	2.841	0.47	0.036
21	2	CT	B2	0.025	2.854	0.431	0.029

Appendix 6/VI. Summary of the fitted parameters (α and n estimated, θ_i and θ_r given) of van Genuchten WRC equation to soil data (360 samples).

Plot	Pit	Type	Layer	α	n	θ_i	θ_r
21	2	CT	C	0.033	2.44	0.405	0.015
21	3	CT	A	0.04	2.067	0.521	0.03
21	3	CT	B1	0.032	2.338	0.48	0.037
21	3	CT	B2	0.028	2.607	0.418	0.032
21	3	CT	C	0.028	3.447	0.408	0.012
22	1	VT	A	0.051	1.725	0.52	0.065
22	1	VT	B1	0.052	2.003	0.509	0.088
22	1	VT	B2	0.054	2.085	0.453	0.052
22	1	VT	C	0.048	2.249	0.403	0.018
22	2	VT	A	0.059	1.644	0.499	0.042
22	2	VT	B1	0.056	1.863	0.462	0.111
22	2	VT	B2	0.061	2.403	0.368	0.039
22	2	VT	C	0.064	3.625	0.377	0.011
22	3	VT	A	0.052	1.64	0.476	0.03
22	3	VT	B1	0.068	1.577	0.514	0.037
22	3	VT	B2	0.06	1.915	0.451	0.032
22	3	VT	C	0.061	3.757	0.427	0.012
23	1	MT	A	0.145	1.428	0.62	0.134
23	1	MT	B1	0.06	1.533	0.596	0.144
23	1	MT	B2	0.039	1.469	0.561	0.134
23	1	MT	C	0.02	1.594	0.436	0.065
23	2	MT	A	0.063	1.586	0.534	0.104
23	2	MT	B1	0.071	1.565	0.472	0.063
23	2	MT	B2	0.07	1.824	0.438	0.084
23	2	MT	C	0.061	1.277	0.498	0.137
23	3	MT	A	0.065	1.544	0.498	0.106
23	3	MT	B1	0.046	1.897	0.513	0.128
23	3	MT	B2	0.059	1.741	0.452	0.093
23	3	MT	C	0.139	1.361	0.404	0.091
24	1	CT	A	0.046	1.434	0.523	0.023
24	1	CT	B1	0.085	1.416	0.534	0.103
24	1	CT	B2	0.046	1.612	0.506	0.141
24	1	CT	C	0.262	1.784	0.264	0.019
24	2	CT	A	0.052	1.362	0.516	0.019
24	2	CT	B1	0.07	1.545	0.584	0.153
24	2	CT	B2	0.098	1.347	0.403	0.047
24	2	CT	C	0.129	1.877	0.318	0.023
24	3	CT	A	0.049	1.475	0.433	0.052
24	3	CT	B1	0.025	1.467	0.57	0.101
24	3	CT	B2	0.109	1.357	0.37	0.031
24	3	CT	C	0.672	1.486	0.301	0.024
25	1	MT	A	0.111	1.383	0.526	0.086
25	1	MT	B1	0.034	1.7	0.516	0.135
25	1	MT	B2	0.032	1.589	0.498	0.128
25	1	MT	C	0.034	1.4	0.419	0.122
25	2	MT	A	0.038	1.539	0.581	0.141
25	2	MT	B1	0.028	1.578	0.641	0.113
25	2	MT	B2	0.023	1.515	0.575	0.161
25	2	MT	C	0.013	1.71	0.394	0.029
25	3	MT	A	0.022	1.64	0.493	0.086

Appendix 6/VII. Summary of the fitted parameters (α and n estimated, θ_s and θ_r given) of van Genuchten WRC equation to soil data (360 samples).

Plot	Pit	Type	Layer	α	n	θ_s	θ_r
25	3	MT	B1	0.025	1.616	0.536	0.102
25	3	MT	B2	0.015	1.896	0.501	0.105
25	3	MT	C	0.021	1.573	0.448	0.081
26	1	CT	A	0.059	1.493	0.632	0.105
26	1	CT	B1	0.059	1.4	0.468	0.055
26	1	CT	B2	0.364	1.353	0.351	0.02
26	1	CT	C	0.795	1.507	0.27	0.013
26	2	CT	A	0.106	1.474	0.641	0.103
26	2	CT	B1	0.094	1.479	0.52	0.093
26	2	CT	B2	0.19	1.509	0.424	0.09
26	2	CT	C	1.414	1.486	0.272	0.019
26	3	CT	A	0.117	1.466	0.6	0.094
26	3	CT	B1	0.173	1.337	0.475	0.072
26	3	CT	B2	1.434	1.439	0.289	0.029
26	3	CT	C	1.165	1.461	0.247	0.02
27	1	CT	A	0.063	1.692	0.537	0.097
27	1	CT	B1	0.076	1.52	0.447	0.032
27	1	CT	B2	0.072	1.805	0.394	0.022
27	1	CT	C	0.074	2.13	0.341	0.014
27	2	CT	A	0.049	1.534	0.536	0.035
27	2	CT	B1	0.05	1.99	0.513	0.124
27	2	CT	B2	0.099	1.784	0.369	0.02
27	2	CT	C	0.101	2.509	0.402	0.015
27	3	CT	A	0.055	1.556	0.53	0.032
27	3	CT	B1	0.098	1.749	0.528	0.108
27	3	CT	B2	0.126	1.836	0.354	0.014
27	3	CT	C	0.051	2.755	0.407	0.018
28	1	OMT	A	0.048	1.444	0.567	0.062
28	1	OMT	B1	0.038	1.587	0.663	0.133
28	1	OMT	B2	0.02	1.719	0.561	0.067
28	1	OMT	C	0.025	1.754	0.391	0.09
28	2	OMT	A	0.02	1.677	0.525	0.087
28	2	OMT	B1	0.02	2.397	0.605	0.171
28	2	OMT	B2	0.02	2.029	0.56	0.07
28	2	OMT	C	0.012	2.225	0.413	0.073
28	3	OMT	A	0.021	1.558	0.493	0.067
28	3	OMT	B1	0.023	1.428	0.502	0.023
28	3	OMT	B2	0.03	1.502	0.499	0.071
28	3	OMT	C	0.053	1.467	0.437	0.134
29	1	VT	A	0.045	1.595	0.456	0.073
29	1	VT	B1	0.076	1.435	0.466	0.101
29	1	VT	B2	0.037	1.6	0.462	0.121
29	1	VT	C	0.171	2.245	0.377	0.018
29	2	VT	A	0.04	1.641	0.487	0.088
29	2	VT	B1	0.088	1.518	0.621	0.114
29	2	VT	B2	0.048	1.825	0.391	0.062
29	2	VT	C	0.026	2.696	0.412	0.021
29	3	VT	A	0.072	1.527	0.492	0.053
29	3	VT	B1	0.055	1.656	0.47	0.064
29	3	VT	B2	0.049	1.597	0.41	0.055

Appendix 6/VIII. Summary of the fitted parameters (α and n estimated, θ_s and θ_r given) of van Genuchten WRC equation to soil data (360 samples).

Plot	Pit	Type	Layer	α	n	θ_s	θ_r
29	3	VT	C	0.104	2.758	0.392	0.012
30	1	CT	A	0.047	1.887	0.538	0.035
30	1	CT	B1	0.064	1.871	0.471	0.057
30	1	CT	B2	0.096	2.125	0.416	0.023
30	1	CT	C	0.098	2.658	0.388	0.011
30	2	CT	A	0.13	1.65	0.538	0.085
30	2	CT	B1	0.065	1.788	0.492	0.053
30	2	CT	B2	0.095	1.941	0.389	0.019
30	2	CT	C	0.107	2.836	0.401	0.017
30	3	CT	A	0.078	1.782	0.564	0.068
30	3	CT	B1	0.064	1.639	0.512	0.049
30	3	CT	B2	0.089	2.202	0.403	0.02
30	3	CT	C	0.173	2.21	0.374	0.011

Appendix 7/I. Swedish arable soil data. R^2 is the coefficient of determination, E_{ave} is the average error at different pressure heads, S_{dev} is the standard deviation of errors, E_{min} is the minimum value and E_{max} is the maximum value of errors at different pressure heads using semi-physical, Jonasson's and van Genuchten's methods of WRC determination. Saturated water content (θ) and residual water content (θ_r) were estimated. S_E is the square sum of errors and θ_{ave} is the average value of all the measurements.

h_s , cm	1	5	16	20	32	50	100	200	316	501	1000	5012	15849
Semi-physical													
E_{ave}	-0.015	0.010	0.018	0.023	0.022	0.019	0.002	-0.017	-0.026	-0.026	-0.017	0.011	0.040
S_{dev}	0.010	0.020	0.025	0.028	0.034	0.041	0.048	0.051	0.049	0.044	0.028	0.025	0.016
E_{max}	0.001	0.035	0.041	0.048	0.060	0.070	0.062	0.040	0.019	0.016	0.025	0.057	0.071
E_{min}	-0.029	-0.027	-0.020	-0.018	-0.031	-0.042	-0.064	-0.093	-0.106	-0.089	-0.060	-0.007	0.024
							$S_E=$		$\theta_{ave}=$		$S_M=$		$R^2=$
							0.134		0.319		1.696		0.921
Jonasson													
E_{ave}	-0.017	0.005	0.007	0.009	0.009	0.002	-0.005	-0.005	-0.007	-0.001	0.013	0.055	0.087
S_{dev}	0.014	0.031	0.040	0.044	0.053	0.064	0.079	0.083	0.083	0.080	0.076	0.099	0.100
E_{max}	-0.042	-0.058	-0.080	-0.083	-0.093	-0.100	-0.106	-0.104	-0.097	-0.088	-0.078	-0.029	0.024
E_{min}	-0.042	-0.058	-0.080	-0.083	-0.093	-0.100	-0.106	-0.104	-0.097	-0.088	-0.078	-0.029	0.024
							$S_E=$		$\theta_{ave}=$		$S_M=$		$R^2=$
							0.460		0.319		1.696		0.729
van Genuchten													
E_{ave}	-0.015	0.011	0.025	0.029	0.035	0.041	0.047	0.039	0.030	0.028	0.029	0.037	0.051
S_{dev}	0.009	0.019	0.020	0.023	0.027	0.034	0.048	0.045	0.041	0.042	0.056	0.052	0.042
E_{max}	0.001	0.033	0.047	0.063	0.066	0.091	0.135	0.115	0.098	0.092	0.102	0.088	0.100
E_{min}	-0.026	-0.023	-0.014	-0.011	-0.011	-0.012	-0.015	-0.018	-0.020	-0.023	-0.035	-0.044	-0.023
							$S_E=$		$\theta_{ave}=$		$S_M=$		$R^2=$
							0.217		0.319		1.696		0.872

$$S_E = \sum_{j=1}^7 \sum_{i=1}^{108} (\theta_{i,j}^M - \theta_{i,j}^C)^2 \quad S_M = \sum_{j=1}^7 \sum_{i=1}^{108} (\theta_{i,j}^M - \theta_{AVE}^M)^2$$

$$R^2 = \frac{S_M - S_E}{S_M}$$

Appendix 7/II. Swedish arable soil data. R^2 is the coefficient of determination, E_{ave} is the average error at different pressure heads, S_{dev} is the standard deviation of errors, E_{min} is the minimum value and E_{max} is the maximum value of errors at different pressure heads using semi-physical, Jonasson's and van Genuchten's methods of WRC determination. Saturated water content (θ) and residual water content (θ) were estimated. S_E is the square sum of errors and θ_{ave} is the average value of all the measurements.

h, cm	1	5	16	20	32	50	100	200	316	501	1000	5012	15849
Semi-physical													
E_{ave}	-0.004	0.017	0.021	0.023	0.022	0.019	0.002	-0.017	-0.028	-0.030	-0.025	-0.002	0.023
S_{dev}	0.011	0.024	0.026	0.028	0.034	0.041	0.048	0.051	0.049	0.042	0.028	0.027	0.029
E_{max}	0.000	0.045	0.043	0.048	0.060	0.070	0.062	0.040	0.019	0.016	0.002	0.057	0.071
E_{min}	-0.029	-0.027	-0.020	-0.018	-0.031	-0.042	-0.064	-0.093	-0.106	-0.089	-0.079	-0.025	0.000
							$S_E=$	$\theta_{ave}=$	$S_M=$	$R^2=$			
							0.135	0.319	1.696	0.920			
Jonasson													
E_{ave}	-0.005	0.013	0.013	0.014	0.011	0.003	-0.004	-0.006	-0.009	-0.006	0.005	0.042	0.069
S_{dev}	0.017	0.034	0.044	0.048	0.054	0.066	0.081	0.086	0.086	0.085	0.083	0.106	0.112
E_{max}	-0.042	-0.058	-0.080	-0.083	-0.093	-0.100	-0.106	-0.104	-0.097	-0.094	-0.085	-0.029	-0.014
E_{min}	-0.042	-0.058	-0.080	-0.083	-0.093	-0.100	-0.106	-0.104	-0.097	-0.094	-0.085	-0.029	-0.014
							$S_E=$	$\theta_{ave}=$	$S_M=$	$R^2=$			
							0.485	0.319	1.696	0.714			
van Genuchten													
E_{ave}	-0.015	0.011	0.025	0.029	0.035	0.041	0.047	0.039	0.030	0.028	0.029	0.037	0.051
S_{dev}	0.009	0.019	0.020	0.023	0.027	0.034	0.048	0.045	0.041	0.042	0.056	0.052	0.042
E_{max}	0.001	0.033	0.047	0.063	0.066	0.091	0.135	0.115	0.098	0.092	0.102	0.088	0.100
E_{min}	-0.026	-0.023	-0.014	-0.011	-0.011	-0.012	-0.015	-0.018	-0.020	-0.023	-0.035	-0.044	-0.023
							$S_E=$	$\theta_{ave}=$	$S_M=$	$R^2=$			
							0.243	0.319	1.696	0.857			

$$S_E = \sum_{j=1}^7 \sum_{i=1}^{108} (\theta_{i,j}^M - \theta_{i,j}^C)^2 \quad S_M = \sum_{j=1}^7 \sum_{i=1}^{108} (\theta_{i,j}^M - \theta_{ave}^M)^2$$

$$R^2 = \frac{S_M - S_E}{S_M}$$

Appendix 8/I. Results of the prediction of the saturated hydraulic conductivity for the UNSODA samples using modified form of Andersson's method and van Genuchten method. K_s is the measured saturated hydraulic conductivity (cm d^{-1}), h_B is the bubbling pressure (cm) determined using the Mualem's method (1976a), $K_{s,bB}$ is the estimated saturated hydraulic conductivity using Andersson's method (see Eq. (3-11)), $h_{B,opt}$ is the optimum bubbling pressure that gives accurate prediction of K_s in Andersson's method, $K_{s,G}$ is the estimated saturated hydraulic conductivity using Eq. (3-36) and $c_{sat,opt}$ is the optimum value for parameter c_{sat} ($108 \text{ cm}^3\text{s}^{-1}$) that gives accurate prediction of K_s (see Eq. (3-36)).

Soil	K_s	h_B	$K_{s,bB}$	$h_{B,opt}$	$K_{s,G}$	$c_{sat,opt}$
3360	2.08	-18.5	0.15	-3.5	19	11.82
3361	2.04	-18.1	0.16	-3.6	17.35	12.7
4001	35.3	-4.6	1.39	-0.65	234.62	16.25
4030	0.41	-5.9	0.95	-0.65	54.66	0.81
4031	3.89	-4.1	1.67	-2.5	382.38	1.1
4040	41.7	-7.2	0.68	-0.55	13.49	333.92
4043	122.7	-7.3	0.66	-0.32	9.68	1369.29
4052	117.5	-4.5	1.47	-0.32	231.99	54.7
4061	30.9	-5.4	1.06	-0.7	114.29	29.2
4062	13	-4.5	1.46	-1.2	231.34	6.07
4070	4	-8.8	0.49	-2.4	11.98	36.05
4071	52	-6.9	0.73	-0.5	16.85	333.2
4080	304	-7	0.71	-0.18	11.98	2739.49
4081	81	-5.4	1.09	-0.4	50.4	173.58
4082	140	-6.1	0.88	-0.3	35.01	431.85
4091	1209	-1	17	-0.1	1044.52	125.01
4092	858	-7.3	0.66	-0.1	34.5	2685.89
4102	72.9	-5.2	1.14	-0.42	108.35	72.67
4110	687	-8	0.57	-0.12	8.51	8715.63
4111	2.5	-9.5	0.44	-3.2	6.31	42.78
Average	189	-7.3	1.67	-1.1	131.9	859.6

Appendix 8/II. Results of the prediction of the hydraulic conductivity function for the UNSODA samples using modified form of Andersson's method and van Genuchten method. E_{ave} is the absolute value of the average logarithmic error: $|\log(K_{i,m}) - \log(K_{i,c})|$, where $K_{i,m}$ is the measured value, $K_{i,c}$ is the calculated value, and M is the number of measurements in soil sample. Average error is given for three different pressure head ranges representing wet ($-100 < h < 0$ cm), medium ($-500 < h < -100$ cm) and dry ($h < -500$ cm) conditions. $E_{ave}/h_{B,opt}$ is the average error when optimum value for bubbling pressure given in Appendix 8/I was used. E_{ave}/λ_{opt} is the average error in van Genuchten's method when the exponent λ in Eq. (3-29) was optimized (standard value for $\lambda=0.5$ was used otherwise).

Soil	Modified Andersson's method					van Genuchten's method						λ_{opt}
	$E_{ave}/$ whole range	$E_{ave}/$ wet	$E_{ave}/$ medium	$E_{ave}/$ dry	$E_{ave}/$ $h_{B,opt}$	$E_{ave}/$ whole range	$E_{ave}/$ wet	$E_{ave}/$ Mediu m	$E_{ave}/$ dry	$E_{ave}/$ λ_{opt}		
3360	0.16	0.17	0.18	0.12	0.1	0.26	0.15	0.27	0.42	0.22	-0.17	
3361	0.05	0.05	0.04	0.05	0.05	0.14	0.12	0.29	0.04	0.13	0.65	
4001	0.7	0.38	1.16	*	0.56	0.48	0.39	0.6	*	0.2	1.75	
4030	2.03	0.65	1.97	2.38	0.55	2.4	0.05	1.7	2.84	0.11	-3.38	
4031	0.25	0.28	0.12	0.45	0.22	0.67	0.07	0.12	1.97	0.09	-1.17	
4040	0.19	0.57	0.21	0.15	0.16	0.64	1.06	1.23	0.5	0.57	1.27	
4043	0.75	1.53	1.27	0.5	0.34	1.46	2.09	2.41	1.11	1.06	2.17	
4052	0.71	0.26	1.06	*	0.54	0.82	0.43	1.12	*	0.51	2.49	
4061	0.21	0.33	0.19	0.21	0.21	0.92	0.43	0.26	2.69	0.5	-0.85	
4062	0.3	0.43	0.28	0.26	0.2	0.38	0.44	0.12	0.81	0.31	-0.32	
4070	0.55	0.17	0.52	0.67	0.15	0.37	0.45	0.5	0.26	0.37	0.47	
4071	0.48	1.61	0.77	0.19	0.4	1.09	1.73	1.87	0.72	0.91	1.68	
4080	1.17	2.28	1.59	0.74	0.49	1.92	2.8	2.75	1.44	1.34	3.4	
4081	0.57	1.5	0.71	0.09	0.52	0.87	1.62	1.13	0.41	0.66	1.84	
4082	1.04	2.02	1.18	0.57	0.48	1.45	2.14	1.72	1.01	1.11	4.06	
4091	0.89	1.69	0.97	0.24	0.59	1.24	2.21	1.32	0.47	1.01	2.19	
4092	1.93	2.9	2.02	1.5	0.44	2.2	2.92	2.42	1.83	1.26	7.78	
4102	0.79	1.59	0.35	0.64	0.79	0.66	1.18	0.15	0.61	0.45	-2.22	
4110	0.99	2.53	1.54	0.49	0.59	1.72	2.66	2.33	1.36	1.04	5.73	
4111	1.23	0.96	0.15	1.44	0.97	0.74	0.95	0.7	0.69	0.39	-2.53	
Average	0.75	1.1	0.81	0.59	0.42	1.02	1.19	1.15	1.07	0.61	1.24	

* No measurements

$$E_{ave} = \frac{\sum_{i=1}^M |\log(K_{i,m}) - \log(K_{i,c})|}{M}$$

